Cape Peninsula University of Technology

PROCESS OPTIMISATION AND TECHNO-ECONOMIC ANALYSIS OF VACUUM ULTRAVIOLET PHOTOLYSIS FOR ETHYLENE REMOVAL IN APPLE STORAGE

by

Nina Ntokozo Mntwini

A thesis submitted in fulfilment of the requirements for the degree of

Master of Engineering in Chemical Engineering

in the

Faculty of Engineering and the Built Environment

at the

Cape Peninsula University of Technology

Supervisors: **Dr Buntu Godongwana**
Dr Bongolwethu Mabusela

Bellville

October 2025

DECLARATION

I, Nina Ntokozo Mntwini, declare that the contents of this dissertation/thesis represent my own unaided work, and that the dissertation/thesis has not previously been submitted for academic examination towards any qualification. Furthermore, it represents my own opinions and not necessarily those of the Cape Peninsula University of Technology.

Signature: 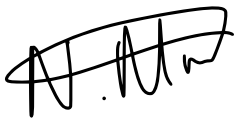 **Date:** **28 October 2025**

ABSTRACT

The nutritional values of apples (*Malus domestica*) is renowned globally. Apples are known to contribute antioxidants, fibre, vitamins, and essential nutrients to the human diet. During storage and transportation, apples remain metabolically active, producing ethylene, a gas responsible for accelerating ripening and senescence, thus contributing to food waste and economic losses. Therefore, the removal of ethylene in overhead atmosphere during transportation and storage is of utmost importance to preserve their shelf-life and the reduction of food waste.

Various techniques have been implemented to ensure the mitigation of ethylene effects during the post-harvest management of fruits and vegetables; however, due to limitations such as rapid saturation, high operational cost, toxicity, additional waste management requirements, and the frequent need for replacement render these conventional methods unsuitable for extended storage.

This study explored vacuum ultraviolet photolysis (VUV) as a promising technology for the removal of ethylene in storage atmosphere. To more accurately represent the process, two complementary modelling approaches were utilized. The first model focused on the fundamental chemical and physical mechanisms that govern ethylene degradation, while the second model examined how different process parameters in the storage system influence performance. Combined, these approaches offered both mechanistic insight and practical relevance. The first model was formulated using a coupled mass and energy balance with ethylene degradation described as a first-order reaction. To assess model sensitivity, key kinetic parameters, including the pre-exponential factor (k_0, 0.10 and 1.00 s^{-1}) and activation energy (E_a,15,000 to 25,000 $J \cdot mol^{-1}$) were varied. This model achieved high predictive accuracy (R^2=0.988, RMSE=0.0572), closely reproducing experimental concentration decay and temperature rise.

However, the first model did not incorporate relative humidity (RH) effects. To address this, a second percentage ethylene removal (PER) model was constructed from a Box–Behnken experimental design, incorporating relative humidity, initial ethylene concentration, and lamp wattage as independent variables. Relative humidity improved removal efficiency at low ethylene concentrations; however, an unexpected result was observed at 50 ppm and 3W. Under these operating conditions, increased relative humidity slightly reduced the percentage of ethylene removal. This was hypothesized to be due to photon competition limiting oxidant generation.

Optimisation combined outputs from both models to minimise total operating cost, defined as the sum of energy use and spoilage-related losses. Cost was more sensitive to incomplete

degradation than to power consumption, meaning that faster conversion directly reduced total cost by lowering spoilage penalties. Sensitivity analysis identified lamp power and activation energy as the most influential parameters, with k_0 and the heat-transfer coefficient exerting smaller effects. The optimal configuration,12 W lamp power, E_a=19,600 J·mol^{-1}, k_0=0.47 s^{-1}, and h_e=15–30 W·m^{-2}·K^{-1}, achieved near-complete degradation within 780 s, with a moderate temperature rise (~2.9× initial) and a cost of 0.148 R/kg apple.

Industrial-scale projections showed a ~90.5 % reduction in ethylene concentration (from 113.27 ppm to 10.81 ppm), spoilage reduction from 31.72 % to 3.03 %, and ~10.5× shelf-life extension. For Golden Delicious apples, this equated to ~R5,785 savings per pallet and ~R 1.82 million per day for 15 truckloads at optimal operation. These findings confirm that VUV photolysis, operated within the identified parameters, offers a scalable, efficient, and cost-effective ethylene control method. By combining mechanistic modelling with environmental sensitivity, the dual model offers a robust foundation for optimising ethylene management in diverse storage systems.

ACKNOWLEGEMENTS

This thesis would not have been possible without the support and encouragement of many individuals.

I extend my deepest gratitude to Dr. Buntu Godongwana, my supervisor, for his unwavering support, expert guidance, and insightful feedback throughout this research. His constructive criticism has been invaluable in shaping the quality and direction of this thesis.

My sincere thanks to Dr. Bongolwethu Mabusela, my co-supervisor, whose guidance, encouragement, and dedication have been instrumental to the successful completion of this work.

I gratefully acknowledge the technical staff of the Department of Chemical Engineering, Ms. Hannelene Small, Ms. Geraldine Lentoor, and Mr. Alwyn Bester, for their willingness to assist and their dedication to ensuring the smooth execution of my experiments.

I am thankful to Miss Zinzi Mbete from Blue Jay Farm for ensuring a steady supply of apples for my research, and to Mr. Sifundo Mathe from the Agricultural Research Council for his assistance with analytical work.

I extend heartfelt thanks to Mike Oluwaseun Ojumu for his steadfast support and for never giving up on me, even during challenging times.

Above all, I owe profound gratitude to my mother, whose unconditional love, sacrifices, and encouragement have been my foundation throughout this journey. Her strength and belief in me have been the greatest source of motivation in completing this work.

DEDICATION

To that little girl who used to dream, your spirit, resilience, and boundless imagination have been my constant inspiration. This work is a testament to your dreams and a reminder that no matter the obstacles, the power of dreaming can transform reality. Thank you for teaching me to dream fearlessly.

NOMENCLATURE

Acronym	Full Form
ANOVA	Analysis of variance
AVG HCl	Aminoethoxyvinylglycine hydrochloride
BB	Box-Behnken
CBA	Cost Benefit Analysis
CCD	Central Composite Design
DCF	Discounted cash flow
DOE	Design of experiments
GAC	Granular activated carbon
LCA	Life cycle analysis
NPV	Net present value
PVOC	Present value of operating costs
RH	Relative humidity
ROS	Reactive oxygen species
RSM	Response surface methodology
TA	Titratable Acids
TEA	Techno-Economic Analysis
TSS	Total soluble solids
1-MCP	1-Methylcyclopropene
VUV	Vacuum ultraviolet

TABLE OF CONTENTS

LIST OF TABLES

LIST OF FIGURES

CHAPTER 1

1. INTRODUCTION

1.1. Background

Due to their diverse range of health benefits, apples *(Malus domestica* (Borkh.)), are cultivated throughout the world. They are a source of antioxidants, dietary fibre, vitamins, and many other nutrients essential for the human diet (Raheema, 2020). Annually, the world produces a staggering 74.8 million tons of apples, with China contributing a substantial 41.0 million tons, the European Union accounting for 12.8 million tons, and South Africa yielding 1.2 million tons (USDA, 2023). Apples currently occupy the second position in global fruit consumption, trailing only behind the widely consumed banana (Vasylieva and James, 2021). To meet the high demand for apples, they must be transported from their cultivation centres to distant consumer markets, necessitating several days of refrigerated storage during transit. However, due to metabolic activity within their living cells, harvested apples remain biologically active even after being harvested (Kulathunga et al., 2018).

This metabolic activity results in the emission of ethylene, a growth phytohormone responsible for ripening and senescence of apples (natural deterioration in quality resulting in loss of texture, flavour, etc.) (Davies, 2010). Exposure of fruits and vegetables to ethylene results in accelerated ripening and senescence, ultimately contributing to food waste (Mahajan et al., 2014). From an economic perspective, such losses represent a loss in investment, since resources, once utilized, become irretrievable. To mitigate these losses, it is imperative to slow down these physiological processes, which can be achieved by minimizing the exposure of fruits and vegetables to ethylene.

Numerous techniques have been researched and implemented to address the inhibition, control, and elimination of ethylene in fruits. AVG is employed for ethylene inhibition, while 1-MCP is utilized for ethylene control at the receptor level (Doerflinger et al., 2019). Additionally, methods such as ozone treatment, catalytic oxidation, air ventilation, oxidizers, absorbers, and adsorbers are employed for ethylene removal (Pathak and Mahajan, 2017). However, each of these methods has its drawbacks in terms of ethylene removal. For instance, using ozone demands extreme caution due to its high human toxicity and potential harm to fruits and vegetables at elevated concentrations (Pathak et al., 2019a). Conversely, air ventilation cannot be employed in controlled atmospheres as it would cause a disruption in set conditions (Pathak and Mahajan, 2017). Catalytic oxidation is an energy-intensive process that would result in the incurrence of additional costs. Adsorbers, absorbers, and oxidizers quickly reach

saturation, necessitating frequent replacement and creating a waste disposal issue (Pathak and Mahajan, 2017). These conventional approaches all possess drawbacks that render them unsuitable for extended storage and long-distance transportation. Thus, a cost-effective, low-waste, safe, and highly efficient method is imperative.

Vacuum Ultraviolet (VUV) photolysis, a technology that remains relatively untapped for ethylene removal in apple preservation, has previously demonstrated its effectiveness in wastewater and air purification applications, as demonstrated by Kutschera et al. (2009) and Huang et al. (2011, 2014). VUV irradiation, characterized by its high-energy photons, is capable of triggering the dissociation of water and oxygen molecules in a gaseous state within the atmosphere of fruits. This photolytic process generates reactive oxygen species (ROS) such as ozone (O_3), atomic oxygen ($O(^1D)$), atomic oxygen ($O(^3P)$), and hydroxyl radicals (·OH) which possess high oxidation potential and are self-sufficient in rapidly facilitating the breakdown of ethylene into its constituent components, carbon dioxide and water as outlined by (Kulathunga et al., 2018).

This technique shows considerable potential for extending the shelf life of fruit by slowing ethylene-driven ripening, although prior research in this field has been somewhat limited. Pathak et al. (2017) reported that vacuum ultraviolet (VUV) photolysis was effective in removing ethylene during short-term storage of apples and kiwifruit. Their reactor consistently lowered the gas concentration inside the storage chamber. A later investigation by Mabusela et al. (2023) went further, comparing VUV photolysis with the widely used ethylene adsorbent potassium permanganate. Under mixed-fruit loading conditions, VUV achieved an efficiency of 86.9%, substantially higher than the 47% recorded for potassium permanganate. The study also considered fruit-quality parameters. While VUV reduced ethylene levels and slowed respiration, it caused surface damage to apples when the fruit was directly exposed to irradiation. This suggests that protective strategies are needed to harness the benefits of VUV without compromising fruit quality.

These findings highlight the potential of VUV photolysis in prolonging the shelf life and quality of fruits by mitigating the detrimental effects of ethylene. Although VUV photolysis is a promising technology, no research has reported its economic feasibility. Therefore, there is a strong need to assess the economic feasibility of this technology to evaluate whether the technology will be economically viable for practical application.

1.2. Problem Statement

The global demand for apples requires the use of effective postharvest management methodologies. A significant challenge in the transportation and storage of apples is the management of ethylene, a plant hormone responsible for accelerated ripening, leading to the deterioration of apple quality. Current postharvest ethylene management strategies, such as oxidation with potassium permanganate, catalytic oxidation, and adsorption/absorption, are ineffective for long-distance transportation and long-term storage, where continuous removal of ethylene is required. Therefore, there is an urgent need for a cost-effective and highly efficient method to manage ethylene and extend the shelf life of apples during transportation and storage. Vacuum ultraviolet photolysis emerges as a promising strategy for effectively removing ethylene due to its ability to continuously remove ethylene, thus maintaining the quality of apples. However, while its technical potential has been demonstrated, no known published work has examined its overall economic feasibility and operating conditions.

1.3. Research questions and hypothesis

1.3.1. Research questions

The study will attempt to answer the following questions:

a) Is VUV photolysis efficacious in removing ethylene in apple storage environments?

b) What are the optimum process variables (humidity, UV lamp power, and initial ethylene concentration) and storage conditions (relative humidity) required to achieve the targeted degradation amount?

c) Is VUV photolysis an economically feasible process for degrading ethylene in fruit and vegetable storage?

1.3.2. Hypothesis

The initial ethylene concentration, lamp power, and relative humidity are the primary determinants of the efficacy and economic feasibility of a vacuum ultraviolet photolysis reactor employed for reducing ethylene concentration levels in apple storage environments.

1.4. Aims and objectives

This study aims to evaluate the application of VUV photolysis for ethylene removal in apple storage environments and to conduct an economic feasibility analysis. This will be achieved by the following objectives:

- To optimise process parameters (initial ethylene concentration, wattage) and storage conditions (relative humidity) using surface response methodology.
- To evaluate the electrical energy per order of VUV photolysis under optimised conditions.
- To use optimised parameters to develop a techno-economic analysis of the degradation of ethylene by VUV photolysis.

1.5. Thesis Outline

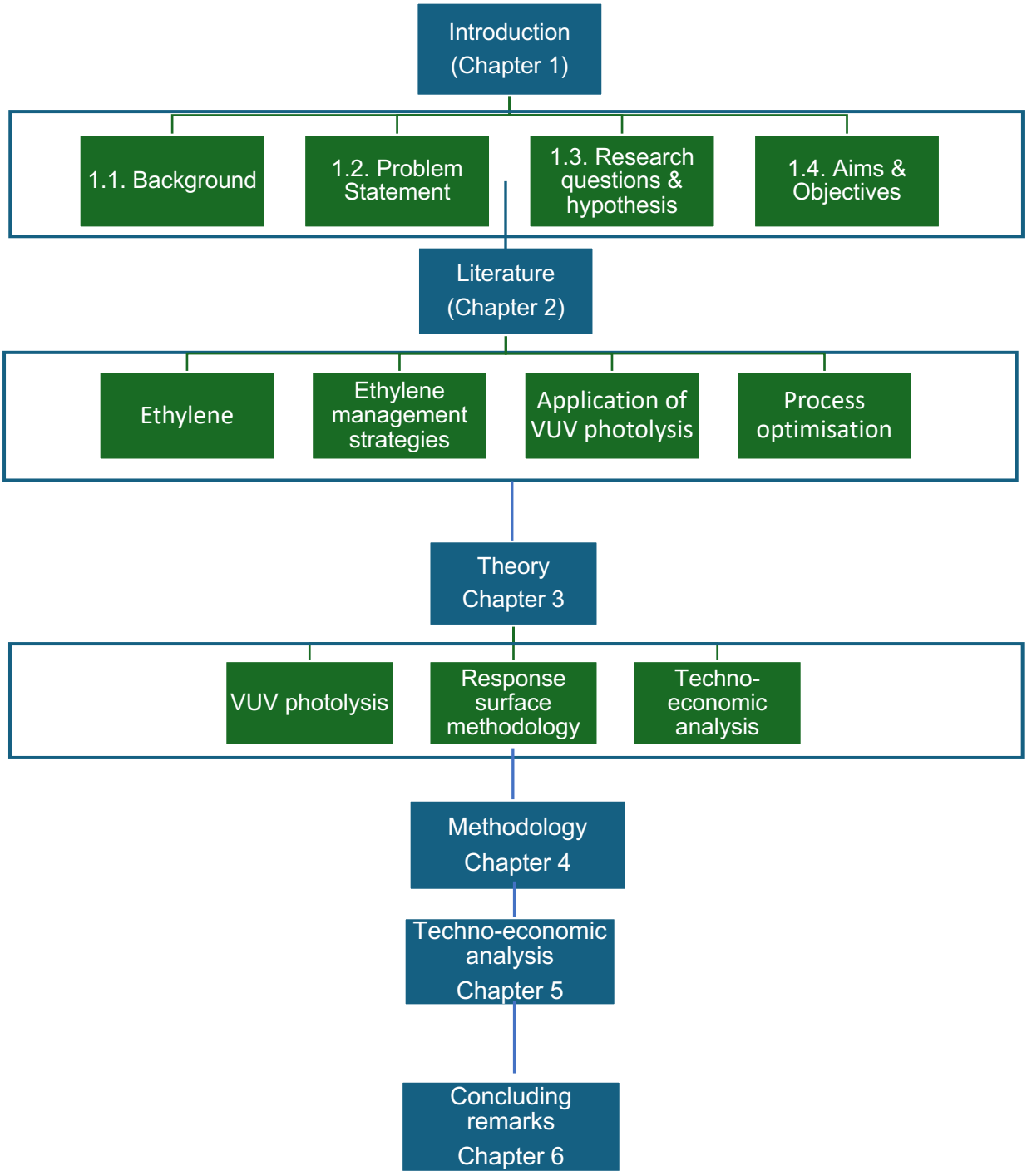

Figure 1.1 Thesis outline

CHAPTER 2

2. LITERATURE REVIEW

2.1. Background

Over the past two decades, advances in post-harvest management have greatly expanded our understanding of ethylene, A simple yet highly influential plant hormone that controls ripening in climacteric fruits. As an unsaturated hydrocarbon, ethylene plays a key role in coordinating the biochemical and physiological changes involved in ripening, which directly impact fruit quality, shelf life, and market value both before and after harvest. Because its production triggers a cascade of metabolic responses, the presence of ethylene is relevant not only at the orchard level but throughout the entire supply chain. The following sections of this chapter explore these dynamics in greater depth.

The discussion begins with ethylene biosynthesis, tracing the pathway from methionine through several enzymatic conversions, and considers the downstream physiological effects that drive fruit maturation. Beyond its biological role, the chapter also examines current strategies for mitigating ethylene's impact during storage. These include chemical approaches such as the application of 1-methylcyclopropene (1-MCP), which binds to ethylene receptors to slow ripening, and the use of physical adsorbents such as activated carbon and zeolites, which remove ethylene gas from storage environments to prolong shelf life.

In addition to these established practices, attention has recently shifted toward more innovative interventions. Techniques such as photocatalytic oxidation and vacuum ultraviolet (VUV) photolysis have emerged as promising tools for degrading ethylene directly. Although these methods are still under active investigation, they represent the frontier of post-harvest technology and suggest new possibilities for maintaining fruit quality while reducing post-harvest losses.

2.2. Role of ethylene in fruit ripening

Ethylene, commonly known as the 'ripening hormone', plays a critical role in the agricultural and horticultural industries by controlling the quality and shelf life of fruits and vegetables both before and after they are harvested. This gaseous unsaturated hydrocarbon consists of two carbon atoms and four hydrogen atoms as depicted in Figure 2.1 (Davies, 2010). Produced by the tissues of fruits and vegetables in extremely low concentrations, ethylene is crucial for regulating physiological processes and stress responses within these plants (McKeon et al., 1995). Despite its simple molecular structure, ethylene controls essential processes like

ripening, senescence, seed germination, leaf abscission, and stress responses, particularly in climacteric fruits (McKeon et al., 1995; Ebrahimi et al., 2021).

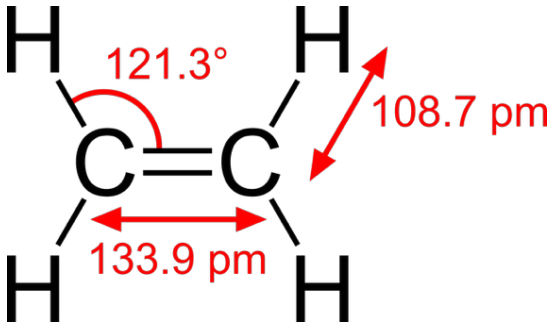

Figure 2.1 Chemical structure of ethylene

Ripening, a primary effect of ethylene's key effects, gives distinctive characteristics to fruits and vegetables. In the horticultural industry, fruits and vegetables are often harvested before full ripeness to satisfy supply chain and market demands. However, they remain metabolically active and susceptible to ethylene's effects, accelerating ripening and potentially leading to quality loss and reduced storability. Given this, various techniques have been developed to inhibit or remove external ethylene, especially within storage environments, to prolong quality and shelf life. The recent focus on ethylene removal highlights its significance in preventing accelerated ripening and ensuring the storability of fruits and vegetables. If ethylene levels are not properly managed, substantial post-harvest losses can occur.

Ethylene plays a critical role in the ripening of many climacteric fruits, influencing key quality attributes. For instance, it drives changes in colour, texture, and nutritional content, therefore enhancing overall quality (Liu et al., 2024). Xiao et al. (2013) highlighted the crucial role of ethylene in regulating gene expression during banana ripening, directly affecting ripeness and quality. Similarly, studies on apples show that ethylene modulates cell wall metabolism and sugar accumulation, leading to fruit softening and sweetness (Li et al.,2016). In tomatoes, Boe (1967) reported that ethylene accelerates both ripening and respiration rates, indicating its significant impact on the ripening process.

Moreover, although kiwi fruit produces only minimal ethylene during ripening, they are highly sensitive to external ethylene with concentrations as low as little as 0.01–0.03 ppm sufficient in speeding up fruit softening (Huang et al., 2021). These results collectively highlight ethylene's essential role as a ripening hormone in a variety of fruits.

2.3. Ethylene biosynthesis

The hormone ethylene is produced through a series of coordinated steps that drive the ripening of fruits and vegetables. This process starts with the conversion of the amino acid methionine into S-adenosylmethionine (SAM) by the enzyme SAM synthase (Adams & Yang, 1977). SAM is then transformed into the cyclic non-protein amino acid 1-aminocyclopropane-1-carboxylic acid (ACC) by ACC synthase (Adams & Yang, 1979). The final step involves converting ACC to ethylene via the enzyme ACC oxidase (Kende, 1993). Additionally, SAM also produces 5'methylthioadenosine (MTA) (Adams & Yang, 1979), which is utilized to regenerate methionine, ensuring its concentration remains stable even with high ethylene production (Abeles et al., 1992). The Yang cycle (Figure 2.2) begins with the breakdown of MTA into methylthioribose (MTR) and adenine. MTR is then phosphorylated and subsequently oxidized to α-keto-γ-methylthio-butyric acid (KMB). The final step adds an amino group to KMB, forming L-methionine (Yang and Hoffman, 1984).

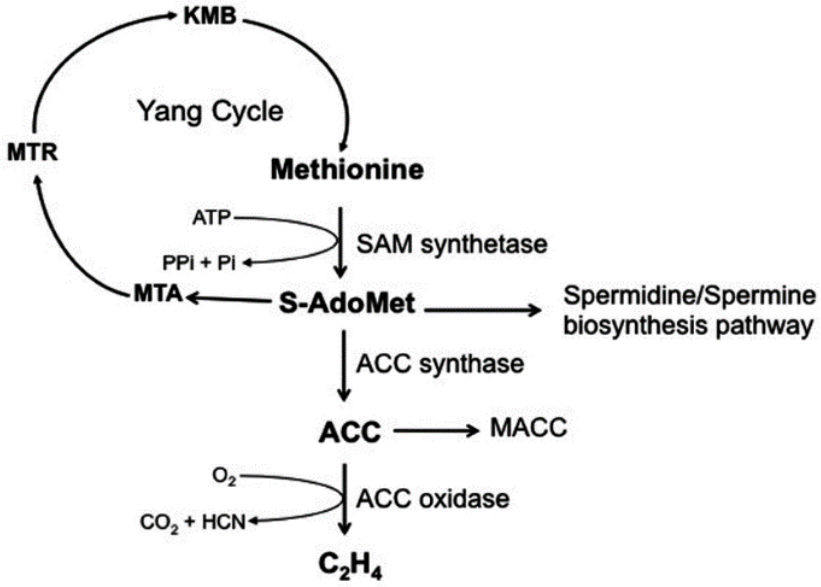

Figure 2.2 The Yang cycle, adapted from (Arc et al., 2013)

2.4. Effects of ethylene on fruits and vegetables

As fruits and vegetables ripen, they undergo changes that enhance their taste, texture, and colour, making them more appealing to consumers (Pech et al., 2012). These changes include the accumulation of pigments leading to colour changes, improvement in sensory qualities through the conversion of sugars to carbohydrates, which enhances aroma, and the breakdown of the cell wall resulting in softening (Sisler and Yang, 1984). A complex network of genes coordinates these changes (Liu et al., 2015). Fruits are categorized into climacteric and non-climacteric types, distinguished by an increase in ethylene production and respiration

during ripening (Mcmurchie et al., 1972). Climacteric fruits, such as apples, tomatoes, and avocados, undergo an ethylene-dependent ripening process (Sisler and Yang, 1984), whereas non-climacteric fruits like citrus, grapes, and strawberries do not rely on ethylene for ripening, though their ripening can be influenced by external ethylene (Pech et al., 2012).
Ethylene production increases exponentially once ripening begins, highlighting the critical role of its regulation (Oetiker and Yang, 1995). Ethylene's effects can be either beneficial or detrimental, depending on exposure levels. Excessive ethylene exposure may trigger senescence and over-ripening, diminishing quality and storage viability, thus contributing to post-harvest losses (Saltveit, 1999).

Table 2.1 Beneficial and detrimental effects of ethylene on the quality of fruits and vegetables, adapted from (Saltveit, 1999)

Beneficial effects of ethylene	**Detrimental effects of ethylene**
Promotes colour development in fruits.	Accelerates senescence.
Stimulates ripening of climacteric fruit.	Stimulates chlorophyll degradation.
Promotes de-greening of citrus.	Enhances excessive softening of fruits.
Stimulates dehiscence in nuts.	Stimulates sprouting of potato.
Alters sex expression in cucurbitaceae.	Promotes abscission of leaves and flowers.
Promotes flowering in bromeliaceae (e.g. pineapple).	Promotes discoloration (e.g. browning).

2.5. Sensitivity of fruit and vegetables to ethylene

As much as ethylene is required for fruit ripening, the primary objective in industry is delaying the effects ethylene has on fruits and vegetables to prolong storage life. Ethylene concentrations as low as 0.001 ppm could initiate ripening (Wills, 2015). However, this is highly dependent on fruit and vegetable sensitivity to ethylene (Table 2.2) and the extent of exposure.

Table 2.2 Ethylene production and sensitivity of different commodities, adapted from (Martínez-Romero et al., 2007)

Commodity	Ethylene production	Ethylene sensitivity
Climacteric fruit		
Apple, Kiwifruit, Pear, Cherimoya	***	*** (0.03-0.1 $\mu L/L$)
Avocado, Cantataloupe melon, Pasion Fruit	***	** (> 0.4 $\mu L/L$)
Apricot, Banana, Mango	**	*** (0.03-0.1 $\mu L/L$)
Nectarine, Papaya, Peach, Plum, Tomato	**	** (> 0.4 $\mu L/L$)
Vegetables and non-climacteric fruit		
Broccoli, Brussel sprouts, Cabbage, Carrot	*	*** (0.01-0.02 $\mu L/L$)
Cauliflower, Cucumber, Lettuce, Persimmon	*	***
Potato, Spinach, Strawberry	*	***
Asparagus, Bean, Celery, Citrus, Eggplant	*	*** (0.04-0.2 $\mu L/L$)
Artichoke, Berries, Cherry, Grape, Pineapple	*	** (> 0.2 $\mu L/L$)
Pepper	*	*

$*$ low, $**$ medium, and $***$ high ethylene production or sensitivity

2.6. Current ethylene management strategies

2.6.1. Chemical methods

2.6.1.1. Inhibition of ethylene biosynthesis

Aminoethoxyvinylglycine hydrochloride (AVG HCl), a naturally occurring non-protein compound, is used to temporarily halt ethylene biosynthesis by inhibiting the production of ACC synthase. (Venburg et al., 2008). Research by Brackmann and Waclawovsky (2001), Yildiz et al. (2012), Batur and Çetinbaş (2017), and Kim et al. (2004) has shown that pre-harvest treatments with AVG effectively suppress ethylene production, decrease pre-harvest fruit drop, and delay ripening in climacteric fruits like apples, pears, and peaches. Despite its ability to retard ethylene production, AVG does not affect ethylene sensitivity, leaving plants treated with AVG susceptible to exogenous ethylene (Venburg et al., 2008). A notable drawback of AVG is its inhibition of tryptophan aminotransferase, an enzyme that shares the pyridoxal-phosphate pathway with ACC synthase (Schaller and Binder, 2017).

2.6.1.2. Blocking of ethylene action at the receptor level

1-Methylcyclopropene (1-MCP) is a volatile, non-toxic gas used as an effective ethylene inhibitor (Watkins, 2006). It competes for ethylene receptor sites with an affinity ten times greater than ethylene, blocking ethylene's action and further biosynthesis (Sisler and Serek, 1997; Blankenship and Dole, 2003). This competitive interaction protects climacteric fruits from both endogenous and exogenous ethylene, delaying ripening and extending shelf life. Studies on bananas by Jiang et al. (1999), on plums by Khan and Singh (2007), on apples by Fan et al. (1999), and avocados by Feng et al. (2000) have demonstrated the efficacy of 1-MCP in delaying fruit ripening through suppressed ethylene production. However, it is important to note that discontinuing its use can lead to various disorders, injuries (Blankenship and Dole, 2003), indicating the need for a method to remove ethylene from storage atmospheres without complications.

2.6.2. Physical and biological methods

2.6.2.1. Activated carbon

Activated carbon has been used as an ethylene adsorbent since the late 1950s. It is characterized by a porous structure of enclosed carbon spaces. The selection of raw materials for producing activated carbon considers factors like ease of activation, accessibility, cost-effectiveness, minimal inorganic content, and low degradation during storage (Martínez-Romero et al., 2007). Activated carbon is available in various forms granular, powdered, or fiber. Granular activated carbon (GAC) is preferred for its traits like natural regeneration and adaptability. Studies by Bailén et al. (2007) and Martínez-Romero et al. (2007) found that GAC efficiently adsorbs ethylene and that its capacity is further enhanced when infused with a palladium (Pd) catalyst. The author further reported on the use of GAC-Pd in removing ethylene in tomato storage led to a notable decrease in ethylene accumulation, maintaining the quality of tomatoes. As much as activated carbon effectively removes ethylene in fruit storage it quickly saturates, requiring costly and impractical frequent regeneration or replacement, and creates environmental waste management challenges upon disposal (Pathak and Mahajan, 2017).

2.6.2.2. Zeolite

Zeolites, as described by (Coloma et al., 2014), are hydrated crystalline aluminosilicates constituting of tetrahedral SiO_4 and AlO_4 units in their framework structure. The inherent negative charge within zeolite frameworks necessitates the introduction of alkali or alkali-earth metals to balance the charge (Coloma et al., 2014). Zeolites are recognized for their eco-

friendly nature, high cation exchange capacity, and excellent thermal stability, rendering them ideal absorbers ((Rashed and Palanisamy, 2018).

In recent times, zeolites have garnered significant attention as ethylene adsorbers. Numerous studies, including those by removal Terry et al. (2007); Tzeng et al. (2019); de Bruijn et al. (2020), have explored the potential of zeolites in ethylene removal. However, it's noteworthy that while adsorbers are effective in eliminating ethylene, they tend to saturate quickly, necessitating frequent removal. Moreover, their suitability for large storage areas is limited (Pathak et al., 2017).

2.6.2.3. Biofilters

A biofilter utilizes immobilized microorganisms to degrade ethylene, with the microorganisms held in place as ethylene flows through a filtering material containing porous substances like compost, soil, or peat, where diffusion into the biofilm triggered(Cabrera et al., 2011).

The porous substance not only supplies nutrients to the microorganisms but also provides a surface for cell attachment (Cabrera et al., 2011). Moghadam et al. (2015) demonstrated the application of a bacterial biofilter for ethylene removal in banana storage. After seven days, it was observed that the quality of bananas in the control group had deteriorated while bananas subjected to the biofilter substrate had maintained their quality (Moghadam et al., 2015). Despite being a cost-effective ethylene removal method, biofilters have drawbacks including being a time-consuming process, requiring a large surface area, and being sensitive to environmental conditions (Cabrera et al., 2011).

2.6.2.4. Thermal catalytic oxidation

Thermal catalytic oxidation involves exposing fruits and vegetables to an oxidizing atmosphere at elevated temperatures (Pathak and Mahajan, 2017). Early investigations such as the large-scale trial by Blidi et al. (1993) in an 1800 m^3 storage reactor for Golden Delicious apples, demonstrated its potential. Using three different catalysts at relatively mild temperatures (100–120 °C), the authors reported 90–100% degradation of ethylene. Remarkably, even after 134 days of storage, apple quality was largely retained.

Despite this impressive efficacy, the method has significant shortcomings. The equipment is capital-intensive, energy demands are high, and ongoing maintenance adds to operational costs. Moreover, the process may generate secondary pollutants such as nitrogen oxides and carbon monoxide, raising environmental concerns (Pathak and Mahajan, 2017) .These factors limit its practical adoption in the fruit industry.

2.6.2.5. Potassium permanganate

Potassium permanganate ($KMnO_4$) has been utilized for more than five decades in food packaging as a chemical oxidiser converting ethylene into carbon dioxide and water (Silva et al., 2009). Its effectiveness in slowing ripening has been documented across several climacteric fruits, including apples (Knee and Hatfield, 1981), bananas (Santosa, Widodo and Kholidi, 2013), papaya (Wills & Warton, 2004).

Despite its proven success in ethylene removal, potassium permanganate has notable limitations. Wills & Warton (2004) observed that its efficiency falls sharply under high relative humidity which in storage environments often exceeds 90%. The compound also saturates quickly, making it viable mainly for short-term storage. Frequent replacement adds cost and complexity (Pathak and Mahajan, 2017).

2.6.2.6. Ozone

The use of ozone dates back to 1840, initially as a disinfectant in drinking water, and it has since found application in horticulture for ethylene removal (Aafia, 2018). As a naturally occurring oxidising gas, ozone reacts readily with ethylene. Skog & Chu (2001) reported successful reductions in ethylene across a range of produce such as broccoli, cucumbers, mushrooms, apples, and pears leading to an extension of shelf life. Nevertheless, ozone poses both safety and quality challenges. At concentrations above 4 ppm, it is toxic to humans and can damage plant tissues. Occupational Safety and Health Administration (OSHA), guidelines restrict occupational exposure to 0.1 ppm over eight hours (Suslow, 2004).This narrow safety margin complicates its practical use in commercial fruit.

2.6.2.7. Air ventilation

Ventilation is among the simplest and least costly approaches to ethylene management. By frequently replacing internal air with fresh external air, the internal concentration of ethylene can be diluted (Pathak and Mahajan, 2017). Its success, however, depends on the quality of the external air supply, which may vary substantially by location and season. For this reason, ventilation alone is rarely sufficient but can serve as a supportive measure.

2.6.3. Advanced oxidation processes

2.6.3.1. Photocatalytic oxidation

Photocatalytic oxidation (PCO) has emerged as an efficient and cost-effective technique that can be applied at low temperature and pressure conditions (Lin et al., 2013). When a semiconductor catalyst is illuminated with UV light, electron–hole pairs form and react with

surface oxygen, generating reactive oxygen species (ROS) such as superoxide anions (Pathak and Mahajan, 2017). In the presence of moisture, hydroxyl radicals are also produced. Together, these species attack ethylene molecules and promote oxidation (Pathak et al., 2017). While promising, PCO suffers from several drawbacks. Catalyst deactivation occurs as intermediate products accumulate on the surface, and recombination of electron–hole pairs reduces efficiency. Elevated humidity further complicates performance, since water and ethylene compete for adsorption sites on the catalyst (Pathak et al., 2017).

2.6.3.2. VUV photolysis

VUV photolysis has recently drawn significant attention as a practical method for degrading pollutants, including ethylene. Unlike chemical oxidants it avoids additive use and associated waste disposal issues. Short-wavelength UV radiation (100–200 nm) drives photodissociation. In this process, pollutant molecules absorb photons and are broken down into simpler and less harmful products, such as carbon dioxide and water (Huang et al., 2011).The major advantage is the absence of external chemicals, which lowers costs and minimises secondary waste (Cuerda-Correa et al., 2020). Moreover, VUV is effective against extending its application to wastewater (Kutschera et al., 2009; Schulze-Hennings et al., 2016; Giri *et al.*, 2014) and air purification (Huang et al., 2011; Huang et al., 2014; Xie et al., 2023 ; Kang, Xi and Hu, 2018). Recent work has begun applying this technology to ethylene control in fruit storage, with promising results. However, the use of high-energy UV light presents operational challenges, as VUV light sources are expensive and require careful management to maintain stable performance.

2.6.3.3. Applications of VUV photolysis

2.6.3.3.1. Wastewater treatment

Vacuum ultraviolet (VUV) photolysis has become a significant innovation in wastewater treatment showing high efficiency in degrading a wide spectrum of pollutants. Giri et al. (2014) demonstrated that VUV outperformed conventional UVC photolysis in breaking down pharmaceutical residues achieving higher degradation rates. Similar findings were reported by Carlson et al. (2015), who observed faster removal of pharmaceutical compounds under VUV irradiation. They attributed the improvement to the molecules stronger absorption and higher quantum yields at VUV wavelengths.

Further evidence of the potential of VUV technology was provided by Schulze-Hennings et al. (2016), using a 193 nm excimer lamp achieved successful elimination of micropollutants such as diclofenac and sulfamethoxazole. Likewise, Kutschera et al. (2009) showed that VUV

photolysis could effectively degrade particularly resistant compounds like geosmin and 2-methylisoborneol which often evade conventional treatment methods. Collectively, these studies suggest that VUV has both broad applicability and unique advantages over established photolytic approaches.

2.6.3.3.2. Air purification

VUV photolysis has also attracted interest for air purification, where it generally outperforms conventional methods in removing volatile organic compounds (VOCs), odours,and pathogens without generating the harmful by-products often associated with chemical oxidants. Sun et al. (2023) observed that removal efficiency decreases at higher initial pollutant concentrations, a trend attributed to the limited availability of reactive oxygen species (ROS). Building on this, Xie et al. (2018) demonstrated that coupling VUV with wet scrubbing significantly enhanced toluene removal, pointing to the potential of hybrid systems. Kang et al. (2018) further explored the mechanistic aspects of photolysis and photooxidation under 185/254 nm irradiation, noting that secondary pollutants can form under certain conditions. Furthermore, Huang et al. (2016) offered a broad review of VUV-based processes, underscoring the central role of hydroxyl radicals and ozone in driving pollutant degradation. Collectively, these studies illustrate both the promise of VUV for air treatment and the need to carefully balance operational conditions to avoid unintended by-products.

2.6.3.4. Fruit storage

Following its successful application in wastewater treatment and air purification, vacuum ultraviolet (VUV) photolysis has gained attention as a potential method for ethylene control in fruit storage. Several studies have evaluated its performance under different conditions, pointing to promising outcomes for extending postharvest freshness.

Pathak et al. (2017) investigated the efficacy of a VUV photolysis reactor utilizing the Box-Behnken design to optimize crucial operational parameters such as flow rate, initial ethylene concentration, and UV lamp power. They reported that the highest removal efficiency, approximately 76%, occurred at 5 ppm initial concentration, 9 W lamp power and a flow rate of 0.5 L/min. Flow rate emerged as the dominant factor with lower flow rates generally enhancing removal when combined with higher lamp power and ethylene concentration. The optimized reactor was later tested in short-term storage trials with apples and kiwifruit, where it successfully lowered ethylene accumulation, producing firmer kiwifruit compared with controls.

In a subsequent study, Pathak et al. (2019b) compared VUV photolysis with photocatalytic oxidation (PCO). Their findings demonstrated a stark contrast: VUV reduced ethylene by 84.8% under storage conditions, whereas PCO achieved only 14.9%. During an eight-day trial with apples, ethylene declined from 70 µL/L to 2.6 µL/L under VUV treatment. They also noted that oxygen concentration modulated both processes, while high humidity impeded PCO but actually enhanced VUV's performance.

A broader review by Mabusela et al. (2022) emphasized VUV's dual advantage of oxidizing ethylene to harmless by-products while simultaneously inactivating surface microbes. Compared with traditional methods such as PCO, VUV consistently provided higher ethylene removal rates and offered the added benefit of pathogen reduction. The review also highlighted that oxygen enrichment generally improved VUV efficiency, although environmental factors such as temperature and humidity strongly influenced outcomes.

More recently, Mabusela et al. (2023) benchmarked VUV against potassium permanganate, a widely used commercial adsorbent. In mixed-fruit storage, VUV reduced ethylene by 86.9% compared with only 25.4% for potassium permanganate. However, direct exposure experiments revealed a trade-off. Although VUV suppressed respiration and ethylene production in apples at 10 °C, over 21 days, it also caused noticeable skin damage and discoloration, underscoring the need for controlled application strategies.

Collectively, the literature points to three process variables of primary importance: flow rate, initial ethylene concentration, and UV lamp power. Storage conditions, particularly relative humidity and oxygen concentration, further influence performance. For this study, the analysis will focus specifically on initial concentration, lamp power, and humidity.

UV lamp power serves as another influential factor in the degradation of ethylene. Increasing lamp output raises photon flux, which accelerates ethylene degradation. Pathak et al. (2017a), for example, observed that raising lamp power from 3 to 9 W at a flow rate below 1 L/min increased ethylene removal from less than 12 ppm to more than 14 ppm, highlighting the direct relationship between intensity and removal efficiency.

2.6.3.5. Initial ethylene concentration

Several authors have explored the impact of the initial ethylene concentration on ethylene degradation. In a study by Pathak, Caleb, Rauh, et al. (2017a), it was observed that an increase in the initial ethylene concentration from 2 to 12 ppm led to an increase in the absolute amount of ethylene removed, while the percentage of ethylene removed decreased (from 82%

to 50%). Another study by Huang et al. (2014) investigated the degradation of benzene and reported a decrease in the percentage of benzene removed, dropping from 48% to 14% with an increase in the initial concentration of benzene from 25 to 200 ppm. This trend suggests that at lower initial concentrations, reactive oxygen species are abundant (ROS), leading to efficient oxidation. However, as the initial concentration rises, ROS becomes limited, resulting in a reduction in the percentage of removal.

2.6.3.6. Relative humidity

The increase in relative humidity (RH) promotes the formation of hydroxyl radicals and other reactive oxygen species which play a key role in accelerating the oxidation of ethylene Findings from a study by Huang et al. (2014) revealed that benzene removal efficiency was initially 12.5% at 0% RH but tripled to 37.9% at 50% highlighting the significant impact of relative humidity. Pathak et al. (2019) evaluated reaction rates using half-time measurements, where a smaller half-time corresponds to faster oxidation. When both relative humidity and oxygen concentration were increased to (84.9 ± 6%) and (20.8 ± 0.08%), respectively, a smaller half-time was achieved. Thus, high RH and oxygen concentration prove advantageous, leading to a faster reaction.

2.6.3.7. Kinetics of VUV photolysis

The kinetics of VUV photolysis are critical for evaluating its efficiency and effectiveness as an advanced oxidation process. Kinetic studies quantify the rate at which ethylene degrades under VUV irradiation while also examining how key variables such as initial ethylene concentration, UV light intensity, and humidity affect these rates.

A study by Mabusela et al. (2023) provided valuable insights into the kinetics of ethylene degradation by VUV photolysis in mixed-fruit storage environments. Using a VUV photolysis reactor, they examined degradation behaviour at different initial ethylene concentrations. Kinetic modelling showed that the reaction followed first-order kinetics with rate constants determined from changes in ethylene concentration over time.

The experiments revealed an interesting trend: increasing the initial ethylene concentration improved the degradation rate. This was attributed to the greater availability of ethylene molecules interacting with the reactive species generated during photolysis, which in turn accelerated the oxidation process.

For example, the rate constant increased sharply when the initial ethylene concentration was raised from 7 mg/kg to 55 mg/kg. Beyond this point, however, further increasing the

concentration to 67 mg/kg caused both the percentage removal and the rate constant to decline. This suggests the presence of an optimal concentration threshold for VUV photolysis.

The reduction in efficiency at higher concentrations was attributed to a saturation effect, where the number of available photons became insufficient to sustain effective degradation across the elevated pollutant load. This finding highlights the practical limits of the system and emphasises the importance of optimising process variables to maintain high removal efficiencies under different operating conditions.

The Box-Behnken Design (BBD) is a type of experimental design used in the response surface methodology (RSM) that provides a quadratic model for the response variable without involving full factorial designs (Rao and Kumar, 2012). The design is efficient in estimating the first and second-order terms necessary for creating a full quadratic model with fewer runs than required by other experimental designs like the central composite design (CCD) (Rao and Kumar, 2012). This aspect is particularly valuable in complex, resource-intensive settings such as VUV photolysis, where experimental runs can be costly and time-consuming. In the context of VUV photolysis, the Box-Behnken design has been utilized to determine key optimal operating conditions that influence the degradation efficiency. Key parameters often include VUV lamp intensity, humidity, flow rate, and the initial concentration of the pollutants (Pathak et al., 2017).

A study by Pathak et al. (2017) demonstrated the application of BBD in VUV photolysis. BBD was utilized to optimize the removal of ethylene in fresh produce storage using VUV photolysis. The study focused on three process variables: flow rate, initial ethylene concentration, and UV lamp power. The application of BBD allowed for the determination of optimal conditions that increased the ethylene removal efficiency. It was noted that a reduction in flow rate combined with an increase in lamp power and initial ethylene concentration significantly improved ethylene removal. This approach was validated in practical applications, significantly reducing ethylene levels in storage environments for apples and kiwifruits, which is crucial for prolonging the storage life and maintaining the quality of fresh produce.

Im et al. (2013) also utilized the Box-Behnken design to optimize the photolysis of diclofenac, a common pharmaceutical compound. In the study four variables were varied: intensity, Fe(III) concentration, NO_3^- concentration, and humic acid. BBD analysis revealed that humic acid significantly inhibited the photolytic process, whereas other factors exerted a positive influence. The design facilitated the efficient identification of optimal conditions that achieved nearly 95% removal of diclofenac under specified parameters. This method demonstrated

significant interactions and provided a high predictive capability with an adjusted R^2 value of 0.981, proving the model's accuracy and effectiveness in optimizing the VUV photolysis process.

Additionally, Yang et al. (2023) also used the BBD to explore the degradation of Orange IV in nitrite-containing wastewater under UV light. The authors' design explored three factors: initial dye concentration, light intensity, and nitrite concentration. The results highlighted that higher light intensities and nitrite concentrations significantly enhanced the degradation rate. From the BBD analysis, detailed contour and surface plots were generated, which clearly illustrated the interactions between these variables. These plots indicated that an increase in light intensity and nitrite concentration significantly enhanced the degradation rate of Orange IV. The optimal degradation efficiency was achieved at a light intensity of 32 W, a nitrite concentration of 12.91 mM, and a neutral pH of 7. Under these conditions, the degradation rate of Orange IV reached approximately 79.5%.

Furthermore, the application of BBD in VUV photolysis goes beyond simply optimizing degradation parameters. It also contributes to the understanding of the underlying photolytic mechanisms. The results of studies by Yang et al. (2023), Pathak et al. (2017), and Im et al. (2013) used detailed contour and surface plots generated from BBD analysis to effectively illustrate the interaction effects among the tested variables. These plots provided both a visual and statistical representation of how each variable and its combinations influenced degradation efficiency. Particularly, the contour plots were instrumental in identifying the optimal conditions that maximize degradation efficiency, clearly indicating the regions of highest response within the experimental range.

2.6.3.8. Apples

Apples are renowned for their abundance in antioxidants, vitamins, and minerals, as well as their exceptional carbohydrate content (Asale et al., 2021). Apples are consumed globally due to their numerous health benefits, such as a decreased likelihood of contracting cardiovascular conditions, respiratory conditions, and some forms of cancer (Amao, 2018). In 2019, apples were among the most cultivated deciduous fruits in South Africa, comprising almost 46% of deciduous produce (DAFF, 2019). Apples are considered as an important fruit due to their contribution to the agricultural economy of the country. Apples accounted for an R6.1 billion portion of the total gross value of deciduous fruits (R18.2 billion) throughout the 2017/2018 growing season (DAFF, 2019). In the Southern Hemisphere, Chile is the largest apple exporter, followed by South Africa (HORTGRO, 2019). As shown in Table 2.3, the South

African apple growing region is mainly found in the Western Cape (Groenland, Ceres, Villiersdorp) and Eastern Cape (Langkloof East).

Table 2.3 Apple Production Areas in South Africa, adapted from (HORTGRO, 2019)

Region	Number of Trees	Area (HA)
Ceres	11 281 266	7 549
Groenland	10 372 174	7 139
Villiersdorp/Vyeboom	5 338 771	4 141
Langkloof East	3 914 601	3 155
Langkloof West	1 660 632	1 253
Free State	811 048	534
Pikeberg	458 947	313
Klein Karoo	373 776	312
Mpumalanga	285 939	203
Boland	386 886	157
Northern Provinces	71 078	65
Worcester	107 459	64
Wolseley/Tulbagh	30 363	22
Eastern Cape	3 739	15
Berg River	14 258	9
Total	35 110 937	24 930

According to Midgley (2016), 43% of apples that are produced annually are exported, suggesting that the apple industry is primarily fuelled by exports. Given the vast supply chains utilised to transport apples to distant consumer markets, it is imperative to maintain the quality and freshness of the produce throughout the process of transportation. The quality of fruit can be adversely affected by the lengthy transit times and fluctuations in storage conditions, leading to a decline in its market value and shelf life. Therefore, it is imperative to develop and optimise effective post-harvest treatments and storage techniques to ensure that exported apples arrive in the best possible condition, thereby preserving their nutritional value, texture, and freshness. The significance of the emphasis on freshness extends beyond the fulfilment of consumer standards; it also contributes to the global competitiveness of apple-producing regions. Within this context, it is imperative to assess the holdups that apples encounter during transportation. The transit periods of apples intended for international markets may exceed a month, and they may remain in shipping containers for several weeks, depending on the destination (Tru-Cape, 2021). During this period, apples are subjected to a fluctuation in

storage parameters such as temperature, humidity, and accumulation of ethylene gas, all of which may accelerate the process of ripening as well as deterioration. The longer travel durations pose significant challenges to preserving the quality of apples throughout the process of transportation.

On the contrary, apples destined for local markets have substantially shorter travel durations, usually reducing the need for long-term storage under controlled circumstances. Nevertheless, regardless of the local area, apples need to be preserved in an optimal condition to satisfy the requirements of consumers for high-quality food.
In addition, apples are typically harvested during the autumn season, although supply and demand extend throughout the entirety of the year, with a storage period of 3-5 months (Domoto, 2008). Therefore, it requires the use of effective storage methods that can maintain the quality of apples for prolonged durations, even after the harvesting period has passed.

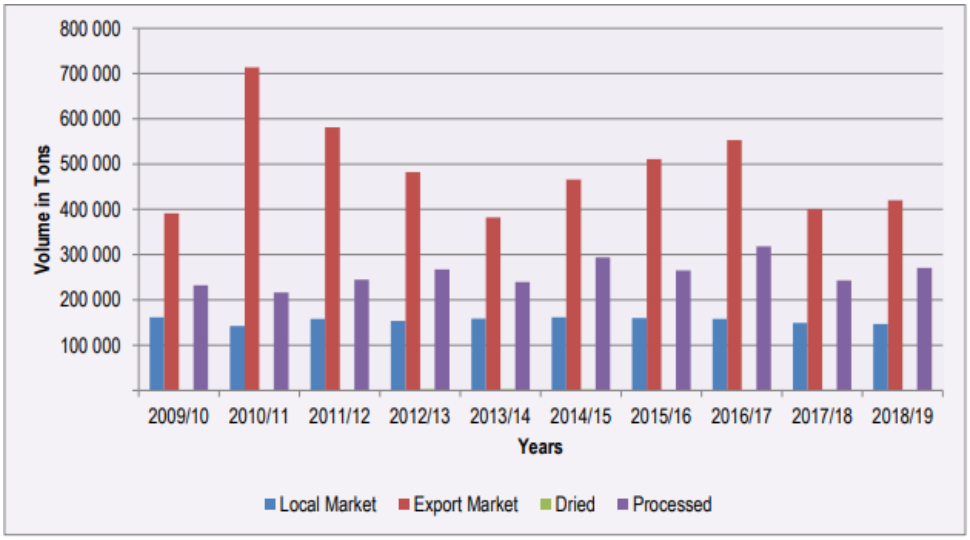

Figure 2.3 Apple crop distribution, 2009/10 – 2018/19, adapted from (DAFF, 2019)

2.6.3.9. Physiochemical Quality Parameters of apples

2.6.3.9.1. Weight loss

Apples consist of 80-85% water (Link et al., 2004), and the primary cause of apple mass loss is the transpiration of this water into the surrounding environment, resulting in an overall reduction in weight. The rate of this loss is significantly influenced by both the storage temperature of the fruit and the relative humidity of the storage atmosphere (Wills et al., 1972). According to (Nistor et al., 2011), apples should be stored at a relative humidity ranging from 90-95%. Failure to maintain these humidity levels may result in dehydration and shrivelling of

the apples. When humidity levels fall below 90%, all mass loss is attributed to transpired water (Maguire et al., 2000). This reduction in water content subsequently leads to shrivelling, browning, and a diminished fruit texture (Lufu et al., 2020).

In contrast, a high relative humidity (>95%) may result in the development of a mealy texture (Tu et al., 2000). De Smedt et al. (1998) investigated mealiness in three different apple cultivars: '*Jonagold*', '*Cox's Orange Pippin',* and '*Boskoop*'. The author induced mealiness by storing the apples at 20 ℃ and 95 % RH for a period depending on the cultivar. The study revealed distinct differences in mealiness among cultivars, with *Cox's Orange Pippin'* and '*Boskoop*' exhibiting a more rapid development of a mealy texture compared to '*Braeburn*', '*Jonagold*', and '*Granny Smith*'. Tu et al. (2000) similarly identified a mealy texture in apples subjected to 95% RH and 20 ℃, linking it to low tensile strength and an increase in cell separation during simulated shelf storage.

It is therefore crucial to maintain the water content of the surrounding environment as closely aligned as possible with the water content of the product. Hence, it is crucial to store fruit under carefully regulated conditions, typically within the range of 90-95% (Lufu et al., 2020).

2.6.3.10. Changes in fruit colour

When consumers select apples, their very first judgment is often visual; colour strongly dictates initial appeal and buying decisions (Wang et al., 2020). Beyond simple aesthetics, colour creates an expectation of flavour and ripeness, and it can even influence appetite. For this reason, skin colour is tightly linked to both market value and maturity assessment at harvest.

In most apple cultivars, immature fruit appears distinctly green. As ripening progresses, this hue fades and is gradually replaced by shades of red or yellow, depending on the variety. The shift results from the degradation of chlorophyll and the parallel synthesis of pigments such as anthocyanins (Whale and Singh, 2007). Importantly, colour development is not driven by ripening alone. Orchard conditions, particularly pre-harvest temperatures, harvest timing, and the local ethylene environment, all play a decisive role.

Ethylene, in particular, has been shown to trigger anthocyanin accumulation by regulating enzymatic pathways. Faragher and Brohier (1984) reported that it promotes pigment formation by inhibiting phenylalanine ammonia-lyase (PAL), a rate-limiting enzyme in anthocyanin biosynthesis. This mechanistic insight highlights how physiological cues and environmental factors converge to produce the visual traits most valued by consumers.

2.6.3.11. Firmness

Fruit texture remains one of the most decisive attributes of apple quality, with firmness commonly regarded as the most reliable single indicator (Saei et al., 2011). Consumers typically associate firm fruit with freshness and high quality, whereas a noticeable loss of firmness is often interpreted as a sign of deterioration. This decline not only shortens shelf life but also complicates marketing, since softer apples attract lower consumer preference and, in turn, influence pricing and turnover dynamics (Harker et al., 2008).

Firmness also shapes the sensory profile of apples. Crispness, juiciness, and resistance to mealiness are all enhanced in fruit that maintains higher firmness levels (Abbott, Watada, and Massie, 2022). From a logistical perspective, firmer apples are less vulnerable to bruising and mechanical damage, making them advantageous for early harvest and for withstanding the stresses of post-harvest handling and transportation (Zhang et al., 2015). Farcuh (2023) suggested that apples intended for long-term storage (over three months) should ideally have a firmness of 6.80 kg. Conversely, apples designated for short-term storage (1-2 months) should exhibit a firmness within the range of 5.8-6.8 kg.

Furthermore, DeEll et al. (2001) proposed that apples with a firmness below 4.5 kg are typically rejected by consumers, establishing this as the minimum acceptable firmness level. Salas et al. (2011) conducted experiments on Golden Delicious apples treated with AVG, and a significant 41% decrease in firmness was observed at the end of the storage period compared to the initial firmness value. Similarly, Mabusela et al. (2023) reported a 16% drop in firmness over a 21-day storage period for 'Fuji' apples treated with VUV photolysis. The author hypothesized that the loss of firmness may be attributed to cell wall deterioration induced by VUV radiation.

2.6.3.12. Total soluble acids and titratable acidity

Total Soluble Solids (TSS) describe the pool of dissolved compounds within fruit cells encompassing sugars, organic acids, phenolics, pigments, proteins, minerals, and certain vitamins (Little and Holmes, 2000; Magwaza and Opara, 2015). In apples, the accumulation of TSS is closely tied to ripening physiology. Starch reserves are mobilized and broken down, and they are converted into simple sugars, which steadily raise the Brix value (Farcuh, 2023). By the later stages of maturity, sucrose, fructose, glucose, and sorbitol dominate the soluble fraction, reflecting the biochemical shift from storage to sweetness (Yang et al., 2021). In practical terms, this makes TSS a widely used proxy for perceived sweetness and overall fruit palatability (Hoehn et al., 2003).

Hoehn et al. (2003) further provided a sensory benchmark for 'Golden Delicious' apples, noting that a minimum TSS of 12 ºBrix is generally required to achieve acceptable eating quality. Brix, in this context, functions as a standardized measure of sugar concentration and is routinely employed by growers and postharvest technologists to guide harvest timing and storage decisions (Magwaza and Opara, 2015).

Alongside sweetness, acidity strongly influences apple flavour. Titratable acidity, expressed through the characteristic sourness of the fruit, arises primarily from malic acid which accounts for roughly 90% of the total organic acid content in apples (Mezey and Mezeyová, 2018). Smaller contributions come from citric, tartaric, and quinic acids, along with mineral acids that together establish the balance between sweetness and tartness (Mignard et al., 2022). These organic acids play crucial roles in respiratory processes and exhibit a decline in concentration as the apples undergo the ripening process (Han et al, 2023).

Jha et al. (2012) investigated the physio-chemical quality parameters of apple fruit over a 28-day period. The research revealed a decrease in the acidity of apples from 0.161 g 100 mL^{-1} to 0.079 g 100 mL^{-1} during the study period. This reduction was attributed to the use of malic acid to aid the ongoing respiration of the fruit, which continues after harvest and ultimately contributes to the ripening process (Ackermann et al., 1992). As starch content decreases and sugar increases, the acidity of most fruits tends to decrease. (Ahmad et al., 2021) reported similar findings, where the acidity of the tested apples decreased from 0.163 to 0.081 during the storage period.

2.6.4. Summary of significance of literature study and Research Gaps

Ethylene plays a central role in the ripening of fruits, a fact that is now widely acknowledged in both agricultural and horticultural research. Earlier work treated it simply as one of many by-products of plant physiology but later discoveries demonstrated its regulatory power. This recognition fundamentally altered how post-harvest handling is approached especially in the management of climacteric fruits.

Research progress has produced a wide toolbox for controlling ethylene and by extension fruit quality after harvest. Chemical inhibitors such as aminoethoxyvinylglycine (AVG) and 1-methylcyclopropene (1-MCP) are now routinely tested in storage facilities. Parallel to this, absorption methods ranging from activated carbon to zeolite-based systems and even biofilters have been developed to physically remove ethylene from the storage atmosphere.

In recent years, interest has also shifted to more experimental approaches, including photocatalytic oxidation (PCO) and vacuum ultraviolet (VUV) photolysis. These newer techniques are often promoted for their potential sustainability benefits, though their industrial uptake remains limited.

Although the technical progress is clear, what is missing is an equally rigorous evaluation of cost and feasibility. Few studies have quantified whether these methods are economically viable at commercial scale. A thorough techno-economic assessment could therefore provide much-needed guidance on cost-effectiveness, scalability, and practical deployment. For growers, distributors, and engineers, such evidence would be invaluable in deciding which strategies to adopt. Filling this research gap would not only improve decision-making but could also strengthen profitability and sustainability across storage and distribution systems.

CHAPTER 3

3. THEORY

3.1. Introduction

This chapter outlines the theoretical foundations of vacuum ultraviolet (VUV) photolysis with a focus on its role in ethylene degradation. The discussion begins with the interaction of VUV radiation and organic molecules highlighting how photon absorption excites electrons and disrupts chemical bonds ultimately producing simpler compounds. Particular attention is given to ethylene where VUV exposure generates reactive oxygen species that drive oxidation pathways and accelerate degradation.

Beyond the reaction chemistry, the chapter also considers the advantages of VUV photolysis relative to conventional ethylene control methods. Its operation without added chemicals, capacity for energy-efficient performance, and effectiveness across diverse environmental conditions make it a compelling alternative. To improve system efficiency, optimization tools such as response surface methodology (RSM) and design of experiments (DOE) are introduced, offering strategies to fine-tune operating parameters.

Additionally, heat transfer correlations including those based on dimensionless numbers such as Nusselt, Peclet, and Stanton are highlighted for their role in capturing convective and radiative effects within the reactor. Such theoretical models are critical for understanding reactor-scale performance and extrapolating laboratory observations to industrial systems.

3.2. VUV photolysis of ethylene

VUV photolysis is governed by the principles of photochemistry. Radiation in the vacuum ultraviolet range (140–200 nm) carries sufficient energy to be absorbed by organic molecules, promoting electrons to excited states and destabilizing covalent bonds (Gonzalez et al., 2004). This process, termed photodissociation, initiates the breakdown of complex molecules into simpler, less reactive intermediates (Gao, 2021). In the case of ethylene, these reactions produce short-lived radicals and reactive oxygen species that play a central role in its oxidative degradation.

The mechanism begins when ethylene or other volatile organic compounds absorb VUV photons. The energy absorbed is sufficient to overcome the bond dissociation energy of chemical bonds within the molecules. This results in the formation of free radicals and other reactive intermediates, which subsequently undergo a series of spontaneous and rapid chemical reactions leading to the formation of stable, non-volatile end products such as carbon

dioxide and water. This reaction is highly efficient due to the high energy carried by VUV photons, which can initiate multiple degradation pathways simultaneously.

When ethylene is exposed to VUV radiation at 185 nm, it undergoes oxidation, this process is primarily facilitated by a UV lamp (Figure 3.1). This lamp primarily emits UV light at 254 nm, with a smaller proportion (6%) emitted at 185 nm (Alapi and Dombi, 2007). Upon UV irradiation, energetic photons capable of dissociating water and oxygen into reactive oxygen species (ROS) are produced.

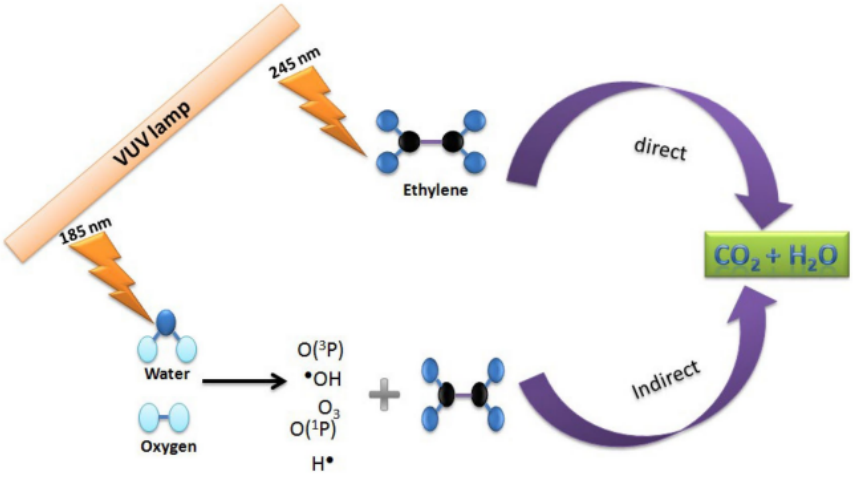

Figure 3.1 Schematic diagram showing mechanism of VUV when degrading ethylene, adapted from (Mabusela et al., 2022)

Both water and oxygen can absorb VUV radiation in both their gaseous and aqueous states. However, in its aqueous form, water is less effective at absorbing VUV radiation due to the limited penetration depth of light, leading to rapid decay or deactivation of radicals. In contrast, photolysis in the gas phase is more effective because the photons have a much greater penetration depth (Ye et al., 2013). Below 190 nm, water in the gaseous phase absorption increases, leading to the dissociation of water molecules and the subsequent production of hydroxyl radicals (·OH) and hydrogen atoms equation (3-1) (Jakob et al., 1993). On the other hand, oxygen undergoes dissociation to form reactive oxygen species (ROS) such as ozone (O_3), atomic oxygen $O(^1D)$, $O(^3P)$ as shown in equation (3-2 to 3-5) (Huang et al., 2016). The ozone generated by photolysis is also broken down (Eqn.6) (Ye et al., 2013). The ROS and hydroxyl radicals formed readily oxidise ethylene into carbon dioxide and water as shown in equation (3-7) and (3-8)

Photolysis of water

$$H_2O \xrightarrow{h\nu\ (185\ nm)} H + \cdot OH \qquad (3\text{-}1)$$

Photolysis of molecular oxygen

$$O_2 \xrightarrow{hv\ (185\ nm)} O(^1D) + O(^3P) \quad (3\text{-}2)$$

Relaxation of singlet Oxygen

$$O(^1D) + M \rightarrow O(^3P + M) \quad (\text{M}=O_2\ or\ N_2) \quad (3\text{-}3)$$

Ozone formation

$$O(^3P) + O_2 + M \rightarrow O_3 + M \quad (3\text{-}4)$$

Water and singlet oxygen formation

$$O(^1D) + H_2O \rightarrow 2 \cdot OH \quad (3\text{-}5)$$

Ozone photolysis

$$O_3 \xrightarrow{hv\ (185+245\ nm)} O_2 + O(^1D) \quad (3\text{-}6)$$

Reactive oxygen species reactions

$$O(^1D) + C_2H_4 \rightarrow CO_2 + H_2O \quad (3\text{-}7$$

Hydroxyl radical reactions

$$OH + C_2H_4 \rightarrow CO_2 + H_2O \quad (3\text{-}8)$$

3.2.1. Justification for using VUV photolysis for ethylene degradation

3.2.1.1. Chemical free process

VUV photolysis effectively degrades ethylene without the use of added chemicals, oxidants, or catalysts, thereby eliminating the potential for secondary pollution (Xie et al., 2023; Sun et al., 2023)

3.2.1.2. Energy and cost efficiency

The process operates at ambient temperatures and does not require high temperatures like catalytic oxidation, making it more energy-efficient and suitable for a temperature-sensitive environment (Blidi et al., 1993)

3.2.1.3. Less waste residues

Ethylene is permanently removed from the storage environment, unlike oxidisers, adsorbers, and absorbers that temporarily trap ethylene on the surface but do not destroy it, requiring periodic replacement or regeneration of adsorbent materials, creating a waste problem (Pathak and Mahajan, 2017).

3.2.1.4. Ease of integration and scalability

Unlike many other ethylene removal methods, VUV photolysis can be integrated into existing storage facilities with relative ease. Alternative technologies often demand larger equipment or extensive modifications to infrastructure, which complicates implementation and increases costs.

3.2.1.5. Effectiveness in diverse conditions

VUV photolysis demonstrates high effectiveness across a broad range of operating conditions and does not rely on narrow temperature windows for optimal performance. By contrast, methods such as air ventilation are strongly influenced by environmental factors, including temperature and humidity, which can restrict their reliability in certain storage environments (Pathak et al., 2017).

3.3. Optimisation studies

3.3.1. Response surface methodology

Response Surface Methodology (RSM) is a set of mathematical and statistical tools designed for experimental design and optimization (Morshedi and Akbarian, 2014). It enables researchers to model complex processes, analyse variable interactions, and identify conditions that yield optimal responses. The concept was first formalized by Box & Wilson, (1951) , who introduced the use of first-order polynomials as an approximation tool for locating optimal operating points. Building on this foundation, several theoretical developments were made, optimal design theory was proposed by Kiefer & Wolfowitz (1952) and later expanded by Chernoff (1953) and Myers et al. (1989) followed by the introduction of second-order response surface by Box & Draper (1963) and subsequently higher-order rotatable designs (fourth- and fifth-order). These advances collectively established RSM as a flexible and widely applicable framework for process optimization. The procedural steps used in this study are summarised in Figure 3.2.

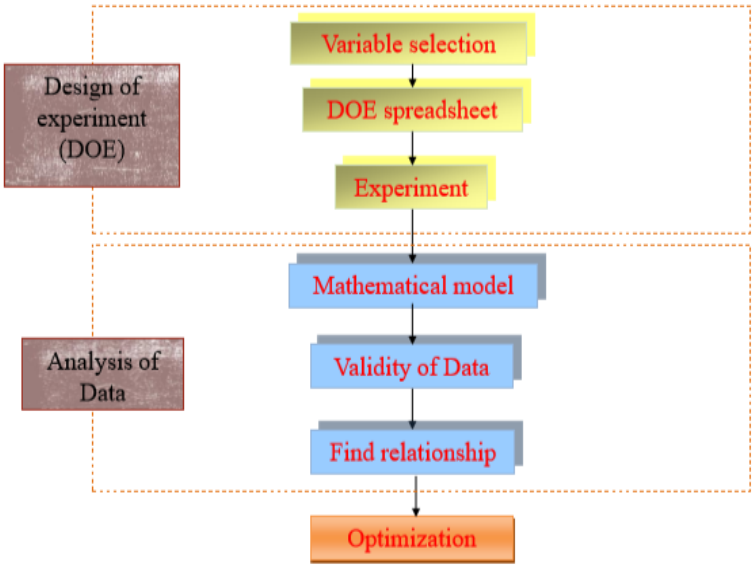

Figure 3.2 Response surface methodology flow

3.3.2. Design of experiment (DOE)

The systematic process of conducting experiments with careful consideration to examine output data using statistical methods is referred to as the Design of Experiments (DOE) (Durakovic, 2017). Understanding the intricacies of DOE requires a grasp of the fundamental workings of an experiment. As noted by Jones (2002), an experiment encompasses a series of tests, referred to as runs, where adjustments are made to input variables with the aim of discerning the underlying causes for alterations in the output response. Within DOE, deliberate modifications are made to input variables to investigate their impact on the output response. This approach enables the analysis of results, ultimately leading to meaningful conclusions. DOE was initially pioneered by Ronald Fischer in the early 1920s. Its evolution has revolutionized the methodology of conducting experiments, shifting from the traditional practice of altering one parameter at a time to concurrently varying multiple parameters, thus establishing a more comprehensive understanding.

3.3.3. Box Behnken Design

Numerous design techniques are available for fitting second-order response surface models, and one widely employed approach is the Box-Behnken (BB) design. This design is a blend of the two-level factorial and incomplete block design methodologies, as introduced by (Box and Behnken, 1960). These designs belong to the category of rotable or nearly rotable second-order designs, and they are instrumental in approximating quadratic models. While they necessitate a higher number of experimental runs for an equivalent number of variables compared to the Central Composite Design (CCD), they are still favoured for their

advantageous design properties. As shown in (Figure 3.3), the BB design comprises a central point and midpoints along the edges (Souza, Dos Santos and Ferreira, 2005). The formula to determine the number of experiments for the BB design is given as follows:

$$N = 2k(k-1) + cp \quad (3\text{-}9)$$

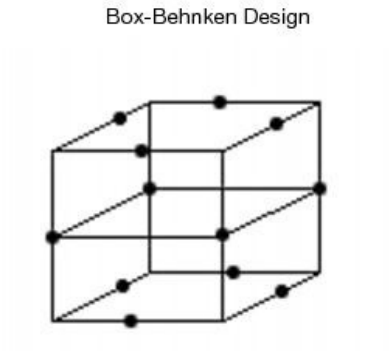

Figure 3.3 Representation of Central Composite design and Box Behnken design

3.3.4. Techno-economic analysis

Techno-economic analysis (TEA) serves as a crucial method for evaluating both the technical feasibility and economic viability of a project, product, or process technology (Leng, 2022). This analysis occurs before engaging in detailed and resource-intensive design and scoping activities (Leng, 2022). Utilizing preliminary feasibility estimates, often in the form of order-of-magnitude or study estimates, TEA relies on less detailed information compared to firm estimates (Turton, 2013). These assessments play a pivotal role in comparative design, assisting in the decision-making process regarding whether to proceed with a proposed project (Peters et al.,2003).

Techno-economic analysis (TEA), grounded in the cost–benefit principle provides a systematic framework for evaluating the economic feasibility of a project. It not only considers cash flows over the full lifetime of the system but also allows researchers to explore different technology scales and applications while benchmarking performance against competing alternatives to highlight opportunities with higher profit potential. In practice TEA follows a structured sequence of evaluations. These typically begin with process design and modelling, proceed through equipment sizing and both capital and operating cost estimation, and culminate in a cash flow analysis that integrates all preceding steps (Chai et al., 2022).

3.3.4.1. Methodologies in TEA

Several methodological approaches are commonly employed within techno-economic analysis (TEA) to capture the economic feasibility of a project, technology or product across

its full life cycle. These tools not only provide financial estimates but also enable a broader evaluation of environmental and operational implications. Among the most widely applied are life cycle analysis, cost–benefit analysis and sensitivity analysis.

3.3.4.1.1. Life Cycle Analysis

Life cycle analysis (LCA) offers a holistic perspective by evaluating both environmental and economic impacts throughout the entire lifespan of a product or process (Turton, 2013). It traces inputs and outputs from raw material acquisition through manufacturing, use, maintenance and eventual disposal or recycling. In the context of TEA, LCA is particularly valuable because it links economic feasibility with sustainability considerations highlighting trade-offs between resource consumption, environmental performance, and cost efficiency.

3.3.4.1.2. Cost Benefit Analysis

Cost–benefit analysis (CBA) provides a structured way to weigh the benefits of a technology or project against its associated costs. The goal is to determine whether the expected returns, monetary or otherwise justify the required investment. By converting both tangible and intangible impacts into a common evaluative framework, CBA equips decision-makers with a clear basis for comparing alternatives and identifying the most economically viable option.

3.3.4.1.3. Sensitivity Analysis

Sensitivity analysis tests the robustness of TEA outcomes by examining how results change when input parameters are varied (Turton, 2013). This approach is essential in contexts where uncertainty is high as it highlights which variables most strongly influence feasibility. By identifying thresholds and ranges of plausible outcomes, sensitivity analysis enables researchers and practitioners to better anticipate risk and refine decision-making under uncertainty.

3.4. Heat transfer on vertical surfaces

Heat transfer refers to the movement of thermal energy from a region of higher temperature to a region of lower temperature (Incropera, 2007). This transfer can occur through three fundamental mechanisms: conduction, convection and radiation. Conduction is the transfer of heat facilitated by molecular interactions between objects in direct contact while radiation is the electromagnetic radiation emission from a surface (Incropera, 2007). Convection, which is emphasized in this work describes the transfer of heat between a solid surface and an adjacent fluid in motion (Incropera, 2007).

In convection the rate of heat transfer depends on the velocity and properties of the fluid, the geometry of the surface and the temperature difference between the surface and surrounding

medium (Dascalaki et al., 1994). To account for these complex interactions the heat transfer co-efficient (h_e) is introduced. As seen in equation (3-10) , the heat transfer co-efficient is a proportionality factor that relates heat flux from a surface to the temperature difference enabling the transfer (Incropera, 2007).

$$q'' = h_e(T_S - T_\infty) \tag{3-10}$$

Where q" is the surface flux, T_s is the surface temperature and T_∞ is the ambient temperature.

Due to thermal resistance at the fluid-solid interface , a temperature variation between the surface and bulk fluid exists resulting in a thermal boundary layer (Incropera, 2007) . Similarly in vicious fluids , a velocity boundary layer develops where the fluid velocity changes from zero at the wall to the free stream velocity (Incropera, 2007). Unlike material properties such as thermal conductivity and viscosity, the heat transfer co-efficient is not a fixed value for a fluid but changes based on the interaction between the fluid, the surface geometry and flow conditions (Hall and Allinson, 2010). Because of its dependence on so many factors all at once , h_e is usually expressed through dimensionless numbers that highlight the interaction of these factors.

3.4.1. Prandtl number

The Prandtl number is a dimensionless parameter that compares the relative thickness of the velocity and thermal boundary layers (Patience, 2017). It is defined as:

$$P_r = \frac{\mu}{\gamma} \tag{3-11}$$

Where γ *is the thermal diffusivity and* μ *is the kinematic viscosity.*

3.4.2. Rayleigh number

In natural convection, fluid motion is driven entirely buoyant forces that arise from variations in density due to temperature (Goldstein and Madanan, 2022). The strength of this buoyancy driven flow is characterized by the Rayleigh number (R_a) which combines effects of buoyancy (through the Grashof number, G_r) and the relative thickness of velocity and thermal boundary layers (through the Prandtl number, P_r) (Zeneli et al., 2020). A high Rayleigh number indicates strong buoyancy forces leading to accelerated fluid motion, a thinner thermal boundary layer, a higher heat transfer co-efficient and a smaller temperature interface difference (Mallya and Haussener, 2021) . Conversely a low Rayleigh number corresponds to weaker buoyancy forces leading slower fluid motion , a thicker thermal boundary layer lower heat transfer and a larger temperature interface difference. It is defined as;

$$N_{Ra} = \frac{\rho g \varphi (T_e - T_\infty) L_e^3}{\gamma \mu} \quad (3\text{-}12)$$

Where φ is the thermal expansion co-efficient; L_e is the characteristic vertical length and g is the gravitational acceleration.

3.4.3. Nusselt number

The heat transfer co-efficient is then expressed in terms of the Nusselt number (N_u), a dimensionless ratio that compares convective to conductive heat transfer across the boundary layer as shown by (Caket et al., 2022). When the Nusselt number is equal to one, conduction dominates and when the Nusselt number is greater than one convection dominates (Roy and Roy, 2020). It is defined as:

$$N_{Nu} = \frac{h_e L}{\kappa} \quad (3\text{-}13)$$

Where k is the thermal conductivity.

3.4.4. Peclet number

In natural convection , the Peclet number (P_e) is the ratio of advective heat transport to diffusive heat transport (Banerjee et al., 2019). When the Peclet number is lesser than one then advection dominates and when the Peclet number is greater than one then diffusion dominates (Blecher, Palmer and Debroy, 2012). It is defined as:

$$N_{Pe} = \frac{\rho u L c_p}{\kappa} \quad (3\text{-}14)$$

3.4.5. Stanton number

The Stanton number expresses the ratio of heat transferred from a surface to the fluid to the thermal capacity of the fluid flow (Taylor et al., 1992). It is defined as:

$$S_t = \frac{h}{\rho c_p U} \quad (3\text{-}15)$$

3.4.6. The Churchill and Chu correlation

The combined effects between the Rayleigh number , Prandtl number and the Nusselt number for natural convection is given by the Churchill and Chu correlation (Churchill and Chu, 1975). For a laminar natural convection over vertical surfaces Churchill & Chu (1975) proposed:

$$N_{st} = \frac{N_{Nu}}{N_{Pe}} = \frac{1}{N_{Pe}}\left[0.68 + \frac{0.67{N_{Ra}}^{1/4}}{\left(1 + \left({}^{0.492}/_{N_{Pr}}\right)^{9/16}\right)^{4/9}}\right] \quad N_{Ra} < 10^9 \tag{3-16}$$

CHAPTER 4

4. METHODLOGY

This chapter outlines the experimental methodology used to address the research objectives presented in Chapter 1. The primary focus is on assessing the economic feasibility of ethylene removal in fruit storage through VUV photolysis for practical application in postharvest management. The experimental approach involves optimizing key process parameters, including initial ethylene concentration, wattage, and relative humidity. These optimized variables were then used as inputs for the techno-economic assessment, which enabled the evaluation of the costs associated with ethylene degradation under VUV treatment
All experiments were conducted in the Chemical Engineering department at Cape Peninsula University, Bellville, Cape Town.

4.1. Experimental set-up

Experiments were conducted using a custom-designed reactor, adapted from the configuration described by Pathak (2019) and Mabusela et al. (2023). The reactor was fabricated from stainless steel and constructed in a cylindrical form with dimensions of 12 cm in diameter and 0.22 cm in height (see figure 4.1). Inlet and outlet ports were positioned at the top and bottom of the reactor. The reactor's lid was made of an acrylic sheet material and had openings to accommodate the electrical fittings of Vacuum Ultraviolet (VUV) lamps, as well as sensors for monitoring temperature and humidity. Three VUV lamps, each with a power input of 3W, were positioned along the central axis of the reactor. The primary emission wavelength of the reactor was observed at 254 nm, with a secondary emission comprising 5-8% of the total output at 185 nm.

Figure 4.1 Experimental setup

4.2. Optimisation studies

4.2.1. Response surface methodology (RSM) optimization tests

A Box-Behnken, response surface methodology (RSM) 3-factor experimental design was prepared using the Design-Expert II Software program. The factors and their upper and lower limits chosen are shown in Table 4.1 below. This input data generated the experimental matrix for optimisation studies.

Table 4.1 Experimental conditions for optimisation studies

Factor	Name	Units	Type	minimum	maximum
A	Initial ethylene concentration	ppm	numeric	5	50
B	Humidity	%	numeric	0	90
C	Wattage	W	numeric	3	9

4.2.2. Experimental procedure

The experimental matrix obtained from the Design-Expert II Software program generated 17 runs in total. All experimental procedures were conducted according to the setup in Figure 4.2 and in a batch mode. Ethylene concentrations were measured at one-minute intervals using the SCS56-ethylene analyser, equipped with both an inlet and outlet pump to facilitate gas recirculation into the reactor, thereby maintaining consistent gas concentrations.

Operational parameters were manually configured within the system. Desired ethylene concentrations were achieved by mixing ethylene from a 100-ppm ethylene standard with synthetic air. Critical to this process was the pre-experimental treatment of synthetic air, which passed through a saturated salt solution prepared 24 hours before experiments or silica gel to achieve the desired humidity level before being mixed with ethylene.

Once the target ethylene and humidity concentrations were obtained, all valves were closed, and UV lamps were switched on based on the desired wattage. Following ethylene degradation in the reactor, the lamps were switched off and the reactor was purged with synthetic air and prepared for the subsequent run.

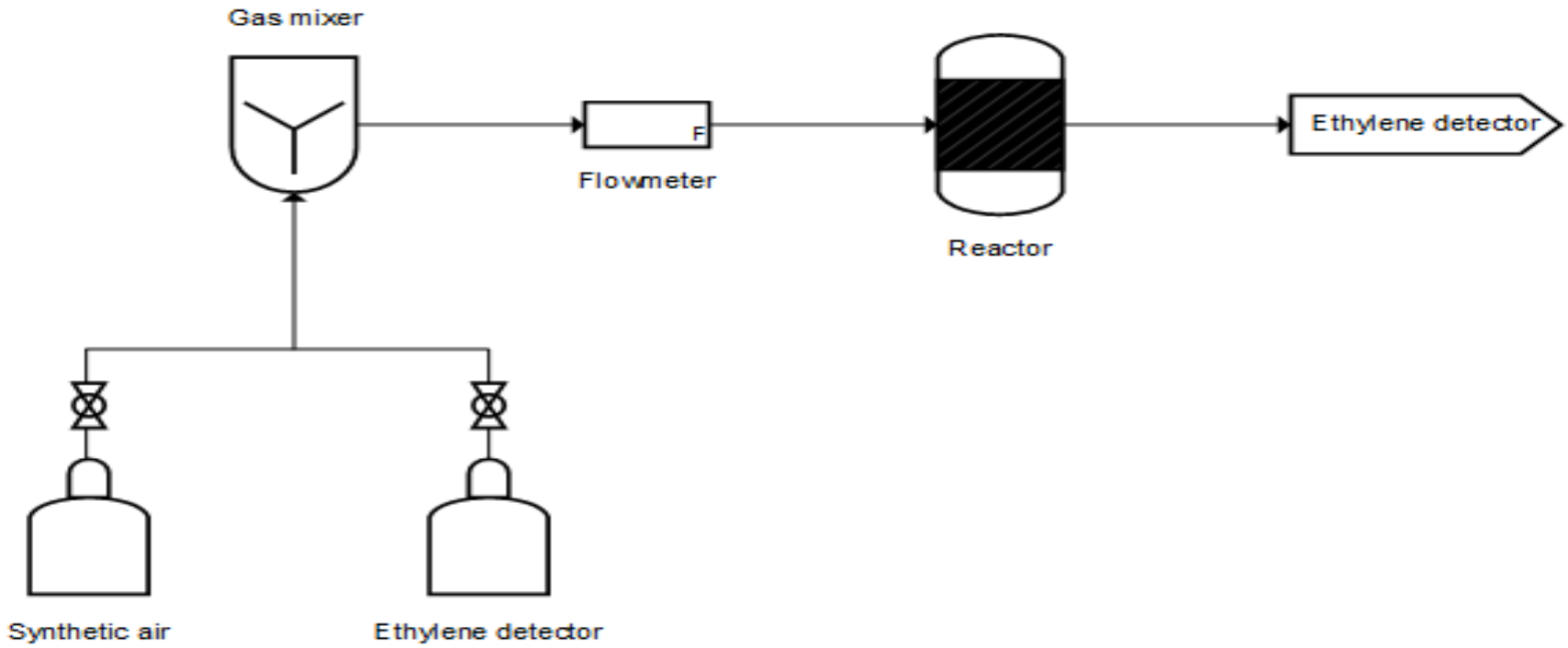

Figure 4.2 PFD of experimental setup

4.3. Techno-economic evaluation

Fresh 'Golden Delicious' apples sourced from the Timberlea Farming Trust farm in Stellenbosch, South Africa, were transported under controlled temperature conditions to the Chemical Engineering Research Lab in Bellville, Cape Town, South Africa. Upon arrival, the fruit samples were sorted to ensure the selection of healthy apples free from bruises or damages.

For the techno-economic evaluation, 23 apples were divided into three treatment groups. The first group contained apples stored in a storage chamber connected to a VUV photolysis reactor for continuous removal of ethylene, as illustrated in Figure 4.4. A pump was used to circulate the air through the reactor and back into the storage chamber. An ozone filter was incorporated to remove residual ozone. A second storage chamber served as a control, containing apples stored without any ethylene removal technique as depicted in Figure 4.5. These experiments were conducted at ambient temperature for a duration of 15 days. A third group of apples were stored in a chamber placed inside a cold room at 10℃.

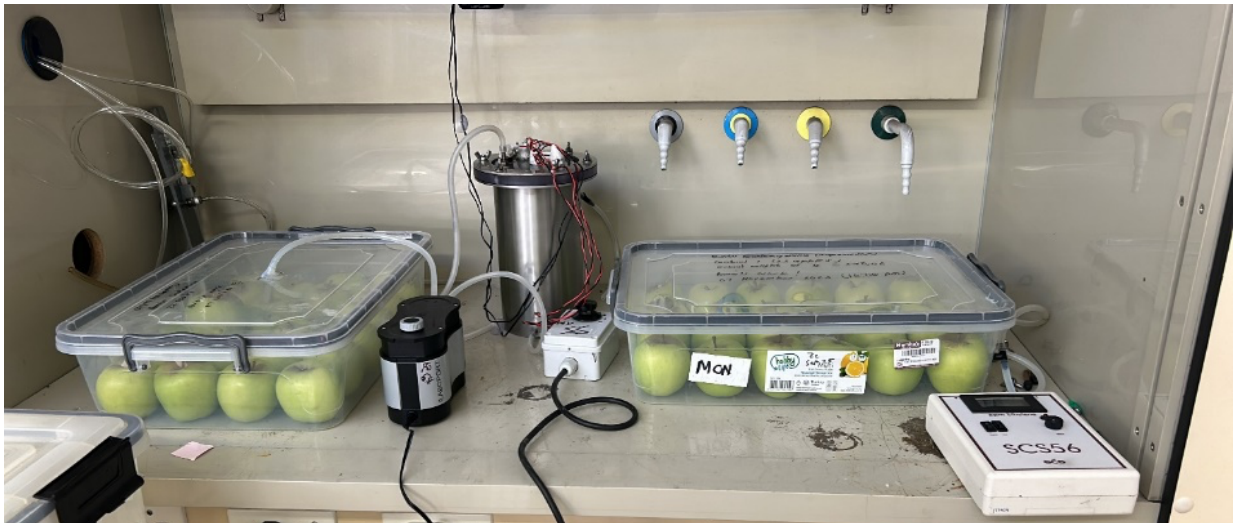

Figure 4.3 Experimental setup for fruit storage experiments

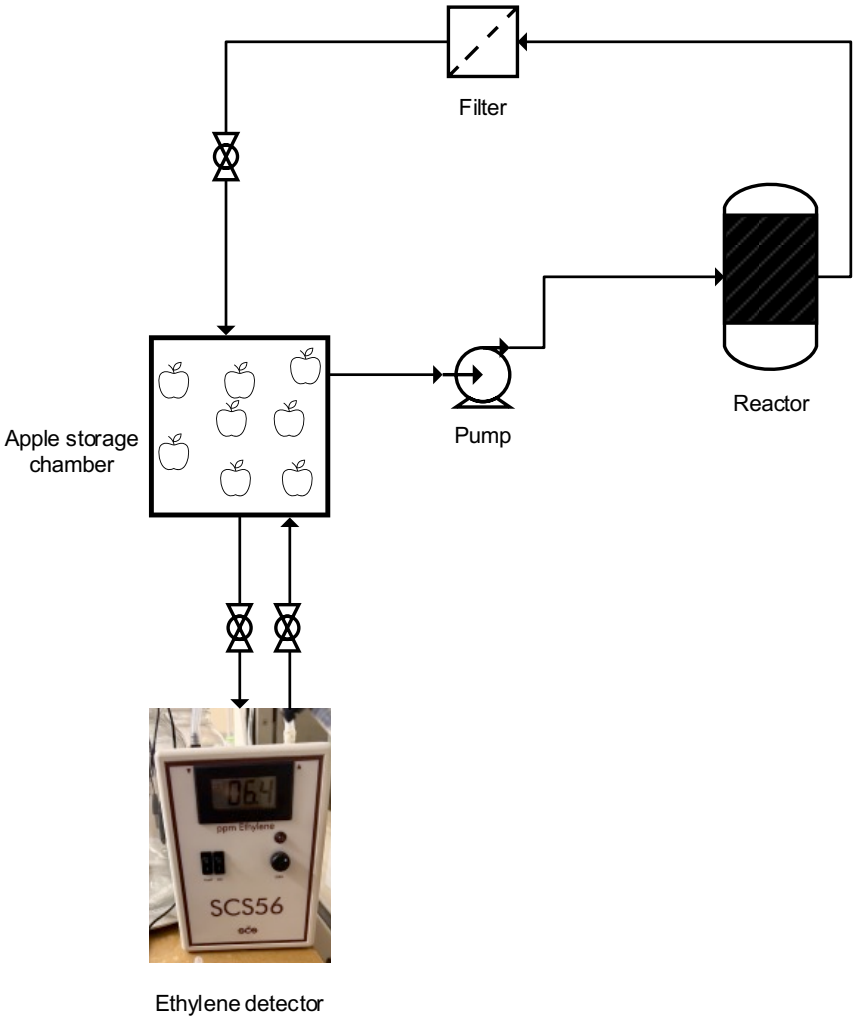

Figure 4.4 Schematic experimental setup for VUV photolysis fruit storage

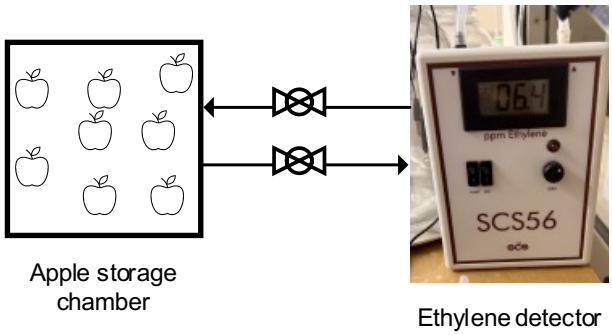

Figure 4.5 Schematic experimental setup for cold storage and control chamber fruit storage

CHAPTER 5

5. RESULTS & DISCUSSION

5.1. Introduction

Vacuum ultraviolet (VUV) photolysis has emerged as a promising advanced oxidation process for the degradation of low-concentration volatile organic compounds such as ethylene, particularly in controlled environments where rapid and residue-free decomposition is critical. However, despite its effectiveness, the practical implementation of VUV photolysis is often constrained by high operational costs. The main contribution to the operational costs is attributed to the sustained power demand of VUV lamps. These lamps consume significant electrical energy over prolonged periods to maintain the required photon flux for effective molecular dissociation. It is therefore important to identify and optimise key reactor parameters that influence both degradation efficiency and energy consumption. This chapter presents a coupled mass and energy balance model for a batch VUV photolysis reactor. The model is further used to develop a parametric optimisation framework aimed at minimising the running costs of a VUV photolysis reactor while maintaining or enhancing its ethylene removal efficiency.

5.2. VUV model development

5.2.1. The VUV reactor

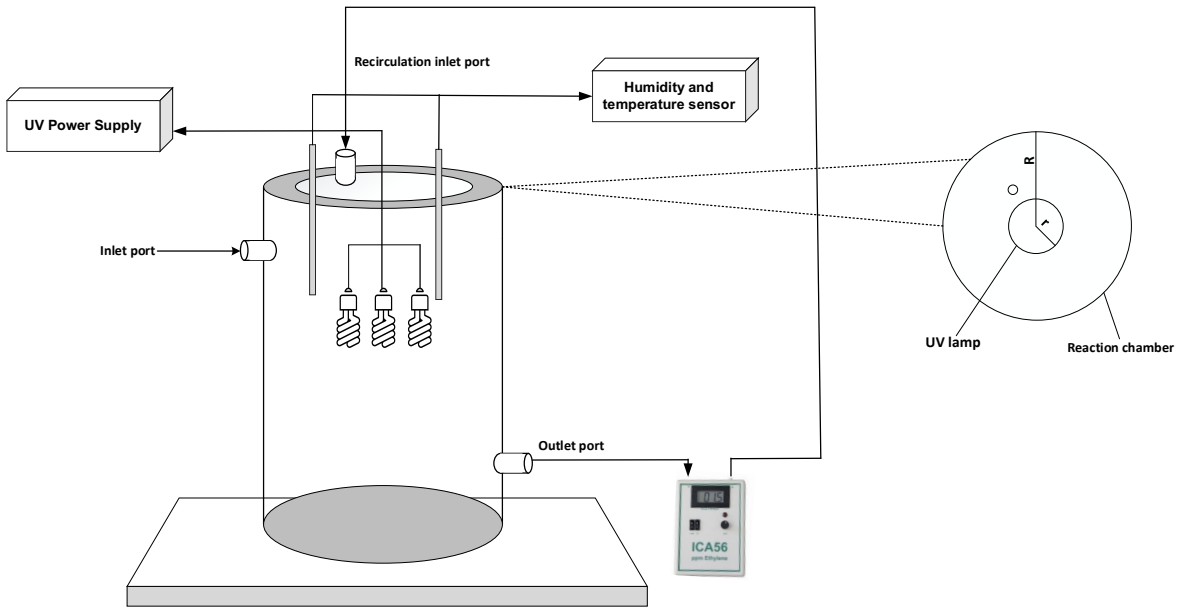

Figure 5.1 A schematic of the VUV photolysis reactor

The model presented in this chapter is applicable to a vacuum ultraviolet photolysis reactor, with UV lamps mounted on the inside of the reactor. The construction of the reactor is illustrated in Figure 5-1. The vacuum ultraviolet (VUV) light source is a low-pressure and medium-pressure mercury lamp with approximately 85% output at 254 nm and 15% output at

185 nm (Kang, Xi and Hu, 2018b; Xu et al., 2019). The reactor is constructed from stainless steel and the lid constructed from borosilicate glass and features openings for VUV lamp fittings and a temperature and humidity sensor.

5.2.2. Model assumptions

The model is based on the following assumptions: (1) the oxidation of ethylene involves two mechanisms, namely the direct mechanism and indirect oxidation. The hydroxyl radicals generated in the indirect oxidation have a very short shelf-life. The photolysis therefore can be assumed to be dominated by direct oxidation; (2) heat loss to the surroundings is negligible; (2) no forced convection, only natural convection and radiation; (3) ideal gas behavior; (4) ethylene-air physical properties are approximated using properties of air, this is due to the low concentrations of ethylene; (5) no significant pressure changes in the reactor.

5.3. Mathematical Formalism

5.3.1. Mass and Energy Balances

The required model seeks to describe the concentration of ethylene in the reactor as a function of time, with the influence of process parameters (e.g. reactor geometry, temperature of lamp, ethylene-air mixture physical properties, etc.). The model will be expressed in terms of ethylene conversion $x_{C_2H_4}$, with the relationship between conversion and concentration given by (Levenspiel, 1999).

$$C_A = C_{A0}\frac{1 - x_A}{1 + \varepsilon_A x_A}\left(\frac{T_0 P}{T P_0}\right) \tag{5-1}$$

For brevity, the subscript *A* has been used in place of C_2H_4. Where C_{A0} is the initial concentration of ethylene; ε_A is the fractional change in volume of the system; T_0 and P_0 are the initial temperature and pressure of the system, respectively. Assuming the oxidation to be dominated by direct oxidation, the fractional change in volume $\varepsilon_A = 0$ since the total moles of reactants is equal to moles of products. A material balance of ethylene inside the batch reactor is therefore given by:

$$\left(C_{A0}\frac{T_0}{T}\right)^{1-n}\frac{dx_A}{dt} = \Pi k_0 e^{-E/RT}(1 - x_A)^n \tag{5-2}$$

where *n* is the order of reaction; k_0 is the pre-exponential factor; *E* is the activation energy of the reaction, *t* is time; and *R* is the universal gas constant. The dimensionless photon flux Π is given by:

$$\Pi = \frac{\lambda \phi \eta I_0}{k_0 hc} \tag{5-3}$$

where λ is the dominant photon wavelength; ϕ is the quantum yield (number of oxidized C_2H_4 molecules per number of photons absorbed); η absorption cross-section; I_0 is the light intensity (W/m^2); h is Planck's constant; and c is the speed of light.

(Mabusela et al., 2024) demonstrated that the reaction follows 1st order kinetics, with respect to concentration, under the operating conditions considered in this study. Equation (5-2) is made dimensionless by introducing the following additional dimensionless variables:

$$\tau = k_0 t;\ \theta = \frac{T}{T_0};\ \psi = \frac{T_e}{T_0};\ \beta = \frac{E}{RT_0} \tag{5-4}$$

Substituting the dimensionless variables in Eq. (5-4) into Eq. (5-2) results in:

$$\frac{dx_A}{d\tau} = \Pi e^{-\beta/\theta}(1 - x_A) \tag{5-5}$$

The energy balance of the VUV reactor is given by:

$$\rho c_p V \frac{dT}{dt} = h_e A_e (T_e - T) + \epsilon \delta A_e (T_e^4 - T^4) + H_{rxn} \cdot r_A \cdot V \tag{5-6}$$

where ρ is the density of the gas mixture; c_p is the specific heat capacity of the gas mixture; V is the volume of the reactor; h_e is the heat transfer coefficient on the external surface of the lamp; A_e is the surface area of the lamp; T_e is the temperature of the lamp; ϵ is the emissivity of the lamp; δ is the Stefan-Boltzmann constant; H_{rxn} is the heat of reaction; and r_A is the rate of reaction. Equation (5-6) is made dimensionless by introducing the following dimensionless variables:

$$N_{st} = \frac{h_e}{\rho c_p}\left(\frac{A_e}{V k_0}\right);\ N_{Bo} = \frac{\epsilon \delta T_0^3}{\rho c_p}\left(\frac{A_e}{V k_0}\right);\ \alpha = \frac{C_{A0} H_{rxn}}{\rho c_p T_0} \tag{5-7}$$

Substituting the dimensionless variables in Eq. (5-7) into Eq. (5-6) gives:

$$\frac{d\theta}{d\tau} = N_{st}(\psi - \theta + N_{Bo}(\psi^4 - \theta^4) + \frac{\alpha \Pi}{\theta}(1 - x_A)e^{-\beta/\theta} \tag{5-8}$$

The dimensionless energy balance of the VUV lamp is given by:

$$\frac{d\psi}{d\tau} = \Gamma_{uv} + \gamma(\psi - \theta) + \sigma(\psi^4 - \theta^4) \tag{5-9}$$

where

$$\Gamma_{uv} = \frac{\Phi}{m_e c_{pe} k_0 T_0};\ \gamma = \frac{h_e A_e}{m_e c_{pe} k_0 T_0};\ \sigma = \frac{\epsilon \delta A_e T_0^3}{m_e c_{pe} k_0} \tag{5-10}$$

where Φ is the power rating of the UV source; m_e is the mass of the lamp; and c_{pe} is the specific heat capacity of the lamp. The input values required to solve Equations. (5-5), (5-8) and (5-9) are listed in Table 5-1, and the dimensionless parameters are listed in Table 5-2.

The Stanton number N_{St} correlation for natural convection adjacent to a vertical lamp, in Equation (8), is given by Churchill and Chu (Popiel, 2008).

$$N_{st} = \frac{N_{Nu}}{N_{Pe}} = \frac{1}{N_{Pe}}\left[0.68 + \frac{0.67{N_{Ra}}^{1/4}}{\left(1 + \left({}^{0.492}/_{N_{Pr}}\right)^{9/16}\right)^{4/9}}\right] \quad N_{Ra} < 10^9 \tag{5-11}$$

where N_{Nu} is the Nusselt number, N_{Pe} is the Peclet number, and N_{Ra} is the Rayleigh number, respectively given by:

$$N_{Nu} = \frac{h_e L}{\kappa};\ N_{Pe} = \frac{\rho u L c_p}{\kappa};\ N_{Ra} = \frac{\rho g \varphi (T_e - T_\infty) L_e^3}{\gamma \mu} \tag{5-12}$$

where φ is the thermal expansion coefficient, γ the thermal diffusivity, κ is the thermal conductivity and g is gravitational acceleration.

Table 5.1 Model input parameter values for the VUV photolysis of ethylene

Description	Parameter	Value	Units
Initial concentration	C_{A0}	51	ppm
Ambient air temperature	T_0	298.15	K
Reactor pressure	P_0	101325	Pa
Reactor length	L	0.22	m
Reactor diameter	D	0.12	m
Lamp length	L_e	0.052	m
Lamp diameter	D_e	0.017	m
Density of gas mixture	ρ	1.184	kg/m^3
Density of lamp	ρ_e	2500	kg/m^3
Heat capacity of gas mixture	c_p	1005	J/kgK
Heat capacity of lamp	c_{pe}	750	J/kgK
Activation energy of reaction	E	19600	J/mol
Heat of reaction	H_{rxn}	30000	J/mol
Pre-exponential factor	k_0	25.00	s^{-1}
Heat transfer coefficient	h_e	30	W/m^{2}K
Power rating of UV lamp	Φ	9	W
UV light intensity	I_0	0.0021	mW/m^2
Absorption cross-section	η	10^{-20}	cm^2
Quantum yield	ϕ	1	-
Lamp emissivity	ϵ	1	-

Table 5.2 Dimensionless parameter values for the model

Dimensionless Group	Parameter
α	1.901 x10^{-4}
β	7.907
γ	5.05 x10^{-7}
σ	7.54 x10^{-6}
Γ_{uv}	5.455 x10^{-5}
N_{st}	0.001125
N_{Bo}	5.64 x10^{-5}
Π	8.06 x10^{-12}

Equations (5-5), (5-8) and (5-9) are not amenable to analytical solutions and require a numerical solver. The equations were solved using the *ode45* numerical solver on MATLAB®.

5.3.2. Parametric cost optimization model

Figure 5-7, which is a solution of Equations (5-5) - (5-9), demonstrates that operating the VUV lamp at Phi (power symbol) = 9W requires a long operating time to reach the final conversion values (tau = 30000). This time is drastically reduced for higher wattage to tau = 25000 (for Phi = 12W) and tau = 15000 (for Phi = 20W), as shown in Figure 5-7 (c). These results immediately present an optimization challenge: what UV lamp power is required to minimize the running costs of electricity while maintaining an acceptable rate of conversion of the ethylene. The objective function for the optimization is therefore:

$$\min_{P} C_{total} = C_{elec}(\Phi) + C_{unreacted}(\Phi) \quad (5\text{-}13)$$

$$C_{elec} = \omega \cdot \Phi \cdot t_{batch} \quad (5\text{-}14)$$

$$C_{unreacted} = \varpi \cdot [1 - x_A(\Phi)] \cdot C_{A0}(ppm) \quad (5\text{-}15)$$

where ω is the unit cost of electricity (R/kWh); ϖ is the cost of unreacted ethylene (R/ppm C_2H_4); $x_A(P)$ is the conversion as a function of lamp power.

Table 5.3 Model input parameter values for Cost Optimisation

Description	Parameter	Value	Units
Unit of electricity	ω	50	R/kWh
Market value of apples (golden delicious, ~200g)	Λ	20.00	R/kg
Spoilage coefficient	k_s	0.00028	ppm^{-1}
Cost of unreacted ethylene	$\varpi = k_s\Lambda$	0.0056	R/ppm C_2H_4
Initial concentration of C_2H_4	C_{A0}	51.0	Ppm

The cost of unreacted ethylene ϖ is obtained by first estimating the spoilage coefficient k_s from the following equation:

$$\frac{M_{spoilage}}{M_{total}} = \frac{[TSS/TA]_{t1} - [TSS/TA]_{t0}}{[TSS/TA]_{t0}} = k_s[C_2H_4] \quad (5\text{-}16)$$

The total soluble solids to titratability acidity ratio (TSS/TA) is a key maturity and quality index for measuring the ripening rate of climacteric fruits. This ratio represents the balance between sweetness derived from total soluble solids (TSS, primarily sugars such as sucrose, fructose, glucose, and sorbitol, along with minor contributions from acids, vitamins, proteins, pigments, phenolics and minerals) and tartness derived from titratable acidity (TA, predominantly malic acid, which accounts for approximately 90% of organic acids in apples) (Magwaza and Opara, 2015; Ma et al., 2018). During ripening, TSS increases due to the enzymatic hydrolysis of starch into sugars, while TA decreases as organic acids especially malic acid, are metabolized during respiration (Lwanami et al., 2024). This shift results in a rising TSS/TA ratio which signals advancing maturity of fruit (Mabusela et al., 2024).

However, an excessively high TSS/TA ratio, often driven by elevated ethylene concentrations, accelerates ripening and can lead to spoilage (Khedr and Al-Khayri, 2023). Spoilage manifest as structural degradation (e.g. mealiness, softening and or shrivelling), increased susceptibly to fungal degradation, enzymatic browning and reduced firmness, all of which diminish shelf life, consumer acceptability and market value (Harker et al., 2008; Abbott, Watada and Massie, 2022). For golden delicious apples, a minimum TSS of 12 °Brix is required for satisfactory eating quality (Magwaza and Opara, 2015).

TSS is measured using a calibrated refractometer to determine the Brix value, which quantifies the percentage of soluble solids in filtered fruit juice extracted from homogenized apple samples. The juice is typically obtained by blending apple flesh, filtering to remove pulp and placing a few drops on the refractometer prism to measure light refraction, which correlates with soluble solids content (Pathak, Caleb, Wegner, et al., 2017). On the other hand, TA is determined by titration, where a known volume of juice is titrated with a standard base by a pH endpoint using an automatic titrator or phenolphthalein as an indicator, The result is expressed as grams of malic acid per 100 mL of juice (Mabusela et al., 2023)
Mabusela et al. (2024) reported a 42% increase in the TSS/TA ratio over 28 days for ‘Fuji’ apples stored under vacuum ultraviolet (VUV) photolysis conditions, with an ethylene generation rate of 6.66 µL/kg·h for apples stored under the same conditions as this study. This translates to a cost of unreacted ethylene of R0.0056/ppm, highlighting the economic implications of ethylene management in storage.

5.4. Results

5.4.1. Validation of PER empirical model

This section presents results of optimization experiments conducted to evaluate ethylene degradation via VUV photolysis. The objective was to maximize ethylene degradation by varying three process parameters: initial ethylene concentration, lamp wattage and relative humidity. Experimental design and statistical analysis was performed using Stat-Ease 360 by employing a Box–Behnken design. The initial ethylene concentration was varied between 5-50 ppm, relative humidity between 0-90 %, and lamp wattage between 3-9W as seen on Table 5.4. The primary aim of this study was to identify the optimal combination of these parameters that achieves the highest ethylene degradation efficiency.

Table 5.4 The factors and levels used in the Box-Behnken design of experiment

Level	Code	Independent Variables		
		X_1: $[C_2H_4]_0$ (ppm)	**X_2: Humidity (%)**	**X_3: Power (W)**
Max. level	+1	50	90	9
Central level	0	27.5	45	6
Min. level	-1	5	0	3

The relationship between the process variables and the response was described using a second-order polynomial model generated in Stat-Ease 360. Due to the difference in the units of the independent variables, a coded approach was used to standardise the range of variables, as shown in Table 5.4 and the experimental combinations are listed in Table 5.5.
In this model, x_1 corresponds to the initial ethylene concentration, x_2 to relative humidity, and x_3 to lamp wattage. Negative coefficients indicate an inhibitory effect on ethylene removal efficiency, meaning that increasing the corresponding factor reduces the percentage of ethylene removed. In contrast, positive coefficients denote a promotive effect, whereby increasing the factor enhances the percentage of ethylene removed.

It is important to note that the model outputs were subject to practical constraints. At the highest lamp power (9W), Design-Expert predicted percent ethylene removal efficiencies greater than 100%. Although such outcomes are statistically valid within the coded model, they are not physically possible. To maintain a realistic interpretation of the results, predicted removals at 9W were therefore capped at 100%.

Table 5.5 Experimental results of the Box-Behnken design for the effect of humidity, lamp wattage and initial C2H4 concentration on the percentage ethylene removal (PER).

Run	Coded variables			Actual C_2H_4 removed (%)	Predicted C_2H_4 removed (%)
	x_1	x_2	x_3		
1	0	+1	-1	13.5	10.55
2	-1	0	+1	100	100
3	+1	+1	0	17.2	20.75
4	-1	-1	0	66	62.45
5	0	0	0	20.6	22.22
6	0	0	0	19.5	22.22
7	+1	-1	0	5.4	9.4
8	+1	0	-1	6.2	5.6
9	-1	0	-1	38	44.95
10	+1	0	+1	18.6	11.65
11	0	-1	-1	9.1	5.7
12	0	+1	+1	55.6	59
13	0	-1	+1	16	18.95
14	0	0	0	21.5	22.22
15	-1	+1	0	100	96
16	0	0	0	29.4	22.22
17	0	0	0	20.1	22.22

The resulting PER estimate from coded data is given by:

$$PER = 22.22 - 32.07x_1 + 11.23x_2 + 15.43x_3 - 5.55x_1x_2 - 12.40x_1x_3 + 8.80x_2x_3 + 21.04x_1^2 + 3.89x_2^2 - 2.56x_3^2 \quad (5\text{-}17)$$

Equation 5.17 reveals that an increase in ethylene concentration results in a decrease in ethylene removal percentage, aligning with existing literature (Huang et al., 2014). Notably, wattage exerts a dominant effect on ethylene removal compared to the other two process variables.

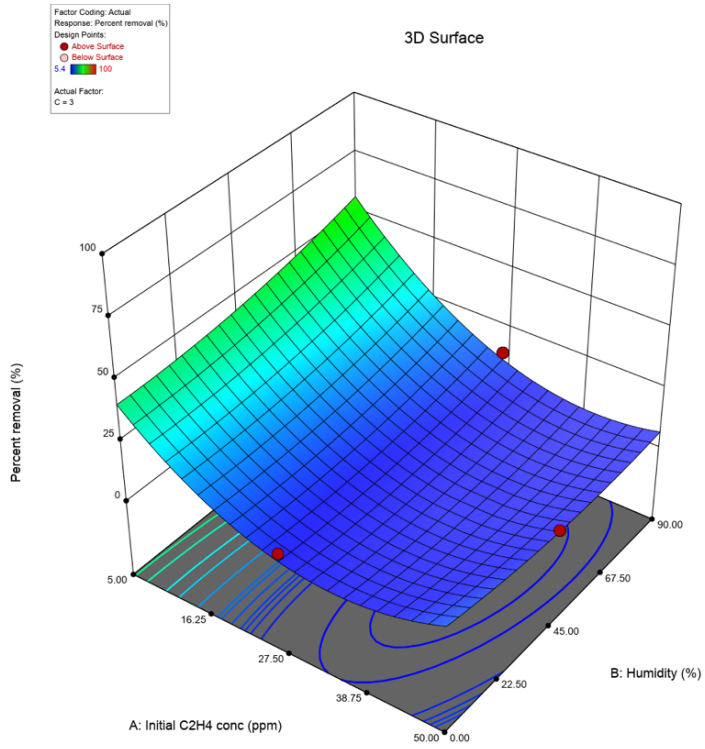

Figure 5.2 Effect of process variables on percentage ethylene removal at 3W

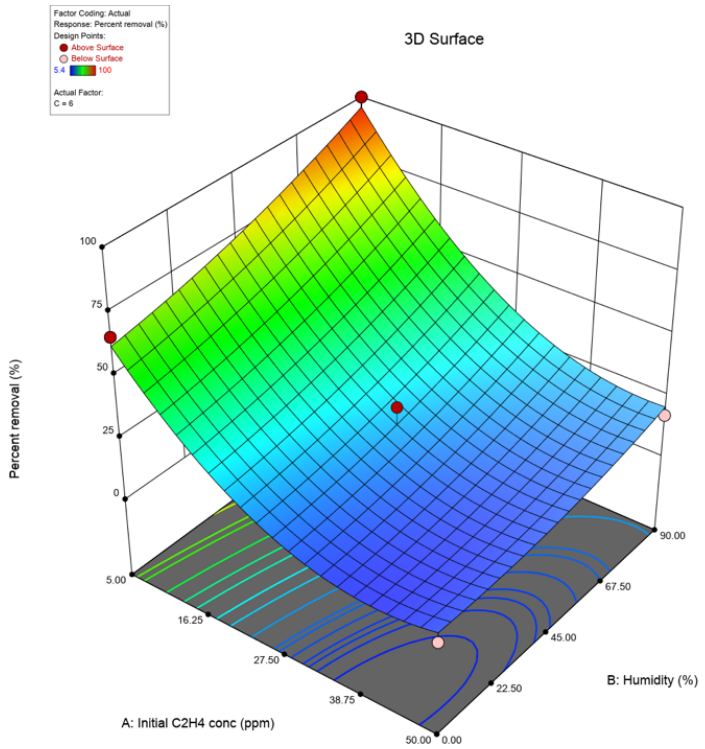

Figure 5.3 Effect of process variables on percentage ethylene removal at 6W

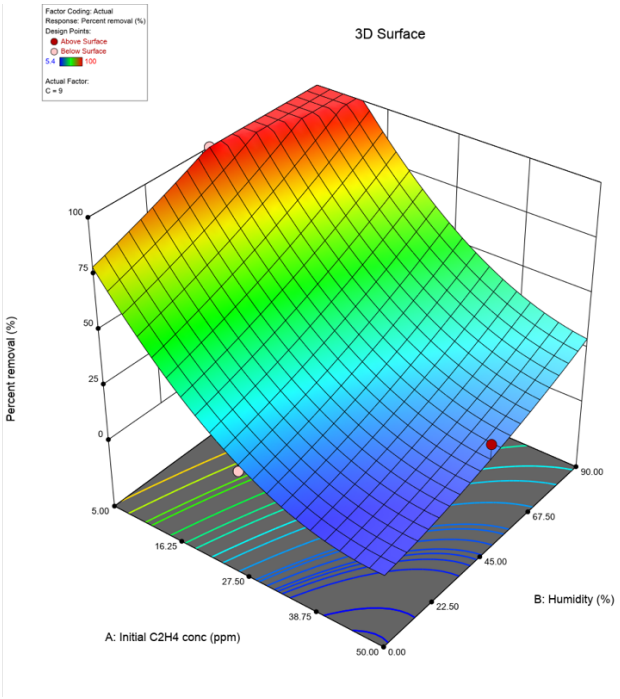

Figure 5.4 Effect of process variables on percentage ethylene removal at 9W

Figures 5-2, 5-3, and 5-4 present the results obtained using 3, 6, and 9 W lamps, across ethylene concentrations ranging from 5 ppm to 50 ppm, and relative humidity (RH) levels between 0 % and 90 %. Across most conditions, a consistent trend is seen, higher lamp power and high humidity lead to higher percentages of ethylene removed. This response is attributed to the increased generation of reactive oxygen species (ROS) and hydroxyl radicals (•OH) under greater photon flux and water vapour availability. These species rapidly breakdown ethylene's C=C bond, initiating oxidation pathways that form carbon dioxide and water (Pathak et al., 2017).

The influence of RH is evident even at low lamp powers. At 5 ppm and 3 W (Figure 5-2), increasing RH from 0 % to 90 % raises removal from ~40 % to ~50 %. At 6 W (Figure 5-3), the same RH change improves removal from ~60 % to >80 %, while at 9 W (Figure 5-4) removal increases from ~80 % to full conversion (100 %). This correlation corresponds with literature showing that water vapour photolysis under VUV light enhances •OH formation, thereby increasing oxidative degradation efficiency (Pathak et al., 2017).

However, a reversal of this behaviour is observed at high ethylene concentrations (50 ppm) and low lamp power (3 W). In this case (Figure 5-2), removal efficiency decreases at high RH. This occurs in a low-photon, high ethylene concentration environment where increasing humidity reduces the available reactive oxygen species.

Creasey et al. (2000) reported that water vapour has a significant absorption cross-section at 185 nm (7.22×10^{-20} cm² molecule^{-1} at 25 °C), meaning it can absorb a portion of the photons emitted at this wavelength before they can initiate photolysis reactions. Because 185 nm radiation is responsible for breaking down O_2 and H_2O to produce key oxidants such as hydroxyl radicals (•OH) and ozone (O_3), this absorption reduces the amount of usable light energy available to drive these processes (Ono et al., 2014).

A study by Huang et al. (2015) revealed that ozone (O_3), though mainly a by-product, can act as a secondary oxidant in ethylene degradation. At 0 % RH, outlet ozone was ~266 ppmv, but dropped to ~100 ppmv at 95 % RH due to enhanced decomposition and photon competition from water vapour. Consequently, ozone's role diminishes under high humidity, with removal dominated by hydroxyl radicals (·OH) and other ROS.

Furthermore, radical production depends on H_2O, O_2, and the lamp's I_{185} and I_{254} ratio, systems with a low I_{185} component are particularly susceptible to RH-induced photon losses (Rowe, Lambe and Brune, 2020).

These results demonstrate that both lamp power and relative humidity are critical determinants of ethylene removal efficiency in VUV photolysis. Higher lamp power and water vapour availability promote ·OH and ROS formation enhancing degradation rates, particularly at low ethylene concentration. However, at high ethylene concentrations and low lamp power, elevated humidity can inhibit removal by competing for 185 nm photons, thereby reducing radical generation.

5.4.2. Validation of the Mass and Energy Balances model

5.4.2.1. Validation of concentration and temperature profiles

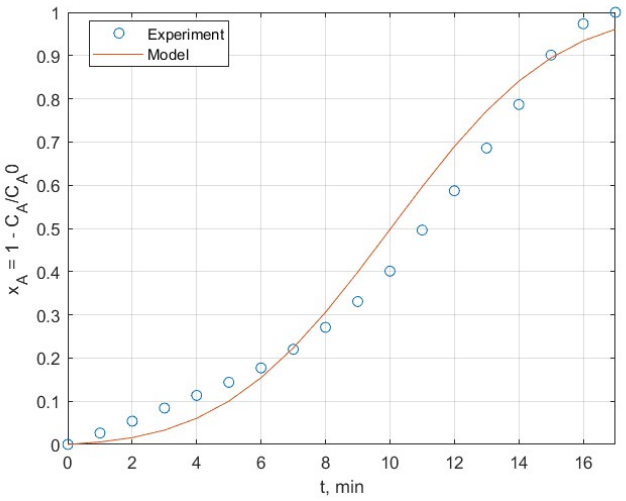

Figure 5.5 Comparison of the theoretical conversion with experimental results (Φ = 9W)

Figure 5-5 is a plot of the experimental conversion results for a 9W VUV lamp, plotted against the theoretical model of Equation (5-5) – (5-9). The correlation coefficient R^2 is related to the root mean square error (*RMSE*) as follows:

$$R^2 = 1 - \frac{n \cdot (RMSE)^2}{(1-n)s_y^2} \tag{5-19}$$

where s_y is the standard deviation of the experimental data. The R^2 and *RMSE* values for the model fit are 0.988 and 0.0572, respectively.

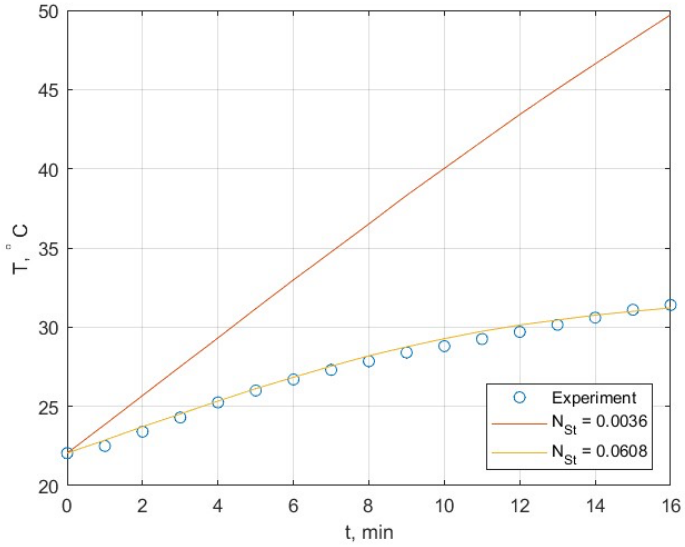

Figure 5.6 Comparison of the theoretical temperature profile with experimental results (Φ= 9W)

In the conversion profile (Figure 5-5), ethylene removal follows a characteristic s-shaped curve, an initial slow phase while radical concentrations build up, a faster mid-phase as radical generation accelerates, and a final plateau as the reactant is depleted. The simulation reproduces both the time to near-complete conversion (16–17 min) and the curve's shape, with only slight deviations in the mid-range (≈10–13 min) that could be due to factors not explicitly modelled, such as local variations in lamp intensity, humidity shifts, or surface interactions.

The temperature profile (Figure 5-6) shows a moderate increase from about 22 °C to 28 °C over 15 minutes, consistent with a process driven primarily by photochemistry rather than thermal effects. The best match is obtained with a Stanton number (N_{st}) of 0.0036, representing natural convection heat transfer; the higher value (0.0608) overestimates heating and does not reflect the experimental setup. Given that the temperature rise is modest, its influence on reaction rate via Arrhenius dependence is minimal, meaning that the observed conversion is governed mainly by photon-initiated chemistry.

The close correspondence between simulated and experimental conversion and temperature profiles indicates that the selected kinetic parameters and heat-transfer assumptions are appropriate. This alignment demonstrates the model's robustness under the tested conditions, with the minor discrepancies likely arising from experimental variability.

5.4.2.2. Sensitivity Analysis (Conversion)

A sensitivity analysis was conducted to evaluate how variations in key model parameters influence ethylene conversion, in a VUV photolysis reactor. Four parameters were investigated: lamp power, activation energy, heat-transfer coefficient, and pre-exponential factor. Each parameter was varied individually while holding all other variables constant, enabling the isolation of its specific impact on reactor performance. Lamp power was adjusted between 6 W and 30 000 W to assess the effect of photon flux on reaction rates and energy consumption. Activation energy was varied from 15 000 to 25 000 J mol^{-1} to determine its influence on kinetic rates. The heat-transfer coefficient was examined across a range of 5 to 30 W m^{-2} K^{-1} to evaluate its role in temperature regulation and conversion efficiency. The pre-exponential factor was altered between 0.10 s^{-1} and 1 min^{-1}. This systematic approach provided a comparative understanding of which parameters most strongly affect process efficiency.

5.4.2.2.1. Power

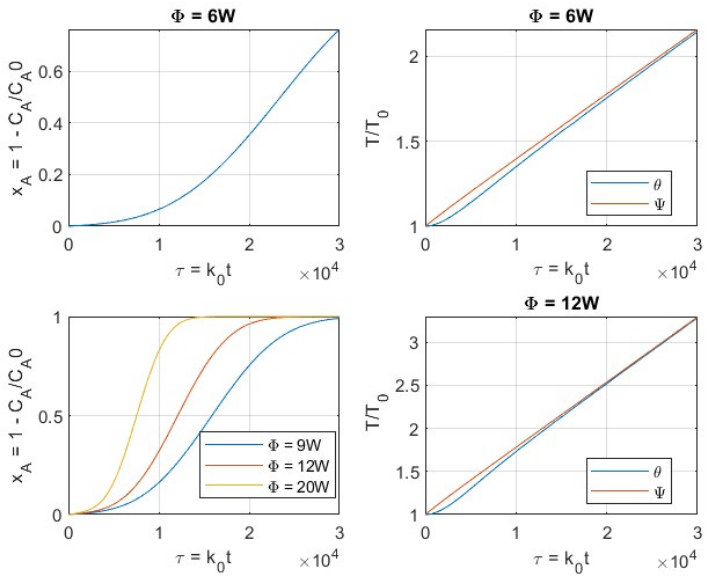

Figure 5.7 Theoretical conversions of ethylene in a VUV photolysis reactor at different lamp power values

The influence of lamp power on ethylene conversion and reactor temperature was evaluated by simulating four input values: 6, 9, 12, and 20 W. In the nondimensional energy balance,

lamp power is represented by the dimensionless parameter, Γ_{uv} directly affecting the heat transfer dynamics of the system. Lamp power controls the photon flux on the reactor and thereby influences the rate of ethylene photodegradation. In the model, increasing the lamp power increases the availability of photons, which increases the rate of reactive oxygen formation thereby accelerates ethylene conversion (Mabusela et al., 2024).

According to Figure 5-7, at a lamp power of 6 W, the model predicted partial conversion, with approximately 80 % of ethylene consumed by 17 minutes. Increasing the lamp power to 9 W leads to near-complete conversion within 7 minutes. Further increases to 12 W and 20 W result in faster complete conversion: 12 W achieves 100 % conversion in approximately 15 minutes, and 20 W requires nearly 3 minutes.

5.4.2.2.2. Activation Energy

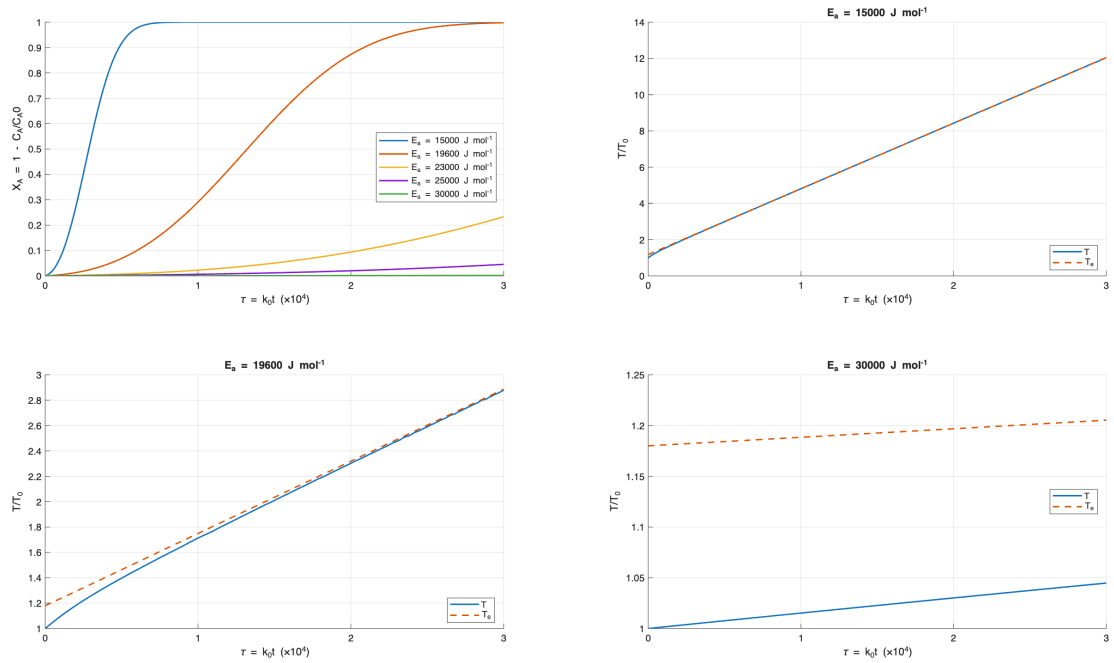

Figure 5.8 Theoretical conversions of ethylene in a VUV photolysis reactor at different activation energy values

Figure 5-8 presents the effect of activation energy on ethylene conversion, with values varied between 15 000 to 30 000 J/mol^{-1}. Within the nondimensional mass and energy balance equations, the activation energy is expressed through the dimensionless parameter, β, which governs the Arrhenius term and thereby exerting a direct influence on the reaction rate and the associated heat generation. Adresi & Pakhirehzan (2023) describe activation energy as the minimum energy required to initiate bond rearrangement and molecular interaction leading to product formation. A higher value of β corresponds to a larger activation energy, resulting in a slower rate of molecular transformation and reduced heat generation, whereas a lower β facilitates more rapid reaction kinetics.

When β corresponds to 15 000 J mol⁻¹, the model predicts extremely rapid conversion, with over 99 % of ethylene consumed in under five minutes. Simultaneously, the reactor temperature rises sharply, reaching approximately 12 times the initial temperature within 17 minutes (Figure 5-8 b). Although the low activation energy promotes rapid conversion, the heat released would, in an operational reactor, drive temperatures beyond material limits, overwhelm cooling systems and increase the likelihood of undesired side reactions.

At an activation energy of 19 600 J mol⁻¹, the conversion profile is more gradual, approaching complete conversion in 4 minutes, and the peak temperature increase is more moderate, at roughly 2.9 times above the initial temperature representing a realistic balance between conversion efficiency and thermal stability (figure 5-8 d). For higher activation energies, 22 000 and 25 000 J mol⁻¹ (larger β), the reaction rate decreases markedly and conversion within this range reaches ~40 % and <10 %, respectively.

These results highlight the sensitivity of both reaction kinetics and thermal behaviour to the dimensionless barrier β. Lower β values accelerate conversion but lead to impractically high reactor temperatures, while higher β values suppress conversion below viable operational thresholds. An activation energy of 19 600 J mol⁻¹ thus emerges as the most representative and operationally stable parameter for model validation and reactor scale-up.

5.4.2.2.3. Heat transfer co-efficient

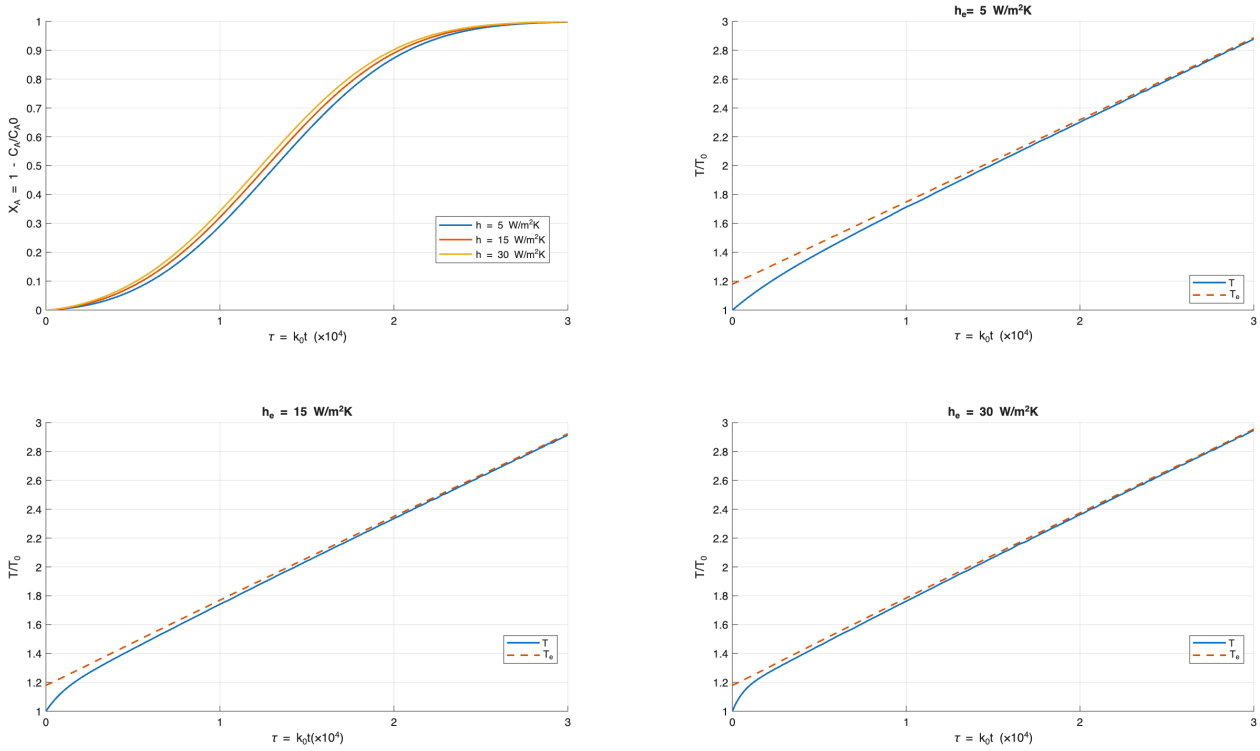

Figure 5.9 Theoretical conversions of ethylene in a VUV photolysis reactor at different heat-transfer values

Figure 5-9 presents the results of the VUV photolysis model analysis, illustrating the impact of varying heat transfer coefficients on the conversion of ethylene over dimensionless time. Within the nondimensional mass and energy balance equations, the heat transfer coefficient is incorporated through the Stanton number (N_{st}), which plays a key role in regulating the heat exchange between the lamp and the gas mixture, thereby impacting the temperature distribution and the reaction kinetics.

The results indicate that the conversion was slightly low during the initial stages when the heat transfer coefficient was set at 5 W/m^{2}K, reaching approximately 100% at a dimensionless time of 2.8 × 10^4 (5.95 minutes), as shown in Figure 5-9a. A further increase to 15 W/m^{2}K resulted in a slight rise, with conversion nearing 100% at a dimensionless time of 2.3×10^4 (4.89 minutes), as depicted in the 5-9c. Further increases to 30 W/m^{2}K showed minimal additional improvement, with conversion curves overlapping and stabilizing at 100% at 2 × 10³ (4 minutes). The initial slight rise in conversion with the heat transfer coefficient increase from 10 to 5-30 W/m^{2}K was likely due to improved heat dissipation, facilitating faster reaction kinetics, whereas the plateau observed beyond 2.3× 10^4 (6,4 minutes), suggests a saturation effect where additional heat transfer does not significantly alter the reaction rate.

Increasing the heat transfer co-efficient from 10 to 30 W m^{-2} K^{-1} results in negligible changes in conversion and only minor decreases in temperature . This indicates that, under the present operating conditions, the VUV reactor performance is governed predominantly by photon flux–driven photochemistry, rather than by heat-transfer or temperature limitations.

5.4.2.2.4. Pre-exponential factor

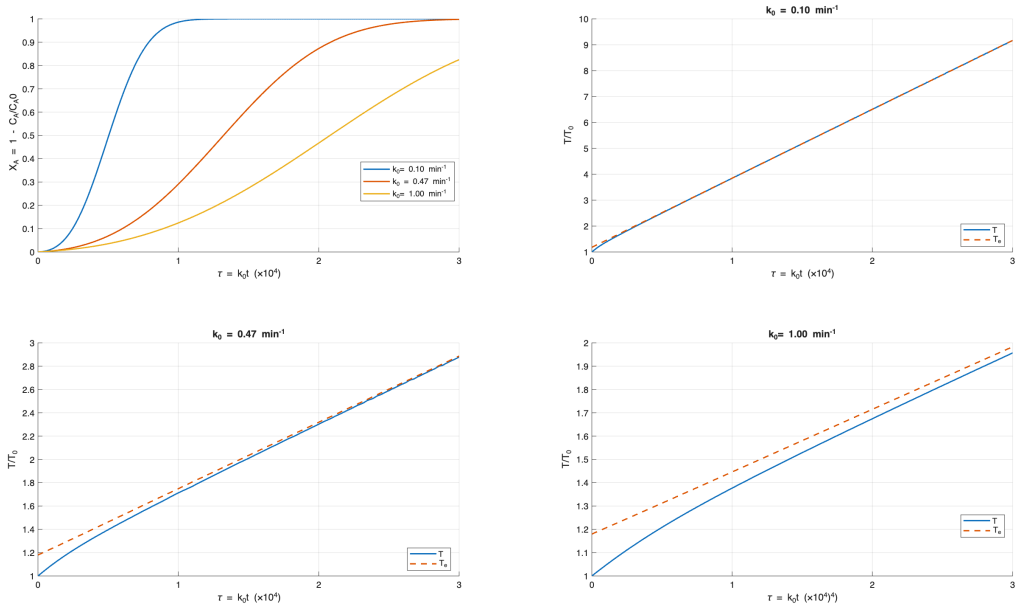

Figure 5.10 Theoretical conversions of ethylene in a VUV photolysis reactor at different pre-exponential factor values

The effects of different pre-exponential factors were studied on figure 5-10. The pre-exponential factor is expressed through the dimensionless time, $\tau = k_0 t$, in the nondimensional mass and energy balances governing the model in figure 5-10. The factor serves as a pre-exponential constant in the Arrhenius equation, indicating the frequency of effective collisions or photon-induced reaction initiations under specific conditions (Jagannadham, 2010). This parameter influences the reaction rate by setting the baseline frequency of molecular encounters or photon interactions that can lead to ethylene degradation in the VUV photolysis process.

Figure 5-10a, illustrates the degradation of ethylene as a function of dimensionless time with k_0 values ranging from 0.10 s^{-1} to 1 min^{-1}. The results reveal a counterintuitive trend; higher pre-exponential factors lead to slower conversion rates. In contrast to classical kinetic expectations, a lower k_0 value (10 s^{-1}) is associated with faster degradation of ethylene.

When τ is defined as $k_0 t$, a smaller $k_0 t$ corresponds to a longer physical runtime ($t=\frac{\tau}{k_0}$). The extended runtime allows the reactor to receive more cumulative radiant energy from the lamp, producing a greater temperature rise. This elevated temperature increases the effective rate constant via the Arrhenius exponential term, thereby accelerating conversion late in the simulation. Conversely, larger k_0 values shorten the physical runtime, limiting both cumulative heating and the associated temperature-driven rate enhancement. Therefore, the inversion observed in Figure 5-10a is a consequence of the modelling framework and time scaling, and not an inherent reversal of the expected kinetic dependence on k_0.

5.4.2.3. Sensitivity Analysis : Cost

A sensitivity analysis was conducted to evaluate how variations in selected process parameters influence the operating cost of a VUV photolysis reactor. The cost model accounts for two main contributions: the electrical cost associated with lamp power consumption and the cost arising from undegraded ethylene, which is linked to product spoilage rates. Four parameters were assessed individually to determine their effect on this cost balance. Lamp power was varied to examine the trade-off between higher energy use and faster conversion which directly impacts cost. Activation energy was adjusted to explore how kinetic barriers influence reaction rates and, consequently, spoilage-related losses. The heat-transfer coefficient was varied to assess whether changes in thermal management affect cost. Finally, the pre-exponential factor was varied to investigate how the intrinsic frequency of reaction-initiating events impacts cost.

5.4.2.3.1. Lamp power

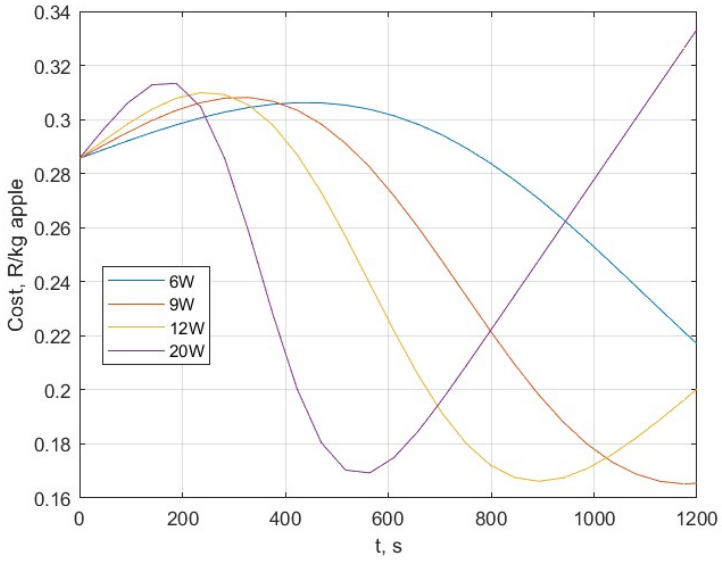

Figure 5.11 Cost (R/kg apple) over time for a VUV photolysis reactor at different lamp power values

Across all wattages, the initial cost reflects undegraded ethylene, which declines with progressive conversion, counterbalanced by escalating electricity costs. At 6W, the cost starts at approximately 0.29 R/kg apple and rises gradually below the other cost profiles but maintains a steeper rise as compared to the other profiles, reflecting a lower photon intensity that results in slower generation of reactive oxygen species (ROS) and hydroxyl radicals (OH) due to reduced light energy, leading to a more gradual breakdown of ethylene. This aligns with findings by Pathak et al. (2017) that lower light intensities result in limited degradation rates, as fewer photons are available to initiate direct and indirect photolysis

For the 6W lamp, at 200 seconds ethylene degradation begins to outpace the accumulation of operational costs, reducing the cost of undegraded ethylene. Thereafter there is a sustained but decelerating degradation process, where the remaining ethylene is broken down more slowly as its concentration decreases, while the linear rise in electricity costs starts to dominate.

A similar trend is observed in the other profiles however as there is an increase in wattage the initial slow gradual rise in cost is less prominent as compared to lower wattages because of the increased intensity that results in an increase in the generation of photons thus the degradation of ethylene progresses faster. However, at elevated wattages, the cost curve exhibits a higher peak, reaching approximately 0.315 R/kg apple and 0.31 R/kg apple for 20 W and 12 W respectively. This is due to the linear accumulation of higher electrical costs as

wattage directly correlates with energy consumption per time. In contrast, lower intensities result lower overall peaks within the observed timeframe.

The 20 W and 12 W curve declines sharply to 0.17 R/kg apple and 0.165 R/kg apple by 480 and 880 seconds and then shoots up to a peak of 0.33 R/kg apple and 0.2 R/kg apple for the given timeframe. Similarly to the 6 W lamp, this behaviour occurs as this rapid degradation outpaces the accumulation of operational costs, reducing the cost associated with undegraded ethylene efficiently. The subsequent sharp rise after is due to the linear increase of electricity costs, which dominate as the high wattage sustains energy consumption over time.

For the 20 W lamp, the sharp cost increase beyond 480 seconds suggests that prolonged operation is economically inefficient, potentially leading to higher overall expenses compared to lower wattages like 12 W or 9 W. The need for cooling at higher temperatures also adds complexity and cost, indicating that 20 W may be best suited for optimized, short-duration applications rather than continuous use in fruit storage systems.

The findings from Figure 5-7a, suggest that an intermediate wattage such as 12 W or 9 W is recommended for the model. This wattage range offers a balanced trade-off, achieving efficient ethylene degradation with a noticeable cost dip (to approximately 0.165 R/kg apple and 0.163 R/kg apple) while maintaining lower long-term operational expenses compared to 20 W, Lower wattages like 6 W provide cost savings but at the expense of slower degradation rates, potentially compromising fruit quality.

5.4.2.3.2. Activation Energy

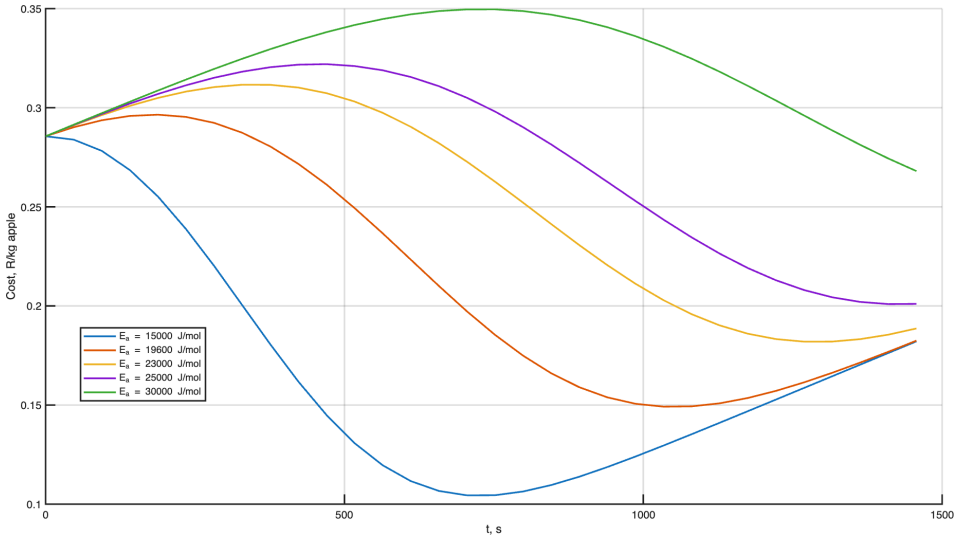

Figure 5.12 Cost (R/kg apple) over time for a VUV photolysis reactor at different activation energy values

Figure 5-12 examines the effect of different activation energies ranging from 10,000 J/mol, 15,000 J/mol, 19,600 J/mol, 20,000 J/mol, to 25,000 J/mol, on the cost of ethylene degradation per kilogram of apple. Activation energy influences the reaction rate constant via the Arrhenius equation, where lower values reduce the energy barrier for ethylene breakdown, thereby accelerating the formation and reaction of reactive oxygen species (ROS) and hydroxyl radicals through direct and indirect photolysis. Across all activation energies, the initial cost comprises the expense of undegraded ethylene and the operational cost of lamp usage, which decreases as degradation progresses but rises due to increasing electricity consumption over time.

The initial cost across all profiles is dominated by the expense of undegraded ethylene, which starts high due to the presence of ethylene in the storage environment. As degradation begins, this cost declines, but the rate and extent of the decline depend on the activation energy. At 15,000 J/mol, the cost starts at approximately 0.28 R/kg apple, drops sharply to around 0.3 R/kg apple due to a low energy barrier enabling rapid ethylene removal, and then rises steadily as electricity costs accumulate. However, figure 5-8b reveals a sharp temperature increase to 12 times the initial value within 17 minutes, incurring additional costs for cooling systems to prevent material damage and unwanted side reactions, which could further elevate operational expenses.

For the intermediate range of 19,600 J/mol, the cost begins at 0.28 R/kg apple, drops to a minimum of about 0.15 R/kg apple, and then increases gradually, reflecting a balanced degradation pace. Figure 5-8d shows a moderate temperature rise of 2.9 times the initial value, reducing the need for extensive cooling and thus limiting additional cost burdens. This intermediate activation energy strikes a cost-effective balance, minimizing both undegraded ethylene losses and thermal management expenses.

For 25,000 J/mol, the cost begins at 0.28 R/kg apple, increases above the lower activation energy profiles due to a higher barrier impeding photon-initiated degradation, leading to sustained undegraded ethylene expenses and a slower cost reduction. The highest modelled activation energy of 30,000 J/mol starts at 0.28 R/kg apple, does not dip during the given time-frame dips as the elevated barrier delays degradation, maximizing undegraded ethylene costs and requiring longer operation times, which amplify electricity expenses.

Based on the findings from Figure 5-12, an intermediate activation energy of 19,600 J/mol is recommended for VUV photolysis in fruit storage. This value achieves a cost minimum of approximately 0.15 R/kg apple, reflecting efficient ethylene degradation that reduces undegraded ethylene expenses, while the moderate temperature increase (2.9-fold) limits cooling costs compared to the 15,000 J/mol scenario (12-fold rise). Higher activation energies like 25,000 J/mol or 30,000 J/mol result in prolonged undegraded ethylene costs and extended operation times, driving up electricity expenses. Conversely, while 15,000 J/mol offers a lower

initial cost dip (0.10 R/kg apple), the substantial thermal costs from overheating outweigh these savings. Thus, 19,600 J/mol optimizes the balance between degradation efficiency, electricity costs, and thermal management expenses, ensuring economic viability for fruit storage applications.

5.4.2.3.3. Pre-exponential factor

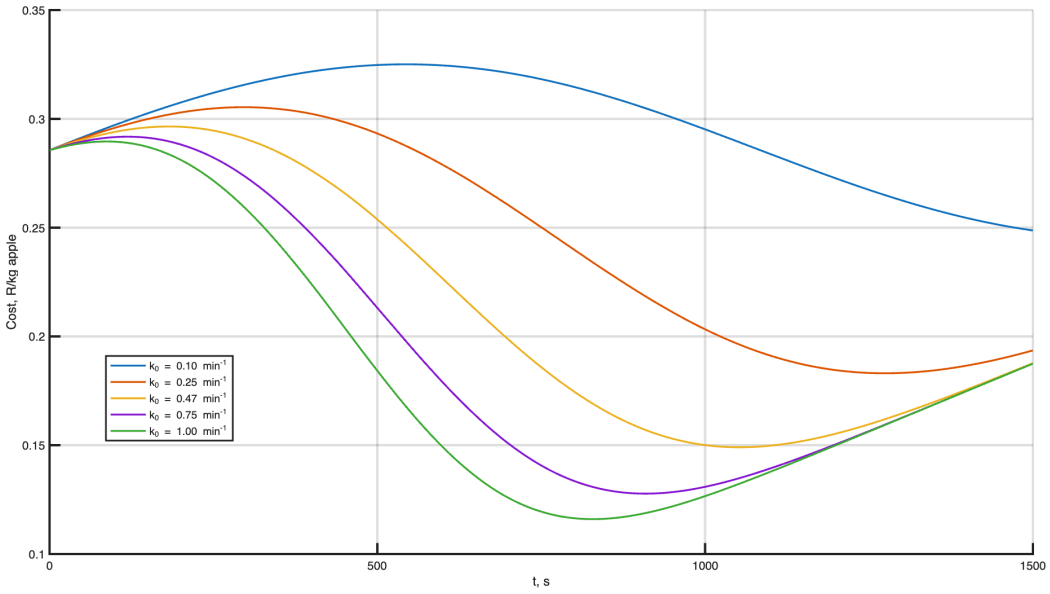

Figure 5.13 Cost (R/kg apple) over time for a VUV photolysis reactor at different pre-exponential factor values

Figure 5-13 examines the effect of different pre-exponential factors (k_0) ranging from 0.10 min^{-1}, 0.25 min^{-1}, 0.47 min^{-1}, 0.75 min^{-1}, to 1.00 min^{-1} on the cost of ethylene degradation per kilogram of apple on the model.

Similarly to the Figure 5.11 and Figure 5.12, the cost across all k_0 values consists of the cost of running the lamps and the cost of undegraded ethylene off which continuously drops as degradation occurs. At the lowest k_0 value of 0.10 min^{-1}, the initial cost is 0.29 R/kg of apple and then rises steeply above the other cost profiles. The steep rise and slow initial decline is a consequence of slow reaction kinetic rates, an attribute associated low k_0 values. This solely means, less ethylene is degraded as the reaction rate is slow thus lamps also stay on longer, consuming more electrical energy contributing to the higher cost.

A similar trend is observed across all the other four k_0, (0.25 min^{-1}, 0.47 min^{-1}, 0.75 min^{-1}, and 1.00 min^{-1}), where costs initially rise but the length of rise is inversely proportional to the k_0 values as faster degradation occurs as higher k_0 values (0.75 min^{-1} and 1.00 min^{-1}) reducing ethylene degradation costs quickly. However, high k_0 values (0.75 min^{-1} and 1.00 min^{-1}) might cause more heat from the reaction, potentially raising costs for cooling to avoid reactor overheating or unwanted side reactions.

At approximately 1400 seconds, the profiles for 0.47 min^{-1}, 0.75 min^{-1}, and 1.00 min^{-1} converge as electricity costs shoot up linearly, overshadowing the earlier cost savings from degradation and aligning their upward trajectories

Based on the findings from Figure 5-13, a middle pre-exponential factor of 0.47 min^{-1} is recommended for the model. This value balances ethylene degradation (with a cost low around 0.15 R/kg apple) and manageable electricity use, avoiding the slow degradation and higher undegraded ethylene costs of lower k_0 like 0.10 min^{-1} or 0.25 min^{-1}. Higher values like 1.00 min^{-1} give a lower cost dip (0.05 R/kg apple) pose possible cooling costs over time, while the convergence with 0.47 min^{-1} and 0.75 min^{-1} suggests diminishing returns at higher k_0.

5.4.2.3.4. Heat transfer co-efficient

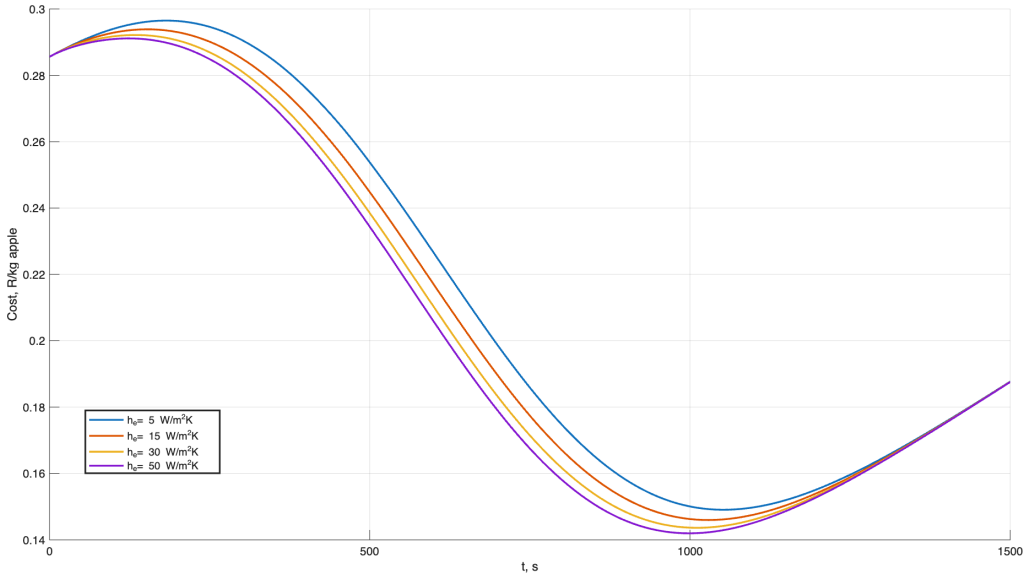

Figure 5.14 Cost (R/kg apple) over time for a VUV photolysis reactor at different heat transfer co-efficient values

Figure 5.14 looks at how different convective heat transfer coefficients (h_e) ranging from 5 to 50 W/m²K affect the cost of ethylene degradation per kilogram of apple in the model.

According to Figure 5.14, the initial cost across all heat transfer coefficients profiles each start at the same baseline. However, as degradation progresses, differences between the profiles become apparent although minor as they all follow a similar trend closely aligning them. The 5 W/m²K profile cost slightly exceeds all others, primarily because of the lower heat transfer co-efficient that results in decreased conversion while the 50 W/m²K heat transfer profile cost yields the lowest cost. However, as the reactor operation continues and approaches ethylene completion and the cost of running the rector lamps on electricity become more prominent, the costs converge indicating that the influence of heat transfer coefficient is more pronounced in the early stages of operation and diminishes as the degradation process progresses.

Although the 50 W/m²K heat transfer profile cost yields the lowest modelled cost and highest conversion as per Figure 5.14, the gain over lower values is minimal. Maintaining such a high co-efficient would increase energy use, capital investment and maintenance requirements. Given the trade-offs, a heat transfer co-efficient in the range of 15-30 W/m²K, offers a balanced solution.

5.4.2.4. Optimum Operating conditions

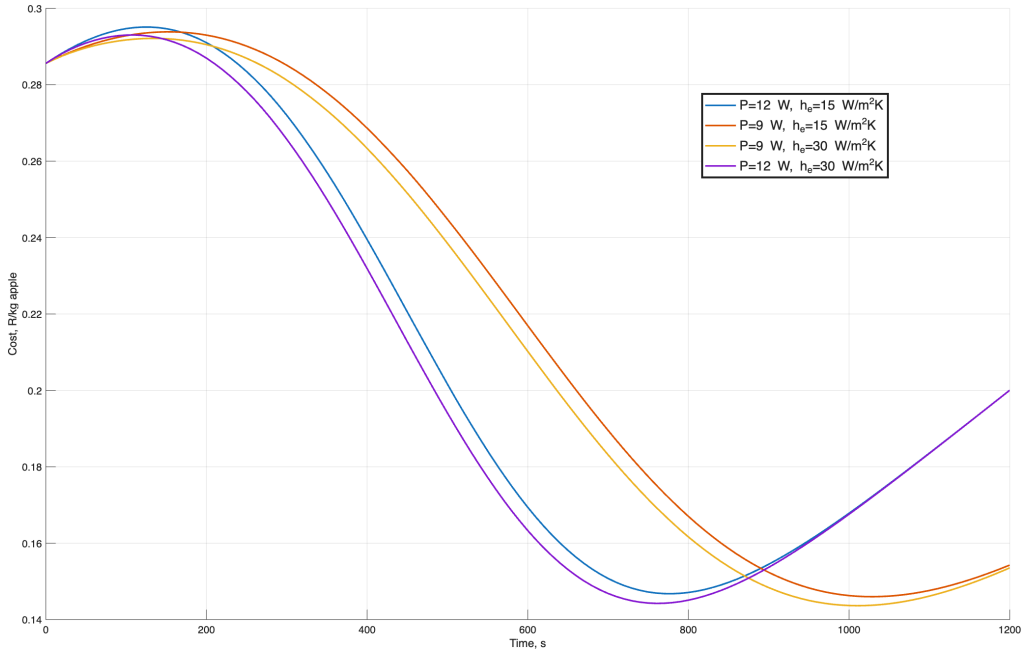

Figure 5.15 Optimum operational costs of VUV photolysis reactor

The optimisation study considered four operating conditions, with activation energy fixed at 19 600 J·mol⁻¹ and the pre-exponential factor fixed at 0.47 s⁻¹. Lamp power was varied between 9 W and 12 W, and the heat transfer coefficient was varied between 15 W·m⁻²·K⁻¹ and 30 W·m⁻²·K⁻¹. The selection of these optimisation values was based on the results obtained on the sensitivity analysis, which evaluated the influence of lamp power and heat transfer coefficient, activation energy and power on both conversion and cost. According to the model lower activation energy values produced high conversion rates and excessive temperature rises, while higher activation energy values slowed degradation to economically unfavourable levels.

Analysis of the model indicated that higher lamp power (12 W) predicted the highest performance in terms of rapid ethylene degradation, with conversion occurring almost instantaneously relative to the other cost profile. In both the 15 and 30 W·m⁻²·K⁻¹ cost profile cases, cost decreases steadily as ethylene is degraded, with the cost profile at 30 W·m⁻²·K⁻¹ initially costing less than the 15 W·m⁻²·K⁻¹ cost profile. Conversion was achieved within

approximately 780 s for both profiles, with only marginal cost differences (0.148 R/kg apple vs. 0.15 R/kg apple). However, once degradation is complete, differences in the heat transfer co-efficient become negligible for the same lamp power, and prolonged operation primarily increases cost due to electricity consumption without improving conversion.
For the 9W lamp power cost profile, degradation was completed at ~1000 s, and while the trends were similar, cost reductions occurred later due to the slower initial conversion due arising from reduced photon availability, which limits the generation of reactive species necessary for ethylene degradation and is further compounded by less effective heat transfer under low heat transfer coefficient conditions.

Overall, results from the model suggest that higher lamp power (12 W) combined with higher heat transfer (30 $W \cdot m^{-2} \cdot K^{-1}$) and moderate pre-exponential factor (0.47 s^{-1}) and activation energy values (19 600 $J \cdot mol^{-1}$) yields the most favourable cost–conversion balance, particularly in the early stages of operation. The choice of 12 W lamp power is particularly important when considering the spoilage factor, which accounts for the economic losses associated with residual ethylene.

In the context of apple storage, even low ethylene concentrations can accelerate ripening and softening, leading to significant postharvest losses (Jabbar and East, 2016). Therefore, conditions that maximise conversion not only reduce operational expenditure but also minimise spoilage-related costs. In the present model, the spoilage factor penalises incomplete degradation by adding a cost proportional to the residual ethylene concentration, meaning that faster and more complete conversion directly translates into economic benefit by preserving fruit quality and extending shelf life.

5.4.3. Industrial Implications

To assess the overall ethylene accumulation during the storage period, the daily average concentration was calculated. This metric provides a representative value for comparing different storage conditions over time. The calculation was performed using, equation (5-18).

$$\overline{x}\ C_2H_4\ conc = \frac{\sum(daily\ C_2H_4\ ppm)}{N} \qquad (5\text{-}18)$$

where N is the total number of days in the storage period.

Quantifying the reduction in ethylene levels allows for evaluating the effectiveness of VUV treatment relative to conventional cold storage. The reduction percentage was determined using Equation (5-19)

$$\% = \frac{\overline{x}\, C_2H_{4\ cold} - \overline{x}\, C_2H_{4\ VUV}}{\overline{x}\, C_2H_{4\ cold}} \quad (5\text{-}19)$$

where $C_2H_{4\ cold}$ *is the average daily ethylene concentration in cold storage;* $C_2H_{4\ VUV}$ *is the corresponding value in the VUV photolysis chamber*

Since ethylene is a ripening hormone that accelerates postharvest deterioration, it is necessary to estimate its impact on spoilage. The spoilage fraction, which represents the proportion of produce lost due to ethylene exposure, was calculated using Equation (5-20):

$$k_{s_{fraction}} = k_s \times \overline{x}\, C_2H_4\ conc \quad (5\text{-}20)$$

where k_s *is the spoilage factor;* $\overline{x}\, C_2H_{4conc}$ *represents the average daily ethylene concentration*

To calculate the proportion of produce lost due to spoilage:

$$mass_{spoiled} = k_{s_{fraction}} \times M \quad (5\text{-}21)$$

where M is the total pallet mass (kg).

The corresponding value lost is calculated as follows:

$$\text{Value lost} = mass_{spoiled} \times \Lambda \quad (5\text{-}22)$$

where Λ *is the market value for golden delicious apples*.

alternatively, the value lost can be calculated as cost of unreacted ethylene:

$$Cost = \sigma \times \Delta\text{ppm} \times \text{M} \quad (5\text{-}23)$$

where σ is the ethylene cost coefficient; Δppm is the difference in average ethylene concentration between treatments ; M is the pallet mass.

Table 5.6 Summary Table of Economic and Spoilage Outcomes

Parameter	Fridge	VUV
Average Ethylene (ppm)	113.27	10.81
Spoilage Fraction (%)	31.72	3.03
Spoiled Mass (kg/pallet)	319.79	30.54
Value Lost (R/pallet)	6395.80	610.80
Cost of Unreacted Ethylene (R/pallet)	6395.80	610.80
Shelf Life Multiplier (approx.)	1× (base)	10.5×

An assessment of the use of VUV photolysis for the degradation of ethylene in fruit storage indicates reduced operating costs, with an increase in potential savings at commercial scale. In a controlled study involving 23 apples stored in a 150 L chamber for 21 days, cold storage at 10 ℃ yielded an average daily ethylene concentration of 113.27 ppm, associated with a spoilage fraction of 31.72%. At ambient temperature, the VUV photolysis treatment reduced the average concentration to 10.81 ppm, lowering spoilage to 3.03% and achieving a 90.5% reduction in ethylene. This magnitude of reduction suggests the potential for extending shelf life by approximately 10.5 times compared with cold storage alone.

For upscaling, one pallet defined according to (Tru-Cape, 2021) industry standards was used as the baseline unit, comprising 5,040 apples. Based on measured average fruit mass (0.2 kg for the Golden Delicious cultivar), the total pallet mass was calculated as 1,008 kg. Under cold storage, spoilage mass reached 319.79 kg (32% loss), while VUV treatment reduced this to 30.54 kg (0.03% loss), preventing 289.25 kg of waste per pallet. At a market value of 20 R/kg, the corresponding loss equated to R 6,395.80 under cold storage and R610.80 under VUV photolysis, yielding per-pallet savings of R5,785.00. This loss correlates directly with unreacted ethylene exposure, calculated using a unit value of 0.056 R/(ppm·kg) and confirming the model's internal consistency through alignment of ethylene reduction with spoilage mitigation.

CHAPTER 6

6. CONCLUSION AND RECOMMENDATIONS

6.1. Conclusion

This study has demonstrated, through both theoretical and empirical investigation, that vacuum ultraviolet (VUV) photolysis is cost-effective approach to postharvest ethylene control in controlled fruit storage facilities. Using different modelling approaches such as mechanistic modelling, statistical analysis, and cost optimisation, this study established a methodology for determining operating conditions that maximise ethylene degradation efficiency while minimising overall operational costs. Two distinct modelling approaches were employed to achieve this objective.

The first was a mass and energy balance formulation, which integrated first-order reaction kinetics, photon–reactant interactions, and radiative–convective heat transfer to predict both ethylene concentration degradation and reactor temperature rise over time. This model, which incorporated validated kinetic parameters, reactor geometry, lamp characteristics, and thermophysical properties, reproduced the experimental conversion and temperature profiles with high accuracy ($R^2 = 0.988$, RMSE = 0.0572). However, because this formulation focused on direct oxidation and did not explicitly include the role of relative humidity (RH), it could not predict the humidity-dependent effects observed experimentally.

To address this limitation, a second model was developed: the percentage ethylene removal (PER) model, based on a Box–Behnken experimental design. This empirical model included initial ethylene concentration, RH, and lamp wattage as independent variables, enabling the quantification of main and interaction effects. Analysis using this model revealed that RH generally promotes removal at low ethylene concentrations by enhancing hydroxyl radical (•OH) generation from water vapour photolysis, which accelerates oxidative degradation. However, a notable observation seen from the results was at high ethylene concentrations (50 ppm) and low lamp power (3 W), were increased RH reduced removal efficiency. This reversal was attributed to photon competition at 185 nm, whereby water vapour absorbs a significant portion of photons before they can dissociate O_2 and H_2O into reactive intermediates, thus limiting oxidant production. This effect was most pronounced in photon-limited conditions, where both low lamp power and high ethylene concentration constrain the availability of reactive species.

The integration of both models enabled a complete understanding of the process: the mass and energy balance model captured the core photochemical and thermal dynamics, while the

PER model resolved humidity effects critical to real-world storage environments. These outputs were then applied to an optimisation model that sought to minimise the sum of electrical energy costs and spoilage-related losses from undegraded ethylene. A sensitivity analysis was carried out by varying lamp power, activation energy, pre-exponential factor, and heat-transfer coefficient individually. Lamp power and activation energy had the greatest influence on both conversion and cost, while the pre-exponential factor had a secondary but non-negligible effect, and heat-transfer coefficient produced minimal gains beyond 15–30 $W \cdot m^{-2} \cdot K^{-1}$. Excessively high lamp power (20 W) achieved rapid degradation but at a high energy cost, while too low a power (6 W) led to prolonged degradation and potential higher spoilage related losses. Similarly, activation energies below ~19,000 $J \cdot mol^{-1}$ caused excessive heating and potential cooling requirements, while higher values slowed degradation to economically unfavourable rates.

The optimal configuration identified from the combined modelling and cost analysis consisted of a 12 W lamp power, an activation energy of 19,600 $J \cdot mol^{-1}$, a pre-exponential factor of 0.47 s^{-1}, and a heat-transfer coefficient in the 15–30 $W \cdot m^{-2} \cdot K^{-1}$ range. This combination achieved near-complete degradation within 780 seconds, limited the temperature rise to about 2.9 times the initial value, and delivered a total cost of approximately 0.148 R/kg apple. The selection of 12 W lamp power was especially important when considering the spoilage cost factor, which penalises incomplete degradation more heavily than marginal increases in energy use.

Application at industry scale underscored the significance of these findings. The VUV treatment maintained an average ethylene concentration of 10.81 ppm as compared to a cold storage value of 113.27 ppm with a reduction of ~90.5 % and a decreased spoilage from 31.72 % to 3.03 %, potentially extending shelf life by approximately 10.5 times. For a pallet of Golden Delicious apples (1,008 kg), this equates to a saving of ~R5,785 R per pallet from reduced spoilage. At a truckload scale of 21 pallets, the saving increases to R121,485.

In conclusion, the dual-model approach presented in this chapter provided both mechanistic accuracy and practical relevance. The mass and energy balance model captured the fundamental kinetics and thermal behaviour of VUV photolysis, while the PER model incorporated humidity-dependent behaviour that is vital in storage environments. Together, these models supported an optimisation strategy that is technically sound, economically justified, and operationally adaptable. VUV photolysis, when operated within the identified optimal parameter range, offers rapid ethylene degradation, minimal operational costs, and an extension of fruit shelf life, making it a scalable and cost-effective solution for commercial postharvest storage.

6.2. Recommendations

Although this study confirms that VUV photolysis is an effective and economically viable method for postharvest ethylene control, one specific performance limitation was observed. At 50 ppm ethylene concentration and low lamp power (3 W), high relative humidity led to reduced removal efficiency. This is likely due to water vapour absorbing part of the 185 nm light, limiting the generation of reactive species required for oxidation. The sensitivity analysis was performed up to 1200 s; however, future studies should extend beyond this duration to capture longer-term system dynamics and steady-state behaviour.

Future research should address this limitation through:

1. Controlled experimental studies that vary humidity, lamp power, and ethylene concentration to determine the conditions under which performance anomalies occur and to quantify their effects.
2. Model refinement to integrate water vapour absorption and photon competition effects into the mass and energy balance framework, improving predictive capability.
3. Expanded techno-economic evaluation comparing the operational and capital costs of VUV photolysis with other postharvest preservation techniques (e.g., catalytic oxidation or controlled-atmosphere storage) to assess its relative cost-effectiveness and scalability.
4. Investigation of system geometry, particularly the distance between the VUV light source and the fruit surface, to evaluate its influence on ethylene degradation efficiency.
5. Quantification of photon flux from the VUV light source, as this parameter is critical for understanding degradation behaviour in large-volume conditions.
6. Verification of degradation products to confirm that ethylene is primarily converted to CO_2 and H_2O, and not to potentially harmful intermediates.

CHAPTER 7

7. REFERENCES

Aafia, S. (2018) 'Ozone treatment in prolongation of shelf life of temperate and tropical fruits', *International Journal of Pure & Applied Bioscience*. https://doi.org/10.18782/2320-7051.6289

Abbott, J.A., Watada, A.E. and Massie, D.R. (2022) 'Sensory and instrument measurement of apple texture', *Journal of the American Society for Horticultural Science*, 109(2), pp. 221–226. https://doi.org/10.21273/jashs.109.2.221

Abeles, F.B., Morgan, P.W. and Saltveit, M.E. (1992) *Ethylene in Plant Biology*. 2nd edn. San Diego, CA: Academic Press.

Ackermann, J., Fischer, M. and Amadò, R. (1992) 'Changes in sugars, acids, and amino acids during ripening and storage of apples (cv. Glockenapfel)', *Journal of Agricultural and Food Chemistry*, 40(7), pp. 1131–1134. https://doi.org/10.1021/jf00019a008

Adams, D. and Yang, S.F. (1977) 'Methionine metabolism in apple tissue: implication of S-adenosylmethionine as an intermediate in the conversion of methionine to ethylene', *Plant Physiology*, 60(6), pp. 892–896. https://doi.org/10.1104/pp.60.6.892

Adams, D.O. and Yang, S.F. (1979) 'Ethylene biosynthesis: identification of 1-aminocyclopropane-1-carboxylic acid as an intermediate in the conversion of methionine to ethylene', *Proceedings of the National Academy of Sciences*, 76(1), pp. 170–174. https://doi.org/10.1073/pnas.76.1.170

Adresi, M. and Pakhirehzan, F. (2023) 'Evaluating the performance of self-sensing concrete sensors under temperature and moisture variations – a review', *Construction and Building Materials*, 373, 132923. https://doi.org/10.1016/j.conbuildmat.2023.132923

Ahmad, F., Zaidi, S. and Arshad, M. (2021) 'Postharvest quality assessment of apple during storage at ambient temperature', *Heliyon*, 7(8), e07714. https://doi.org/10.1016/j.heliyon.2021.e07714

Alapi, T. and Dombi, A. (2007) 'Comparative study of the UV and UV/VUV-induced photolysis of phenol in aqueous solution', *Journal of Photochemistry and Photobiology A: Chemistry*, 188(2–3), pp. 409–418. https://doi.org/10.1016/j.jphotochem.2007.01.002

Amao, I. (2018) ‘Health benefits of fruits and vegetables: review from Sub-Saharan Africa’, in *Vegetables – Importance of Quality Vegetables to Human Health*. InTech. https://doi.org/10.5772/intechopen.74472

Arc, E. et al. (2013) ‘ABA crosstalk with ethylene and nitric oxide in seed dormancy and germination’, *Frontiers in Plant Science*, 4, 63. https://doi.org/10.3389/fpls.2013.00063

Asale, Y. et al. (2021) ‘Phytochemicals and antioxidant activity of different apple cultivars grown in South Ethiopia: case of the Wolayta zone’, *International Journal of Food Properties*, 24(1), pp. 354–363. https://doi.org/10.1080/10942912.2021.1885440

Bailén, G. et al. (2007) ‘Use of a palladium catalyst to improve the capacity of activated carbon to absorb ethylene, and its effect on tomato ripening’, *Spanish Journal of Agricultural Research*, 5(3), pp. 345–351. Available at: www.inia.es/sjar (Accessed: 20 August 2025).

Banerjee, R. et al. (2019) ‘Intervention of microfluidics in biofuel and bioenergy sectors: technological considerations and future prospects’, *Renewable and Sustainable Energy Reviews*, 99, pp. 212–228. https://doi.org/10.1016/j.rser.2018.11.040

Batur, S. and Çetinbaş, M. (2017) ‘Pre-harvest application of ReTain (aminoethoxyvinylglycine, AVG) influences pre-harvest drop and fruit quality of “Williams” pears’, *Tarım Bilimleri Dergisi*, 23(3), pp. 344–356. https://doi.org/10.15832/ankutbd.447704

Blankenship, S.M. and Dole, J.M. (2003) ‘1-Methylcyclopropene: a review’, *Postharvest Biology and Technology*, 28(1), pp. 1–25. https://doi.org/10.1016/S0925-5214(02)00246-6

Blecher, J.J., Palmer, T.A. and Debroy, T. (2012) ‘Laser-silicon interaction for selective emitter formation in photovoltaics. I. Numerical model and validation’, *Journal of Applied Physics*, 112(11), 113108. https://doi.org/10.1063/1.4768537

Blidi, A. El et al. (1993) ‘Ethylene removal for long term conservation of fruits and vegetables’, *Food Quality and Preference*, 4(3), pp. 145–152. https://doi.org/10.1016/0950-3293(93)90154-X

Boe, A.A. (1967) *Ripening Tomatoes: Ethylene, Oxygen, and Light Treatments*. USDA Technical Bulletin.

Box, G.E.P. and Behnken, D.W. (1960) ‘Some new three-level designs for the study of quantitative variables’, *Technometrics*, 2(4), pp. 455–475. https://doi.org/10.1080/00401706.1960.10489912

Box, G.E.P. and Draper, N.R. (1963) 'The choice of a second order rotatable design', *Biometrika*, 50(3–4), pp. 335–352. https://doi.org/10.2307/2333904

Box, G.E.P. and Wilson, K.B. (1951) 'On the experimental attainment of optimum conditions', *Journal of the Royal Statistical Society: Series B (Methodological)*, 13(1), pp. 1–45. https://doi.org/10.1111/j.2517-6161.1951.tb00067.x

Brackmann, A. and Waclawovsky, A.J. (2001) 'Responses of "Gala" apples to preharvest treatment with AVG and low-ethylene CA storage', *Acta Horticulturae*, 553, pp. 237–242. https://doi.org/10.17660/ActaHortic.2001.553.31

Cabrera, G., Ramírez, M. and Cantero, D. (2011) 'Biofilters', in Moo-Young, M. (ed.) *Comprehensive Biotechnology*. 2nd edn. Amsterdam: Elsevier, pp. 583–593. https://doi.org/10.1016/B978-0-08-088504-9.00408-6

Caket, A.G. et al. (2022) 'Recent studies on 3D lattice metal frame technique for enhancement of heat transfer: discovering trends and reasons', *Renewable and Sustainable Energy Reviews*, 162, 112697. https://doi.org/10.1016/j.rser.2022.112697

Carlson, J.C. et al. (2015) 'Direct UV photolysis of selected pharmaceuticals, personal care products and endocrine disruptors in aqueous solution', *Water Research*, 84, pp. 350–361. https://doi.org/10.1016/j.watres.2015.04.013

Chai, S.Y.W. et al. (2022) 'Future era of techno-economic analysis: insights from review', *Frontiers in Sustainability*, 3, 924047. https://doi.org/10.3389/frsus.2022.924047

Chernoff, H. (1953) 'Locally optimal designs for estimating parameters', *The Annals of Mathematical Statistics*, 24(4), pp. 586–602. https://doi.org/10.1214/aoms/1177728915

Churchill, S.W. and Chu, H.H.S. (1975) 'Correlating equations for laminar and turbulent free convection from a horizontal cylinder', *International Journal of Heat and Mass Transfer*, 18(9), pp. 1049–1053. https://doi.org/10.1016/0017-9310(75)90222-7

Coloma, A. et al. (2014) 'Development of an active film with natural zeolite as ethylene scavenger', *Journal of the Chilean Chemical Society*, 59(4), pp. 2674–2678.

Creasey, D.J., Heard, D.E. and Lee, J.D. (2000) 'Absorption cross-section measurements of water vapour and oxygen at 185 nm: implications for the calibration of field instruments to measure OH, HO_2 and RO_2 radicals', *Geophysical Research Letters*, 27(11), pp. 1651–1654. https://doi.org/10.1029/1999GL011014

Cuerda-Correa, E.M., Alexandre-Franco, M.F. and Fernández-González, C. (2020) 'Advanced oxidation processes for the removal of antibiotics from water: an overview', *Water*, 12(1), 102. https://doi.org/10.3390/w12010102

DAFF (2019) *A profile of the South African apple market value chain*. Pretoria: Department of Agriculture, Forestry and Fisheries. Available at: www.daff.gov.za (Accessed: 20 August 2025).

Dascalaki, E. et al. (1994) ‘Natural convection heat transfer coefficients from vertical and horizontal surfaces for building applications’, *Energy and Buildings*, 20(3), pp. 271–282. https://doi.org/10.1016/0378-7788(94)90027-2

Davies, P.J. (2010) ‘The plant hormones: their nature, occurrence, and functions’, in Davies, P.J. (ed.) *Plant Hormones: Biosynthesis, Signal Transduction, Action!*. Dordrecht: Springer, pp. 1–15. https://doi.org/10.1007/978-1-4020-2686-7_1

DeEll, J.R. et al. (2001) ‘Factors affecting apple fruit firmness – a review’, *Fruit Varieties Journal*, 55(1), pp. 1–10.

Doerflinger, F.C. et al. (2019) ‘Preharvest aminoethoxyvinylglycine (AVG) and 1-methylcyclopropene (1-MCP) effects on ethylene and starch concentrations of “Empire” and “McIntosh” apples’, *Scientia Horticulturae*, 244, pp. 134–140. https://doi.org/10.1016/j.scienta.2018.09.031

Domoto, P. (2008) *Harvesting and storing apples*. Ames, IA: Iowa State University Extension. Available at: https://store.extension.iastate.edu (Accessed: 20 August 2025).

Durakovic, B. (2017) ‘Design of experiments application, concepts, examples: state of the art’, *Periodicals of Engineering and Natural Sciences*, 5(3), pp. 421–439. https://doi.org/10.21533/pen.v5i3.145

Ebrahimi, A. et al. (2021) ‘Novel strategies to control ethylene in fruit and vegetables for extending their shelf life: a review’, *International Journal of Environmental Science and Technology*, 18, pp. 2571–2586. https://doi.org/10.1007/s13762-021-03485-x

Fan, X., Blankenship, S.M. and Mattheis, J.P. (1999) ‘1-Methylcyclopropene inhibits apple ripening’, *Journal of the American Society for Horticultural Science*, 124(6), pp. 690–695.

Faragher, J.D. and Brohier, R.L. (1984) ‘Anthocyanin accumulation in apple skin during ripening: regulation by ethylene and phenylalanine ammonia-lyase’, *Scientia Horticulturae*, 22(1–2), pp. 89–96.

Farcuh, M. (2023) *Fruit harvest – determining apple fruit maturity and optimal harvest date*. Ithaca, NY: Cornell University.

Feng, X. et al. (2000) ‘Control of ethylene responses in avocado fruit with 1-methylcyclopropene’, *Postharvest Biology and Technology*, 20(2), pp. 143–150. Available at: www.elsevier.com/locate/postharvbio (Accessed: 20 August 2025).

Gao, H. (2021) ‘Molecular photodissociation in the vacuum ultraviolet region: implications for astrochemistry and planetary atmospheric chemistry’, *Molecular Physics*, 119(7), e1861354. https://doi.org/10.1080/00268976.2020.1861354

Giri, R.R. et al. (2014) ‘Significance of water quality and radiation wavelength for UV photolysis of PhCs in simulated mixed solutions’, *Central European Journal of Chemistry*, 12(6), pp. 659–671. https://doi.org/10.2478/s11532-014-0526-2

Goldstein, R.J. and Madanan, U. (2022) ‘Thermal convection studies at the University of Minnesota’, in Greene, G. and Cho, H.H. (eds.) *Advances in Heat Transfer*. Amsterdam: Elsevier, pp. 1–42. https://doi.org/10.1016/bs.aiht.2022.07.004

Gonzalez, M.G. et al. (2004) 'Vacuum-ultraviolet photolysis of aqueous reaction systems', *Journal of Photochemistry and Photobiology C: Photochemistry Reviews*, 5(3), pp. 225–246. https://doi.org/10.1016/j.jphotochemrev.2004.10.002

Hall, M.R. and Allinson, D. (2010) 'Heat and mass transport processes in building materials', in Hall, M.R. (ed.) *Materials for Energy Efficiency and Thermal Comfort in Buildings*. Cambridge: Woodhead, pp. 3–27. https://doi.org/10.1533/9781845699277.1.3

Han, Y., Su, Z. and Du, J. (2023) 'Effects of apple storage period on the organic acids and volatiles in apple wine', *LWT – Food Science and Technology*, 173, 114389. https://doi.org/10.1016/j.lwt.2022.114389

Harker, F.R. et al. (2008) 'Eating quality standards for apples based on consumer preferences', *Postharvest Biology and Technology*, 50(1), pp. 70–78. https://doi.org/10.1016/j.postharvbio.2008.03.020

Hoehn, E. et al. (2003) 'Efficacy of instrumental measurements for determination of minimum requirements of firmness, soluble solids, and acidity of several apple varieties in comparison to consumer expectations', *Postharvest Biology and Technology*, 27(1), pp. 27–37. https://doi.org/10.1016/S0925-5214(02)00190-4

HORTGRO (2019) *Key deciduous fruit statistics*. Paarl: Hortgro. Available at: www.hortgro.co.za (Accessed: 20 August 2025).

Huang, H. et al. (2011) 'Photocatalytic destruction of air pollutants with vacuum ultraviolet (VUV) irradiation', *Catalysis Today*, 175(1), pp. 310–315. https://doi.org/10.1016/j.cattod.2011.04.015

Huang, H. et al. (2014) 'Photooxidation of gaseous benzene by 185 nm VUV irradiation', *Environmental Engineering Science*, 31(9), pp. 524–531. https://doi.org/10.1089/ees.2014.0100

Huang, H. et al. (2015) 'Enhanced degradation of gaseous benzene under vacuum ultraviolet (VUV) irradiation over TiO_2 modified by transition metals', *Chemical Engineering Journal*, 259, pp. 534–541. https://doi.org/10.1016/j.cej.2014.08.057

Huang, H. et al. (2016) 'Recent development of VUV-based processes for air pollutant degradation', *Frontiers in Environmental Science*, 4, 17. https://doi.org/10.3389/fenvs.2016.00017

Huang, W. et al. (2021) 'The role of ethylene and abscisic acid in kiwifruit ripening during postharvest dehydration', *Postharvest Biology and Technology*, 178, 111559. https://doi.org/10.1016/j.postharvbio.2021.111559

m, J.K., Kim, M.K. & Zoh, K.D., 2013. Optimization of photolysis of diclofenac using a response surface methodology. *Water Science and Technology*, 67(4), pp. 907–914. https://doi.org/10.2166/wst.2012.634

Incropera, F.P., 2007. *Fundamentals of Heat and Mass Transfer*. *Chemical Engineering Research and Design*, 85(A12). https://doi.org/10.1205/cherd.br.0712

Iwanami, H., Moriya-Tanaka, Y., Kudo, S., et al., 2024. Factors explaining variations in soluble solids content of apples during ripening and storage. *Horticulture Journal*, 93(2). https://doi.org/10.2503/hortj.QH-105

Jabbar, A. & East, A.R., 2016. Quantifying the ethylene induced softening and low temperature breakdown of “Hayward” kiwifruit in storage. *Postharvest Biology and Technology*, 113, pp. 87–94. https://doi.org/10.1016/j.postharvbio.2015.11.002

Jagannadham, V., 2010. How do we introduce the Arrhenius pre-exponential factor (A) to graduate students? *Creative Education*, 1(2), pp. 128–129. https://doi.org/10.4236/ce.2010.12019

Jakob, L., Friedrich, J. & Bauer, R., 1993. Vacuum-ultraviolet (VUV) photolysis of water: oxidative degradation of 4-chlorophenol. *Journal of Photochemistry and Photobiology A: Chemistry*, 75(2), pp. 97–103. https://doi.org/10.1016/1010-6030(93)80189-G

Jha, S.N., Rai, D.R. & Sharma, R., 2012. Physico-chemical quality parameters and overall quality index of apple during storage. *Journal of Food Science and Technology*, 49(5), pp. 594–600. https://doi.org/10.1007/s13197-011-0415-z

Jiang, Y., Joyce, D.C. & Macnish, A.J., 1999. Responses of banana fruit to treatment with 1-methylcyclopropene. *Plant Growth Regulation*, 28(2), pp. 77–82. https://doi.org/10.1023/A:1006255505470

Jones, R., 2002. Design and Analysis of Experiments (fifth edition), Douglas Montgomery, John Wiley and Sons, 2001, 684 pages, £33.95. *Quality and Reliability Engineering International*, 18(5), pp. 413–414. https://doi.org/10.1002/qre.458

Kang, I.S., Xi, J. & Hu, H.Y., 2018. Photolysis and photooxidation of typical gaseous VOCs by UV irradiation: removal performance and mechanisms. *Frontiers of Environmental Science and Engineering*, 12(3), pp. 1–12. https://doi.org/10.1007/s11783-018-1032-0

Kende, H., 1993. Ethylene biosynthesis. *Annual Review of Plant Physiology and Plant Molecular Biology*, 44(1), pp. 283–307. https://doi.org/10.1146/annurev.pp.44.060193.001435

Khan, A.S. & Singh, Z., 2007. 1-MCP regulates ethylene biosynthesis and fruit softening during ripening of “Tegan Blue” plum. *Postharvest Biology and Technology*, 43(3), pp. 298–306. https://doi.org/10.1016/j.postharvbio.2006.10.005

Khedr, E.H. & Al-Khayri, J.M., 2023. Synergistic effects of tragacanth and anti-ethylene treatments on postharvest quality maintenance of mango (*Mangifera indica* L.). *Plants*, 12(9), p. 1887. https://doi.org/10.3390/plants12091887

Kiefer, J. & Wolfowitz, J., 1952. Stochastic estimation of the maximum of a regression function. *The Annals of Mathematical Statistics*, 23(3), pp. 462–466. https://doi.org/10.1214/aoms/1177729392

Kim, I.S., Kang, S.M., Lee, S.K. & Choi, S.T., 2004. Effects of aminoethoxyvinylglycine on preharvest drop and fruit quality of “Mibaekdo” peaches. *Acta Horticulturae*, 653, pp. 177–182. https://doi.org/10.17660/ActaHortic.2004.653.24

Knee, M. & Hatfield, S.G.S., 1981. Benefits of ethylene removal during apple storage. *Annals of Applied Biology*, 97(1), pp. 165–174. https://doi.org/10.1111/j.1744-7348.1981.tb03002.x

Kulathunga, J., Ranasinghe, R.A.S.N., Ranaweera, K.K.D.S. & Gunaratne, A., 2018. Strategies used to prolong the shelf life of fresh commodities. *Science and Technology of Traditional Foods of Sri Lanka*. Available at: https://www.researchgate.net/publication/324825644

Kutschera, K., Börnick, H. & Worch, E., 2009. Photoinitiated oxidation of geosmin and 2-methylisoborneol by irradiation with 254 nm and 185 nm UV light. *Water Research*, 43(6), pp. 1733–1741. https://doi.org/10.1016/j.watres.2009.02.015

Leng, R., 2022. *Integration and Optimization of Unit Operations*. Edited by B. Perlmutter. Amsterdam: Elsevier. https://doi.org/10.1016/c2019-0-05070-4

Levenspiel, O., 1999. *Chemical Reaction Engineering*. 3rd ed. New York: Wiley.

Lin, L., Ma, J., Zhou, M. & Ma, F., 2013. Photocatalytic oxidation for degradation of VOCs. *Open Journal of Inorganic Chemistry*, 3(1), pp. 14–17. https://doi.org/10.4236/ojic.2013.31003

Link, S.O., Drake, S.R. & Thiede, M.E., 2004. Prediction of apple firmness from mass loss and shrinkage. *Journal of Food Quality*, 27(1), pp. 13–22. https://doi.org/10.1111/j.1745-4557.2004.tb00634.x

Little, C.R. & Holmes, R., 2000. *Storage Technology for Apples and Pears: A Guide to Production, Postharvest Treatment and Storage of Pome Fruit in Australia*. Melbourne: Department of Natural Resources and Environment. Available at: https://api.semanticscholar.org/CorpusID:128805485

Liu, M., Pirrello, J., Chervin, C., Roustan, J.P. & Bouzayen, M., 2015. Ethylene control of fruit ripening: revisiting the complex network of transcriptional regulation. *Plant Physiology*, 169(4), pp. 2380–2390. https://doi.org/10.1104/pp.15.01361

Liu, M., Su, X., Yin, X. & Chen, K., 2024. Ethylene biosynthesis and signal transduction during ripening and softening in non-climacteric fruits: an overview. *Frontiers in Plant Science*, 15, p. 1368692. https://doi.org/10.3389/fpls.2024.1368692

Lufu, R., Ambaw, A. & Opara, U.L., 2020. Water loss of fresh fruit: influencing pre-harvest, harvest and postharvest factors. *Scientia Horticulturae*, 272, p. 109519. https://doi.org/10.1016/j.scienta.2020.109519

Ma, B., Chen, J., Zheng, H., Fang, T., Ogutu, C. & Li, S., 2018. Determination of predominant organic acid components in *Malus* species: correlation with apple domestication. *Metabolites*, 8(4), p. 74. https://doi.org/10.3390/metabo8040074

Mabusela, B.P., Godongwana, B., Mathe, S., et al., 2022. Advances in vacuum ultraviolet photolysis in the postharvest management of fruit and vegetables along the value chains: a review. *Food and Bioprocess Technology*, 15, pp. 28–46. https://doi.org/10.1007/s11947-021-02703-1

Mabusela, B.P., Godongwana, B., Mathe, S., et al., 2023. Impact of vacuum ultraviolet (VUV) photolysis on ethylene degradation kinetics and removal in mixed-fruit storage, and direct exposure to “Fuji” apples during storage. *Journal of Food Science and Technology*. https://doi.org/10.1007/s13197-023-05775-3

Mabusela, B.P., Godongwana, B., Mathe, S., et al., 2024. Ethylene degradation via vacuum ultraviolet photolysis: nth-order kinetic model, energy consumption assessment, and a case study for “Fuji” apples under retail conditions. *Food and Bioproducts Processing*, 147, pp. 230–238. https://doi.org/10.1016/j.fbp.2024.07.006

Maguire, K.M., Banks, N.H., Opara, L.U. & Bowyer, M.C., 2000. Harvest date, cultivar, orchard, and tree effects on water vapor permeance in apples. *Journal of the American Society for Horticultural Science*, 125(1), pp. 100–104. https://doi.org/10.21273/jashs.125.1.100

Magwaza, L.S. & Opara, U.L., 2015. Analytical methods for determination of sugars and sweetness of horticultural products: a review. *Scientia Horticulturae*, 184, pp. 179–192. https://doi.org/10.1016/j.scienta.2015.01.001

Mahajan, P.V., Caleb, O.J., Singh, Z., Watkins, C.B. & Geyer, M., 2014. Postharvest treatments of fresh produce. *Philosophical Transactions of the Royal Society A: Mathematical, Physical and Engineering Sciences*, 372(2017), p. 20130309. https://doi.org/10.1098/rsta.2013.0309

Mallya, N. & Haussener, S., 2021. Buoyancy-driven melting and solidification heat transfer analysis in encapsulated phase change materials. *International Journal of Heat and Mass Transfer*, 164, p. 120525. https://doi.org/10.1016/j.ijheatmasstransfer.2020.120525

Martínez-Romero, D., Guillén, F., Castillo, S., Valero, D. & Serrano, M., 2007. Tools to maintain postharvest fruit and vegetable quality through the inhibition of ethylene action: a review. *Critical Reviews in Food Science and Nutrition*, 47(6), pp. 543–560. https://doi.org/10.1080/10408390600846390

McKeon, T.A., Fernández-Maculet, J.C. & Yang, S.F., 1995. Biosynthesis and metabolism of ethylene. In *Plant Hormones*. Dordrecht: Springer, pp. 118–139. https://doi.org/10.1007/978-94-011-0473-9_6

McMurchie, E.J., McGlasson, W.B. & Eaks, I.L., 1972. Treatment of fruit with propylene gives information about the biogenesis of ethylene. *Nature*, 237, pp. 235–236. https://doi.org/10.1038/237235a0

Mezey, J. & Mezeyová, I., 2018. Changes in the levels of selected organic acids and sugars in apple juice after cold storage. *Czech Journal of Food Sciences*, 36(2), pp. 154–158. https://doi.org/10.17221/165/2017-CJFS

Midgley, S.J.E., 2016. Commodity value chain analysis of apples. WWF-SA, South Africa.

Mignard, P., Dufour, C., Huet, S., et al., 2022. Effect of genetics and climate on apple sugars and organic acids profiles. *Agronomy*, 12(4), p. 827. https://doi.org/10.3390/agronomy12040827

Moghadam, H.Z., Kheirkhah, B. & Kariminik, A., 2015. Ethylene removal by bio-filters in order to increase storage life of bananas. *International Journal of Life Sciences*, 9(5), pp. 30–36. https://doi.org/10.3126/ijls.v9i5.12696

Morshedi, A. & Akbarian, M., 2014. Application of response surface methodology: design of experiments and optimization – a mini review. *Indian Journal of Fundamental and Applied Life Sciences*, 4(4), pp. 244–249.

Myers, R.H., Khuri, A.I. & Carter, W.H., 1989. Response surface methodology: 1966–1988. *Technometrics*, 31(2), pp. 137–157. https://doi.org/10.1080/00401706.1989.10488509

Nistor, O.V., Borda, D., Popa, M.E. & Ciucu, A., 2011. Study of the apple parameters' variation during refrigeration storage. *Journal of Agroalimentary Processes and Technologies*, 17(2), pp. 204–210.

Oetiker, J.H. & Yang, S.F., 1995. The role of ethylene in fruit ripening. *Acta Horticulturae*, 398, pp. 167–178. https://doi.org/10.17660/actahortic.1995.398.17

Ono, R., Hayashi, N., Uchida, S., et al., 2014. Effect of humidity on the production of ozone and other radicals by low-pressure mercury lamps. *Journal of Photochemistry and Photobiology A: Chemistry*, 274, pp. 13–19. https://doi.org/10.1016/j.jphotochem.2013.09.012

Pathak, N., Caleb, O.J., Rauh, C., et al., 2017. Effect of process variables on ethylene removal by vacuum ultraviolet radiation: application in fresh produce storage. *Biosystems Engineering*, 159, pp. 33–45. https://doi.org/10.1016/j.biosystemseng.2017.04.008

Pathak, N., Caleb, O.J., Wegner, G., et al., 2017. Impacts of mixed fruit loading on postharvest physiological responses and quality of horticultural produce. *Food Packaging and Shelf Life*, 14, pp. 66–73. https://doi.org/10.1016/j.fpsl.2017.08.010

Pathak, N., Caleb, O.J., Geyer, M., et al., 2017. Photocatalytic and photochemical oxidation of ethylene: potential for storage of fresh produce — a review. *Food and Bioprocess Technology*, 10, pp. 982–1001. https://doi.org/10.1007/s11947-017-1889-0

Pathak, N., Caleb, O.J., Rauh, C., et al., 2019. Efficacy of photocatalysis and photolysis systems for the removal of ethylene under different storage conditions. *Postharvest Biology and Technology*, 147, pp. 18–30. https://doi.org/10.1016/j.postharvbio.2018.09.006

Pathak, N., 2019. *Photocatalysis and vacuum ultraviolet light photolysis as ethylene removal techniques for potential application in fruit storage*. PhD thesis, Stellenbosch University.

Pathak, N. & Mahajan, P.V., 2017. Ethylene removal from fresh produce storage: current methods and emerging technologies. In *Reference Module in Food Science*. Amsterdam: Elsevier. https://doi.org/10.1016/B978-0-08-100596-5.22330-5

Patience, G.S., 2017. Experimental methods and instrumentation for chemical engineers. In *Experimental Methods and Instrumentation for Chemical Engineers*. Amsterdam: Elsevier, pp. 325–346. https://doi.org/10.1016/B978-0-44-463782-6.00013-6

Pech, J.C., Purgatto, E., Bouzayen, M. & Latché, A., 2012. Ethylene and fruit ripening. In *The Plant Hormone Ethylene*, pp. 275–304. https://doi.org/10.1002/9781118223086.ch11

Peters, M.S., Timmerhaus, K.D. & West, R.E., 2003. *Plant design and economics for chemical engineers*. 5th ed. New York: McGraw-Hill.

Popiel, C.O., 2008. Free convection heat transfer from vertical slender cylinders: a review. *Heat Transfer Engineering*, 29(6), pp. 521–536. https://doi.org/10.1080/01457630801891557

Raheema, R., 2020. *Apples and health*. ResearchGate. https://doi.org/10.13140/RG.2.2.26052.04485

Rao, J.S. & Kumar, B., 2012. 3D blade root shape optimization. In *10th International Conference on Vibrations in Rotating Machinery*. London: Institution of Mechanical Engineers. https://doi.org/10.1533/9780857094537.4.173

Rashed, M.N. & Palanisamy, P.N., 2018. Introductory chapter: adsorption and ion exchange properties of zeolites for treatment of polluted water. In *Zeolites and their applications*. Rijeka: InTech. https://doi.org/10.5772/intechopen.77190

Rowe, J.P., Lambe, A.T. & Brune, W.H., 2020. Technical note: Effect of varying the λ = 185 and 254 nm photon flux ratio on radical generation in oxidation flow reactors. *Atmospheric Chemistry and Physics*, 20(21), pp. 13417–13424. https://doi.org/10.5194/acp-20-13417-2020

Roy, U. & Roy, P.K., 2020. Advances in heat intensification techniques in shell and tube heat exchanger. In *Advanced analytic and control techniques for thermal systems with heat exchangers*. Amsterdam: Elsevier, pp. 159–190. https://doi.org/10.1016/B978-0-12-819422-5.00007-4

Saei, A., Zamani, Z., Kalantari, S., et al., 2011. Cropping effects on the loss of apple fruit firmness during storage: the relationship between texture retention and fruit dry matter concentration. *Scientia Horticulturae*, 130(1), pp. 256–261. https://doi.org/10.1016/j.scienta.2011.07.008

Salas, N.A., Cruz-Hernández, A., Calderón-Santoyo, M., et al., 2011. Volatile production by 'Golden Delicious' apples is affected by preharvest application of aminoethoxyvinylglycine. *Scientia Horticulturae*, 130(2), pp. 449–455. https://doi.org/10.1016/j.scienta.2011.07.017

Saltveit, M.E., 1999. Effect of ethylene on quality of fresh fruits and vegetables. *Postharvest Biology and Technology*, 15(3), pp. 279–292. https://doi.org/10.1016/S0925-5214(98)00091-X

Santosa, E., Widodo, W.D. & Kholidi, M., 2013. The use of clay as potassium permanganate carrier to delay the ripening of Raja Bulu banana. *Jurnal Hortikultura Indonesia*, 1(2), pp. 88–95. https://doi.org/10.29244/jhi.1.2.88-95

Schulze-Hennings, U., von Sonntag, J., Korth, A., et al., 2016. Improving vacuum-UV (VUV) photolysis of organic compounds in water with a phosphor converted xenon excimer lamp emitting at 193 nm. *Water Science and Technology*, 74(4), pp. 939–947. https://doi.org/10.2166/wst.2016.272

Silva, D.F.P., Alves, R.E., de Brito, E.A., et al., 2009. Potassium permanganate effects in postharvest conservation of the papaya cultivar Sunrise Golden. *Pesquisa Agropecuária Brasileira*, 44(7), pp. 669–675. https://doi.org/10.1590/S0100-204X2009000700003

Sisler, E.C. & Serek, M., 1997. Inhibitors of ethylene responses in plants at the receptor level: recent developments. *Physiologia Plantarum*, 100(3), pp. 577–582. https://doi.org/10.1034/j.1399-3054.1997.1000320.x

Sisler, E.C. & Yang, S.F., 1984. Ethylene, the gaseous plant hormone. *BioScience*, 34(4), pp. 234–238. https://doi.org/10.2307/1309461

Skog, L.J. & Chu, C.L., 2001. Effect of ozone on qualities of fruits and vegetables in cold storage. *Canadian Journal of Plant Science*, 81(4), pp. 773–778. https://doi.org/10.4141/P00-110

De Smedt, V., Barreiro, P., de Baerdemaeker, J. & Segers, J., 1998. Microscopic observation of mealiness in apples: a quantitative approach. *Postharvest Biology and Technology*, 14(2), pp. 151–158. https://doi.org/10.1016/S0925-5214(98)00044-1

Souza, A.S., Dos Santos, W.N.L. & Ferreira, S.L.C., 2005. Application of Box–Behnken design in the optimisation of an on-line pre-concentration system using knotted reactor for cadmium determination by flame atomic absorption spectrometry. *Spectrochimica Acta Part B: Atomic Spectroscopy*, 60(5), pp. 737–742. https://doi.org/10.1016/j.sab.2005.02.007

Sun, X., Chen, Y., Li, J., et al., 2023. Removal of gaseous volatile organic compounds via vacuum ultraviolet photodegradation: review and prospect. *Journal of Environmental Sciences (China)*, 134, pp. 263–277. https://doi.org/10.1016/j.jes.2022.01.020

Suslow, T.V., 2004. *Ozone applications for postharvest disinfection of edible horticultural crops*. University of California Agriculture and Natural Resources Publication 8133. https://doi.org/10.3733/ucanr.8133

Taylor, R.P., Solbrig, C.W., Jackson, J.D., et al., 1992. Measurement and prediction of roughness element shape effects on turbulent heat transfer. In: *Transport Phenomena in Heat and Mass Transfer*. Amsterdam: Elsevier, pp. 377–388. https://doi.org/10.1016/B978-0-444-89851-7.50031-5

Terry, L.A., Ilkenhans, T., Poulston, S., Rowsell, L. & Smith, A.W.J., 2007. Development of new palladium-promoted ethylene scavenger. *Postharvest Biology and Technology*, 45(2), pp. 214–220. https://doi.org/10.1016/j.postharvbio.2006.11.020

Tru-Cape, 2021. Getting an apple from point A to B is a real wonder. Available at: https://tru-cape.com/getting-an-apple-from-point-a-to-b-is-a-real-wonder/ (Accessed: 6 September 2024).

Tu, K., Nicolaï, B. & De Baerdemaeker, J., 2000. Effects of relative humidity on apple quality under simulated shelf temperature storage. *Scientia Horticulturae*, 85(3), pp. 217–229. https://doi.org/10.1016/S0304-4238(99)00148-X

Turton, R., Bailie, R.C., Whiting, W.B. & Shaeiwitz, J.A., 2013. *Analysis, synthesis, and design of chemical processes*. 4th ed. Upper Saddle River: Prentice Hall.

Tzeng, J.H., Chen, P.H., Chang, C.H., et al., 2019. Application of palladium-modified zeolite for prolonging post-harvest shelf life of banana. *Journal of the Science of Food and Agriculture*, 99(7), pp. 3467–3474. https://doi.org/10.1002/jsfa.9565

USDA, 2023. *Fresh apples, grapes, and pears: World markets and trade*. United States Department of Agriculture Foreign Agricultural Service. Available at: https://public.govdelivery.com/accounts/USDAFAS/subscriber/new.

Vasylieva, N. & James, H., 2021. Production and trade patterns in the world apple market. *Innovative Marketing*, 17(1), pp. 16–25. https://doi.org/10.21511/im.17(1).2021.02

Venburg, G.D., Ritenour, M.A., Whitaker, B.D. & Mattheis, J.P., 2008. Recent developments in AVG research. *Acta Horticulturae*, 796, pp. 17–24. https://doi.org/10.17660/ActaHortic.2008.796.3

Wang, W., Liu, D., Xu, J., et al., 2020. Skin color in apple fruit (*Malus* × *domestica*): genetic and epigenetic insights. *Epigenomes*, 4(3), p. 13. https://doi.org/10.3390/epigenomes4030013

Watkins, C.B., 2006. The use of 1-methylcyclopropene (1-MCP) on fruits and vegetables. *Biotechnology Advances*, 24(4), pp. 389–409. https://doi.org/10.1016/j.biotechadv.2006.01.005

Whale, S.K. & Singh, Z., 2007. Endogenous ethylene and color development in the skin of 'Pink Lady' apple. *Journal of the American Society for Horticultural Science*, 132(1), pp. 20–28.

Wills, R., 2015. Low ethylene technology in non-optimal storage temperatures. In: *Advances in postharvest fruit and vegetable technology*. Boca Raton: CRC Press, pp. 119–132. https://doi.org/10.1201/b18489-9

Wills, R.B.H., Scott, K.J. & Zealand, N., 1972. Effect of water loss from apples during cool storage on the water content of the fruit. *Journal of the Science of Food and Agriculture*, 23(6), pp. 743–746

Wills, R.B.H. & Warton, M.A., 2004. Efficacy of potassium permanganate impregnated into alumina beads to reduce atmospheric ethylene. *Journal of the American Society for Horticultural Science*, 129(3), pp. 433–438. https://doi.org/10.21273/jashs.129.3.0433

Xiao, Y.Y., Chen, J.Y., Kuang, J.F., et al., 2013. Banana ethylene response factors are involved in fruit ripening through their interactions with ethylene biosynthesis genes. *Journal of Experimental Botany*, 64(8), pp. 2499–2510. https://doi.org/10.1093/jxb/ert108

Xie, P., Ma, J., Liu, W., Zou, J. & Yue, S., 2018. Degradation of organic pollutants by vacuum-ultraviolet (VUV): kinetic model and efficiency. *Water Research*, 136, pp. 46–57. https://doi.org/10.1016/j.watres.2018.01.019

Xie, R., Li, Y., Zhao, S., et al., 2023. Accelerated oxidation of VOCs via vacuum ultraviolet photolysis coupled with wet scrubbing process. *Journal of Environmental Sciences (China)*, 134, pp. 278–287. https://doi.org/10.1016/j.jes.2022.05.002

Xu, Y. et al. (2019) 'Ultraviolet-C priming of strawberry leaves against subsequent *Mycosphaerella fragariae* infection involves the action of reactive oxygen species, plant hormones, and terpenes', *Plant, Cell and Environment*, 42(3). Available at: https://doi.org/10.1111/pce.13491

Yang, G. et al. (2023) 'Degradation of Orange IV by UV photolysis in nitrite-containing wastewater: Influencing factors, mechanism, and response surface methodology', *Process Safety and Environmental Protection*, 169, pp. 592–603. Available at: https://doi.org/10.1016/j.psep.2022.11.017

Yang, S. et al. (2021) 'Evaluation of physiological characteristics, soluble sugars, organic acids and volatile compounds in "Orin" apples (*Malus domestica*) at different ripening stages', *Molecules*, 26(4). Available at: https://doi.org/10.3390/molecules26040807

Yang, S.F. and Hoffman, N.E. (1984) 'Ethylene biosynthesis and its regulation in higher plants', *Annual Review of Plant Physiology* [Preprint]. Available at: https://doi.org/10.1146/annurev.pp.35.060184.001103

Ye, J. et al. (2013) 'Generation of reactive oxygen species in simulated flue gas under vacuum ultraviolet radiation', *Chemical Engineering Journal* [Preprint]. Available at: https://doi.org/10.1016/j.cej.2013.07.056

Yildiz, K., Ozturk, B. and Ozkan, Y. (2012) 'Effects of aminoethoxyvinylglycine (AVG) on preharvest fruit drop, fruit maturity, and quality of "Red Chief" apple', *Scientia Horticulturae*, 144, pp. 121–124. Available at: https://doi.org/10.1016/j.scienta.2012.07.005

Zeneli, M. et al. (2020) 'Numerical methods for solid-liquid phase-change problems', in *Ultra-High Temperature Thermal Energy Storage, Transfer and Conversion*. Available at: https://doi.org/10.1016/B978-0-12-819955-8.00007-7

Zhang, Z. et al. (2015) 'Identification of differentially expressed genes associated with apple fruit ripening and softening by suppression subtractive hybridization', *PLoS ONE*, 10(12). Available at: https://doi.org/10.1371/journal.pone.0146061